Performance-Based Design of Fire-Exposed Reinforced Concrete Elements using an Equivalent Standard Fire

Robert T. Kuehnen, *The University of Western Ontario*

Supervisor: Youssef, Maged A., *The University of Western Ontario*
A thesis submitted in partial fulfillment of the requirements for the Master of Engineering Science degree in Civil and Environmental Engineering

Abstract

Fire events represent one of the most severe loading scenarios for reinforced concrete (RC) buildings. In lieu of intensive computational analysis, designers need simplified methods to assess RC members exposed to natural fires. This thesis focuses on the development of a time equivalent (t_e) to replace a natural fire with an equivalent standard fire, allowing for the implementation of existing simplified analysis methods.

The proposed t_e is based on the average internal temperature profile (AITP) that develops in a section during fire. Two AITP t_e are proposed to accurately or conservatively approximate the AITP of natural fire exposed sections. A size adjustment factor (φ_{size}) is also proposed to account for the influence of section dimensions. Suitability of the AITP t_e in the performance-based fire design of RC beams and columns was examined based on the relationships of moment-curvature, axial load & axial strain, and moment capacity & axial load capacity.

Keywords

Reinforced Concrete, Fire, Performance-Based Design, Time Equivalent, RC Beams, RC Columns, Average Internal Temperature Profile.

Co-Authorship Statement

All numerical and analytical work presented in this thesis was performed by Robert Kuehnen. Work was reviewed by Dr. Maged Youssef and Dr. Salah El-Fitiany. Chapters 3 of this thesis has been submitted to a scholarly journal as a manuscript co-authored by Robert Kuehnen and Maged Youssef. The case study in Chapter 4 has been submitted as a conference paper co-authored by Robert Kuehnen, Maged Youssef, and Salah El-Fitiany. Chapter 5 and Chapter 4, excluding the case study, will at a later date be submitted to a scholarly journal as a manuscript co-authored by Robert Kuehnen, Maged Youssef, and Salah El-Fitiany.

Acknowledgments

I would like to express my many thanks to Dr. Maged Youssef for his advice and guidance over these past years. When I began searching for where to undertake my Master's program, I had only one goal in mind, select the best advisor, and all else would work itself out. Now, two years on, I believe even more strongly in that original thesis. Dr. Youssef has given me a tremendous opportunity at Western University and broadened my knowledge on the previously unknown world of structural fire design. I appreciate his support during my Master's and look forward to what we will be able to accomplish ahead.

My debts of gratitude to my fellow graduate students who have helped me during my thesis are enormous in both number and degree. Their experience was of great assistance to my work, and their friendship essential to my perseverance. Particular gratitude is due to Dr Salah El-Fitiany, for whom this thesis would have been very different without. Leaving Western, I will miss Salah's thoughtful guidance and late-night conversations.

Finally, this thesis would not have been possible without the love and support of my family. There is no doubt that the opportunities that have been created here will carry with me forever. Opportunities for my future, my education, my career, and my family. These opportunities would not be possible without your sacrifices and dedication.

Table of Contents

Chapter 5

Chapter 6

List of Tables

List of Figures

List of Abbreviations, Symbols, and Notations

a_c	thermal diffusivity (m^2s^{-1})
A_f	floor area of the fire compartment (m^2)
A_s	area of tension steel (mm^2)
b	thermal absorptivity for the total enclosure ($Jm^{-2}s^{0.5}K$)
b_c	beam width (mm)
c	depth of section neutral axis (mm)
C_{cT}	resultant compression force at elevated temperature (kN)
c_s	specific heat ($Jkg^{-1}K^{-1}$)
d	effective depth of the tension reinforcement (mm)
EI_{iT}	initial stiffness at elevated temperature (Nm^2)
F_{agg}	aggregate factor
f'_c	concrete compressive strength at ambient temperature (MPa)
f'_{cR}	residual concrete compressive strength after a heating cycle (MPa)
f'_{cT}	concrete compressive strength at elevated temperature (MPa)
F_{sT}	steel stress at elevated temperature (MPa)
F_u	steel ultimate strength (MPa)
F_y	steel yield strength (MPa)
F_{yT}	steel yield strength at elevated temperature (MPa)
h_c	beam height (mm)
h_{max}	coefficient of heat transfer ($Wm^{-1}K^{-1}$)
k	thermal conductivity ($Wm^{-1}K^{-1}$)

M_{bT}	balance moment resistance at elevated temperature (kNm)
M_r	moment resistance at zero axial load (kNm)
M_{rT}	moment resistance at zero axial load and elevated temperature (kNm)
O	opening factor of the fire compartment ($m^{0.5}$)
P_{bT}	balance axial capacity at elevated temperature (kN)
P_{rT}	axial resistance at zero moment and elevated temperature (kN)
P_T	axial resistance at elevated temperature (kN)
q	heat flux (Wm^{-2})
$q_{f,d}$	design fire load density related to the floor area A_f (MJm^{-2})
t	time (hr)
T	temperature (°C)
T_{av}	average concrete temperature at a given section height (°C)
t_e	time equivalent of a standard fire exposure (min)
T_f	temperature of the standard fire (°C)
t_{final}	natural fire: overall fire duration (min)
t_{max}	natural fire: time of maximum temperature (min)
T_{max}	natural fire: maximum temperature (°C)
T_o	ambient temperature (°C)
T_{sT}	resultant tension force at elevated temperatures (kN)
V_a	volume fraction of aggregates
x	distance from the section point under consideration to the closer of the left or right faces (mm)
y	distance from the section point under consideration to the bottom face (mm)

α_1	average stress block parameter
α_{1T}	average stress block parameter at elevated temperature
α_s	coefficient of thermal expansion
β_1	stress block depth parameter
β_{1T}	stress block depth parameter at elevated temperature
$\Delta\xi$	size of the FDM mesh block
ε	strain (mm/mm)
$\varepsilon_{0.3}$	transient creep strain at $0.3f'_c$
ε_c	concrete total strain at ambient temperature (mm/mm)
ε_{cR}	residual concrete total strain after a heating cycle (mm/mm)
ε_{cT}	concrete total strain at elevated temperature (mm/mm)
ε_{cu}	concrete ultimate strain (mm/mm)
ε_{cuT}	concrete ultimate strain at elevated temperature (mm/mm)
ε_f	effective emissivity
ε_s	steel total strain (mm/mm)
ε_{sT}	steel strain at elevated temperature (mm/mm)
ε_{th}	fire-induced thermal strain (mm/mm)
ε_{tr}	fire-induced transient strain (mm/mm)
η_w	ratio between surface and fire temperature
η_x	ratio between temperature at interior point x and T_f
η_y	ratio between temperature at interior point y and T_f
ρ	density (kgm^{-3})
ρ_s	steel reinforcement ratio

σ	Stefan-Boltzmann constant (WmK^{-4})
φ	section curvature (rad/mm)
φ_{iT}	initial section curvature at elevated temperature (rad/mm)
ψ_{size}	size adjustment factor

Chapter 1

"Structural engineering is the art of modeling materials we do not wholly understand, into shapes we cannot precisely analyze, so as to withstand forces we cannot properly assess, in such a way that the public at large has no reason to suspect the extent of our ignorance."

A.R. Dyke, 1976

1.0 Introduction

There are few subjects for which the epigraph of this thesis enjoys greater reality than in the discipline of fire safety. Despite decades of research, the extreme severity and variability of fire events has eluded our ability to even fundamentally understand fire's influence on structures. From a material perspective, the low conductivity of reinforced concrete (RC) makes it a highly suitable material for fire protection; however, fire's influence on concrete's strength and strain is still not fully understood. Large debates exist regarding the mechanisms of explosive spalling, cooling rates, exposure duration, and the host of available additives (Kodur, 2014). From an analysis perspective, our ability to evaluate elements has vastly improved with the implementation of computational capabilities. Performance-based models, such as that developed by El-Fitiany and Youssef (2009), promise simple and efficient analysis of RC members. Yet still, the building code and standard practices rely on prescriptive fire ratings, focusing on temporary protective measures, as opposed to designing buildings to withstand fire. And finally, from a force perspective, testing performed in furnaces during the early 1920's is still considered as the standard for representing the development of building fires (CAN/ULS-S101, 2014). Rudimentary models for predicting the scale of realistic fire events do exist in the literature and design standards (EN 1991-1-2, 2002); but, the specifics of accurately modelling fire development and its spread within a building, is still largely untrodden ground (Dai et al., 2017).

From 2005 to 2014, Statistics Canada (2017) reported over 200,000 structural fires and 1,490 structural fire-related fatalities. Although these numbers are considered an improvement over the decades before, giving the public the impression of success, further innovation is still possible and necessary. To overcome the gaps in our understanding, research into material mechanics, analysis, and fire development is needed in the field of fire safety. This thesis examines the influence of fire development on RC sections, covering the later of the three research gaps.

1.1 Research Objectives

With the recent focus on performance-based structural fire design, engineers are in need of simple, but accurate methods of assessing concrete's performance during fire events. The proposed research aims to:

1. Present a literature review detailing the influence of natural fire events on the stress-strain relationship of normal strength concrete (NSC),

2. Determine an equivalent standard fire duration (time equivalent) for a natural fire acting on RC beams,

3. Evaluate the influence of variable RC beam dimensions on the average internal temperature profile and the time equivalent,

4. Assess the accuracy of the proposed time equivalent in calculating the sectional moment-curvature response,

5. Repeat steps 2 through 4 to determine and assess a time equivalent for RC columns.

1.2 Methodology

The proposed research is performed using the computational models developed Alhadid (2017) and El-Fitiany and Youssef (2009). Their models allow for analytical evaluation of the thermal and structural response of RC elements exposed to fire loading. The current study adapts these programs to apply natural fire events and identify the effect on RC sections. Models were developed in MATLAB, C++, and Fortran. To validate results, an ABAQUS finite element model was utilized in Chapter 4.

1.3 Outline of Thesis

This thesis is prepared in an "Integrate-Article Format" following the guidelines described in the Western University – School of Graduate and Postdoctoral Studies (SGPS), General Thesis Regulations.

1.3.1 Chapter 2

A literature review is presented in this chapter exploring the effects of natural fires on the stress-strain response of concrete. Background regarding standard and natural fire curves is presented detailing their usage and parameters. The four main variabilities of fire: heating rate, maximum temperature, duration at maximum temperature, and cooling rate are individually explored. The chapter summarizes the impact of each variable in comparison to one another and provides conclusions about ongoing work.

1.3.2 Chapter 3

In the first section of the chapter, a brief literature review is conducted providing the background and limitations of past time equivalent (t_e) methods. Noting the shortcomings of the existing methods, this chapter introduces a new time equivalent method based on the actual internal thermal gradients that develop in a RC beam during fire exposure. An average internal temperature profile (AITP) is a technique used to simplify a section's two-dimensional thermal gradients into a one-dimensional profile. Using a section's AITP, time equivalency is determined based on mean or conservative criteria. The mean criterion accurately matches the AITP of a design fire to that of a standard, while the conservative criterion selects the shortest duration standard fire that produces equal or larger temperatures at every point in the AITP. Following a parametric study, two equations are presented to calculate the AITP t_e. Further evaluation regarding the influence of section dimensions on the value of the t_e revealed the importance of accounting for section width. The section concludes with a study comparing the developed t_e against the existing methods for RC beam sections.

1.3.4 Chapter 4

A parametric study is presented to assess the proposed AITP t_e for RC beams. Using a sectional analysis program developed by El-Fitiany and Youssef (2009), sample RC beam sections are modelled and tested. The sectional moment-curvature responses of the beams are compared for given design fires and corresponding time equivalent fires. The results were found to be in good agreement lending to the validity of the AITP method. The work is further assessed in comparison to existing time equivalent methods to demonstrate the improved suitability of the AITP method. Finally, a case study is presented demonstrating the application of the time equivalent in the use of performance-based design.

1.3.5 Chapter 5

The AITP time equivalent method is investigated for usage with RC columns. The t_e from Chapter 3 is tailored for RC beams undergoing three-sided fire exposure. RC columns typically undergo four-sided exposure, which greatly influences their internal thermal gradients. A parametric study was undertaken to assess the AITP t_e methodology for the application of RC columns. It was found that the conservative t_e is still valid four-sided heating, while the mean t_e is wholly unsuitable. An alternative to the mean t_e is explored, but ultimately found to be unfeasible due to the large errors that arise. The conservative t_e is assessed based the mechanical response of RC columns and in view of existing time equivalent methods.

1.4 References

Alhadid, M. *Behavior of Fire-Exposed RC Frames Before and After Jacketing*. Diss. Department of Civil and Environmental Engineering, Western University, 2017.

CAN/ULC-S101. *Standard Methods of Fire Endurance Tests of Building Construction and Materials*. Underwriters Laboratories of Canada. Toronto, Canada. 1982.

Dai, X., S. Welch, A. Usmani. "A Critical Review of Travelling Fire Scenarios for Performance-Based Structural Engineering." *Fire Safety Journal*, vol. 91, no. 1, 2017, pp. 568-758.

Dyke, A.R. "Chairman's Address to the Scottish Branch of the Institution of Structural Engineers." 1976. Reported by J.A. Schmidt. "The Definition of Structural Engineering." *Structure Magazine*, no. January 2009, 2009, pp. 9.

El-Fitiany, S.F. and M.A. Youssef. "Assessing the Flexural and Axial Behaviour of Reinforced Concrete Members at Elevated Temperatures Using Sectional Analysis." *Fire Safety Journal*, vol. 44, no. 5, 2009, pp. 691-703.

EN 1991-1-2. *Eurocode 1: Actions on Structures - Part 1-2: Actions on structures Exposed to Fire*. European Committee for Standardization. Brussels, Belgium. 2002.

Kodur, V. "Properties of Concrete at Elevated Temperatures." *ISRN Civil Engineering*, vol. 2014, no. 468510, 2014, pp. 1-15.

Statistics Canada. *Fire Statistics in Canada: Selected Observations from the National Fire Information Database 2005 to 2014*. Canadian Centre for Justice Statistics. Kanata, Canada. 2017.

Chapter 2

2.0 Literature Review

In North America, the current practice for structural fire safety involves the implementation of prescriptive methods, requiring compliance with fire-resistance ratings and suppression system specifications. Although this approach has been largely successful in delaying the propagation of fires, allowing for the safe evacuation of occupants, it provides no knowledge about the behavior of the fire-exposed structure. To ensure structural integrity, the North American industry is moving towards performance based structural fire design; as included in the most recent publication of ASCE 7-16 (2016). Implementation of performance design requires knowledge of the general stress-strain relationships for concrete at high temperatures, which are presented within EN 1992-1-2 (2004) and by Youssef and Moftah (2007). However, the major deficiency of these relationships is that they were developed based on the application of standard fire scenarios, ignoring the variability of natural fire events. To develop a clear understanding of these formulations and their application in the performance-based approach, this chapter summarizes the impact of natural fires on the stress-strain response of concrete.

2.1 Standard vs. Natural Fire Definition

To evaluate the fire ratings of different construction elements, standard temperature-time curves are prescribed as in ASTM E-119 (2018) and ISO 834 (2014). These standard curves were generated in the early 1900’s based on observations of the temperature-time relationship measured in laboratory furnaces. By their very nature, standard curves do not even remotely represent the trends of a naturally occurring fire. Instead, they were adopted to simplify and standardize the representation of a severe heating scenario; which was deemed as a conservative assumption of the natural fire, and thus, suitable for design (Cooper and Steckler, 1996).

In contrast to the standard curves, natural fire curves represent the true temperature-time relationship for a compartment, which, ASCE 7-16 (2017) edicts as essential for conducting structural fire analysis. Figure 2.1 compares the standard fire curve prescribed by ISO 834 (2014) with that of a typical natural fire profile. Considering that every compartment is different, each natural fire curve has its own unique profile; however, the main three stages of growth, full development, and decay are always present (Purkiss, 2007). EN 1991-1-2 (2002) provides a simplified approach for the development of natural fire curves based on a number of compartment specific parameters such as floor area, number of openings, and fuel load. In contrast to the simplicity of standard curves, the extensive quantity of data required to generate natural relationships has been a large barrier to their implementation. But with the advent and prevalence of modern computing power, the ability to evaluate every unique compartment is now highly feasible.

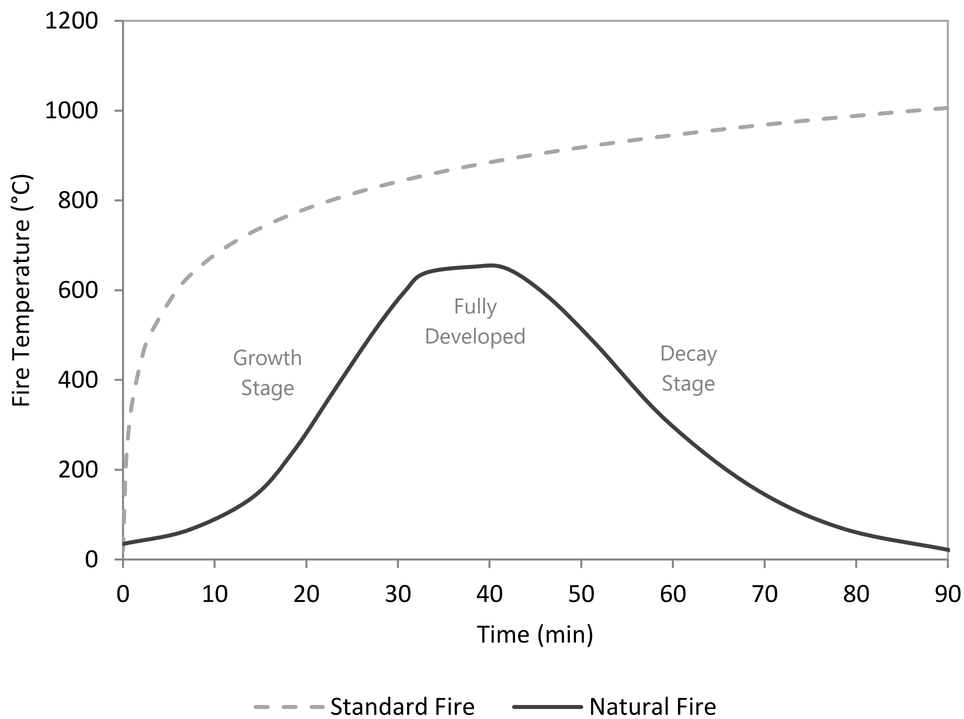

Fig. 2.1: Standard vs. Natural Fire Temperature-Time Curve

2.2 Fire Influence on Concrete Stress-Strain Relationship

Throughout a fire event, concrete properties continue to degrade at all stages. Since standard curves are identical regardless of the structure or the fire, they fail to accurately represent the impact of a realistic fire on concrete's stress-strain relationship. By contrast, the temperature-time curve of a natural fire has four main variabilities that affect the stress-strain relationship of concrete: rate of heating, maximum temperature, duration of maximum temperature, and rate of cooling (Zhang et al., 2001). During the growth stage, variable rates of heating can occur, ranging from near instantaneous to very slow heating. At full development, the value of the maximum temperature as well as its duration play an important role in the degradation of concrete. And finally, in the decay phase, variable rates of cooling can be present ranging from slow air cooling in a smoldering compartment to rapid water cooling from firefighting efforts. Each of these four variabilities play a significant and different role in the deterioration of concrete.

A typical ambient stress-strain relationship for NSC is presented in Figure 2.2. The key points defining the curve are identified by the Eurocode (EN 1992-1-2, 2004) as the maximum compressive strength (f'_c), the corresponding strain at max strength (ε_c), and the ultimate strain (ε_{cu}). When the concrete is at elevated temperatures, these points are denoted as f'_{cT}, ε_{cT}, and ε_{cuT}. When the concrete specimen has undergone a full heating and cooling cycle back to ambient temperature, the residual concrete variables are denoted as f'_{cR}, ε_{cR}, and ε_{cuR}. Concrete properties at residual and hot conditions will exhibit notably different responses depending on the natural fire exposure. Following the ambient profile given in Figure 2.2, the Eurocode provides tables to interchange the three key points at various temperatures for both residual and hot conditions. Connecting the key points, the initial ascending portion of the curve can be calculated using equations found in the Eurocode and the declining portion of the curve can be modeled as a straight line joining the peak of the curve to the ultimate strain.

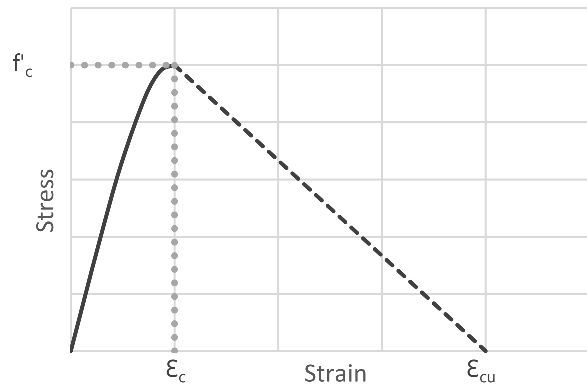

Fig. 2.2: Illustrative Stress-Strain Relationship for Concrete under Elevated Temperatures (EN 1992-1-2, 2004)

2.3 Experimental Work

Researchers have experimentally tested concrete at elevated temperatures for an extensive range of circumstances. Naus (2005) identified fifteen main parameters that affect the response of concrete at elevated temperatures. In this chapter, these parameters have been divided into two groups, variable and controlled. During this chapter's study, variable parameters were assessed at different levels while controlled parameters were locked into a specific state.

Variable parameters were identified based on their critical impact on the properties of normal strength concrete (NSC) and/or the definition of the natural fire curve. They are: (a) aggregate type (siliceous or calcareous), (b) heating rate, (c) cooling rate, (d) maximum temperature, (e) exposure duration, (f) mechanical testing time relative to the fire event, and (g) initial ambient compressive strength.

Controlled parameters reflect: (a) unstressed tests, (b) unconfined tests, (c) unsealed moisture tests, (d) ordinary portland cement (OPC) specimens (no additives such as fly ash, silica, fibers, etc.), and (e) NSC. NSC concrete is assumed to be defined as having a compressive strength up to 50 MPa.

Table 2.1 displays a list of the experimental tests investigated during this literature review. Figure 2.3 outlines the main parameters used in the table. "Residual" testing time indicates that testing occurred after the specimen cooled back to ambient temperature. The specific number of days from cooling to residual testing is provided for each experimental work. "Hot" testing occurs at maximum temperature after the heating duration has been applied. "Uniform" duration is defined as exposing the test specimen to the maximum temperature until a uniform internal temperature is achieved within the specimen. Typically, cylinder specimens heated for longer than a 1-hr duration are considered to have reached a uniform internal temperature (Fu et al., 2005; Diederichs et al., 1988). An "instant" heating rate indicates that the specimen was placed in a furnace preheated to the maximum temperature such that no rate of heating is experienced in the furnace or compartment. Cooling rate is stated as either "slow", "ambient", or "rapid"; comprehensive definitions of those three rates are provided in Section 2.4.4. It should be noted that the heating and cooling rates refer to the temperature change of the testing compartment, not the specimen itself.

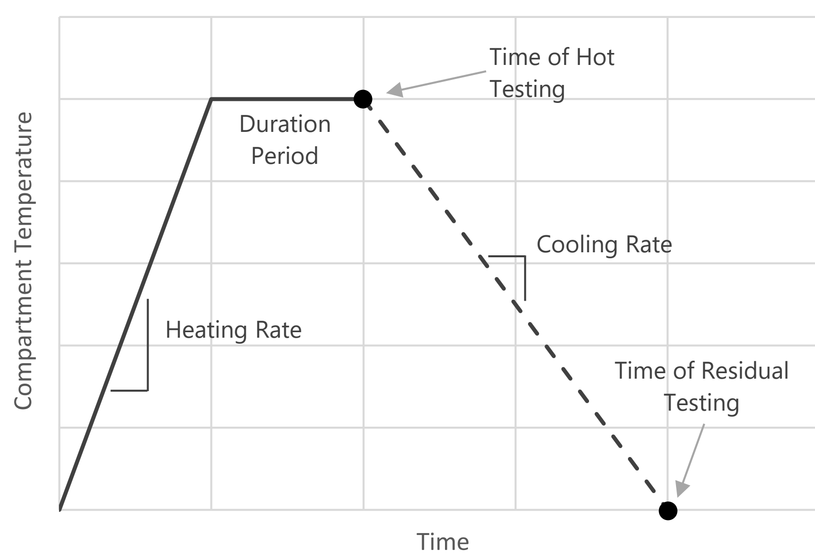

Fig. 2.3: Typical Furnace Heating Profile during Specimen Testing

Table 2.1 List of Evaluated Experimental Work with Test Parameters

Author	f'_c (MPa)	Aggregate	Specimen Size	Duration (hr)	Testing Time	Heating Rate (°C/min)	Cooling Rate
Abramowicz and Kowalski (2010)	30.0, 45.0	Siliceous	103x200 mm cylinder	uniform	residual (0 days)	3.0	varied
Abrams (1971)	27.0, 44.0	Both	75x150 mm cylinder	uniform	hot & residual (0 days)	measured [1]	natural
Anderberg and Thelandersson (1976)	50.0	Siliceous	75x150 mm cylinder	uniform	hot	1.0, 5.0	null
Bingol and Gul (2008)	20.0, 35.0	Calcareous	100x200 mm cylinder	3.00	residual (0 days)	12.0 - 20.0	varied
Botte and Caspeele (2017)	50.0	Siliceous	cube and cylinder [2]	uniform	residual (0 & 56 days) [2]	1.0	varied
Carette et al. (1982)	45.0	Calcareous	102x203 mm cylinder	varied	residual (0 days)	0.3	natural
Castillo and Durrani (1990)	31.0	Calcareous	50x102 mm cylinder	0.17	hot	8.0	null
Chang et al. (2006)	27.0, 40.0	Siliceous	150x300 mm cylinder	2.00	residual (30 days)	3.0	natural
Culfik and Ozturan (2010)	37.5	Calcareous	100x200 mm cylinder	3.00	residual (0 days)	1.0	slow
Diederichs et al. (1988)	32.9	Siliceous	80x300 mm cylinder	2.00	hot	2.0	null
Fu et al. (2005)	35.0	Siliceous	75x100 mm cylinder	1.00	hot	2.0	null
Furumura et al. (1995)	21.0, 42.0	Siliceous	50x100 mm cylinder	2.00	hot	1.0	null
Harada et al. (1972)	30.0	Both	50x100 mm cylinder	uniform	residual (30 days)	1.5	natural
Jaesung et al. (2006)	30.0	Siliceous	100x200 mm cylinder	4.00	residual (0 days)	2.0	varied
Khaliq (2012)	50.0	Calcareous	75x150 mm cylinder	2.00	hot	2.0	null
Li et al. (2004)	42.5	Siliceous	100 mm cube	none	residual (0 days)	10.0	varied
Mohamedbhai (1987)	35.0	Siliceous	100 mm cube	varied	residual (14 days)	varied	varied
Molhotra (1956)	25.0 - 50.0	Siliceous	100x200 mm cylinder	1.00	hot & residual (0 days)	measured [3]	natural
Morita et al. (1992)	19.6 - 41.0	Unknown	100x200 mm cylinders	1.00	residual (0 days)	1.0	natural
Nassif (2005)	45.0	Both	75x150 mm cylinders	uniform	residual (0 days)	9.0	varied
Netinger et al. (2011)	45.0	Both	40x40x160 mm prism	1.50	residual (0 days)	instant	natural
Noumowe et al. (1996)	37.1	Calcareous	110x220 mm cylinder	1.00	residual (0 days)	1.0	natural
Phan et al. (2001)	50.0	Calcareous	102x204 mm cylinder	uniform	hot & residual (0 days)	5.0	natural
Savva et al. (2005)	34.7	Siliceous	150 mm cube	2.00	residual (0 days)	2.5	slow
Shen (1991)	28.0	Siliceous	300x100 mm prism	0.50	residual (0 days)	8.0	rapid
Tan (1990)	28.0	Siliceous	irregular prism "T" section	0.50	residual (0 days)	2.0	natural
Xiaoyong and Fanjie (2011)	35.0, 20.0	Siliceous	150x300 mm cylinder	2.00	residual (0 days)	5.0	natural
Yao (1991)	40.0	Siliceous	irregular prism "plus" section	0.50	hot	5.0	null
Zhang et al. (2000)	50.0	Siliceous	100 mm cube	varied	residual (0 days)	instant	natural

1. Heating was applied such that maximum difference in internal temperatures never exceeded 3%.
2. Residual strength tests on 150 mm cubed specimens at 0 days. Residual strain tests on 106x330 mm cylinder specimens at 56 days.
3. Heating was applied such that maximum difference in internal temperatures never exceeded 100°C.

2.4 Effect of Natural Fire Stages on the Concrete Stress-Strain Relationship

In this section, the influence of natural fires on the stress-strain relationship of concrete is explored. The stress-strain response is evaluated based on the four main variabilities of natural fires: heating rate, maximum temperature, duration at maximum temperature, and cooling rate. The experimental tests from Table 2.1 are isolated to individually investigate the influence of each natural fire variability. Considering that residual and hot tested specimens record fundamentally different responses; experimental work is initially separated based on these two conditions, with later comparisons provided. The stress-strain relationship is assessed based on the key points of $f'_{cT/R}$ and $\varepsilon_{cT/R}$. The full stress-strain relationship is not considered due to limitations of experimental results in the literature. Likewise, the ultimate strain is not commonly recorded prohibiting any meaningful assessment of its response during natural fire.

2.4.1 Heating Rate

At the onset of the heating phase, the temperature within a concrete element is uniform and equal to the ambient temperature, typically assumed to be 20°C. As heating is undertaken, a temperature gradient arises between the outer concrete layers and the inner core. This gradient induces thermal stresses, which in turn influences the section's stress and strain response. The formation and severity of the internal temperature gradient is largely based on the rate of heating (Phan and Carino, 2003).

To evaluate and compare the effect of variable rates of heating, this chapter divides experimental work into slow and rapid rates. The definition of slow and rapid heating was entirely based on the median heating rate of the available experimental work. As such, a slow heating rate is defined as having a rate less than or equal to 2°C/min; while rapid heating is greater than 2°C/min up to instantaneous heating. For comparison, the standard curve defined by ISO 834 (2014) has an average heating rate of 34°C/min between 0°C and 800°C. Experimental work is further divided into hot tested specimens and residually tested specimens.

Figures 2.4 and 2.5 display the influences of slow and rapid heating on the residual relative strength of concrete. The work is reported for siliceous aggregate samples, unless otherwise labelled as calcareous (cal.). The profiles of these experiments for both slow and rapid heating were found to be in good agreement with one another. Figure 2.6 displays the averaged results. No significant disparity is observed between the two averages, with both rates indicating comparable strengths at all temperatures. Considering the average loss across all temperatures, slow heating causes slightly greater average strength loss at 38 %, compared to rapid heating at 35 %. The largest disparity in strength loss occurs at 800°C, wherein slow heating resulted in a strength reduction that is 11 % greater than rapid heating. Figure 2.6 also shows the recommended strength by EN 1992-1-2 (2004) with values adjusted from hot to residual conditions as described in Implementation of Eurocodes (2005). Results from Netinger et al. (2011) are presented to compare against instantaneous heating, the most sever heating rate possible. The high correlation of Netinger's work gives indication that even highly rapid heating of concrete will exhibit similar responses to that of slower rates.

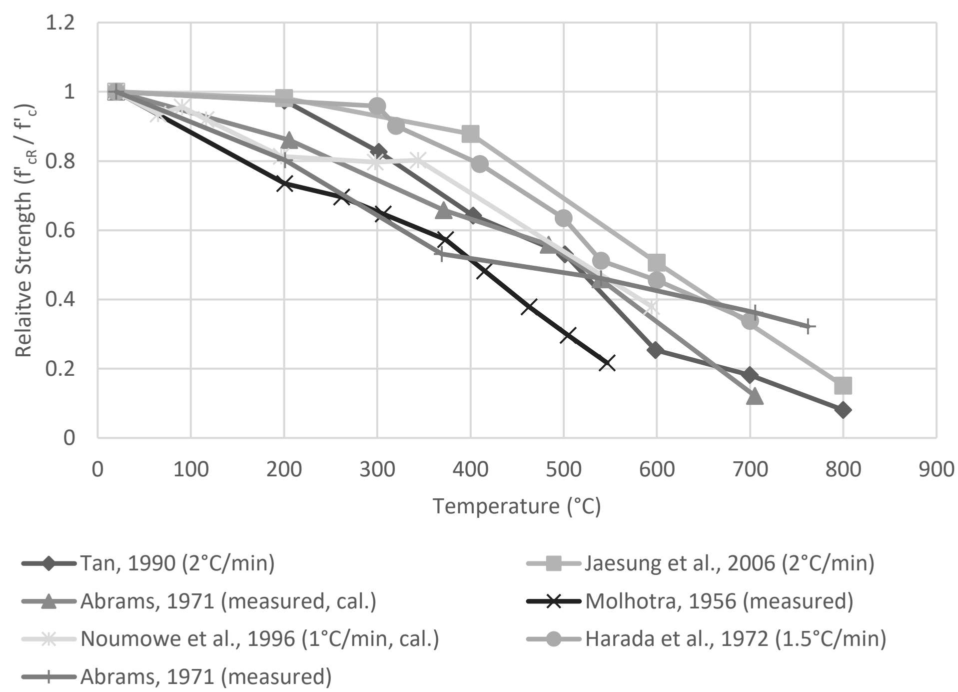

Fig. 2.4: Relative Residual Strength of Concrete after Exposure to Slow Rates of Heating and Natural Cooling

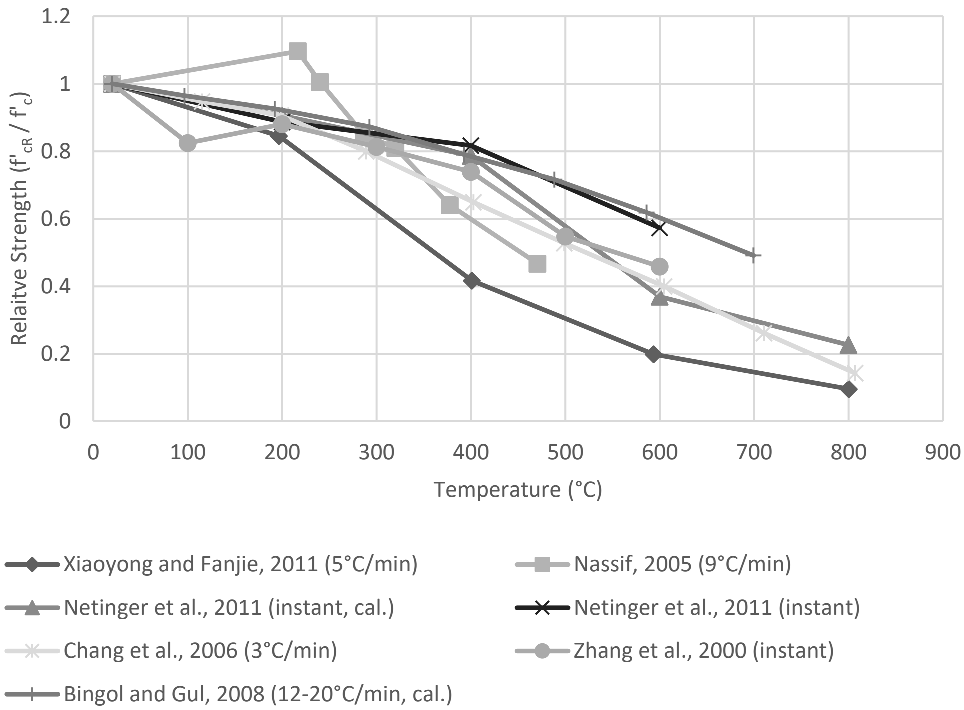

Fig. 2.5: Relative Residual Strength of Concrete after Exposure to Rapid Rates of Heating and Natural Cooling

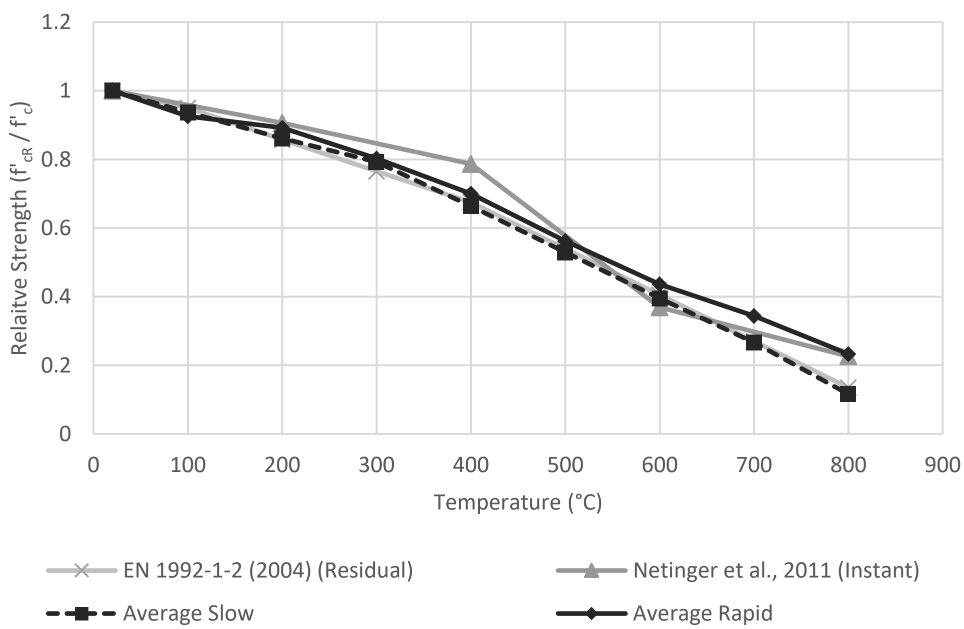

Fig. 2.6: Relative Average Residual Strength of Concrete after Exposure to Slow or Rapid Heating and Natural Cooling

Figures 2.7 and 2.8 present the relative strength versus temperature at slow and rapid heating under hot conditions. The strength of the slow and rapid samples was found to be in reasonably good agreement with one other. Greater fluctuation is observed as compared to the residual tests, possibly due to the greater difficulty of hot testing or larger variation in specimen specific properties. Figure 2.9 features the averaged slow and rapid profiles, with EN 1992-1-2 (2004) provided as a baseline. Similar to the residual results, the three curves follow a very similar path without significant deviation. Slow heating still results in a slightly greater average strength loss of 28 %, as compared with rapid heating at 23 %. The largest and only notable disparity occurs at 400°C, wherein slow heating results in 20 % higher strength loss as compared to rapid heating. The exact cause of this proportionally high strength increase for the rapidly heated samples can be attributable to the short maximum temperature duration applied to all three evaluated samples.

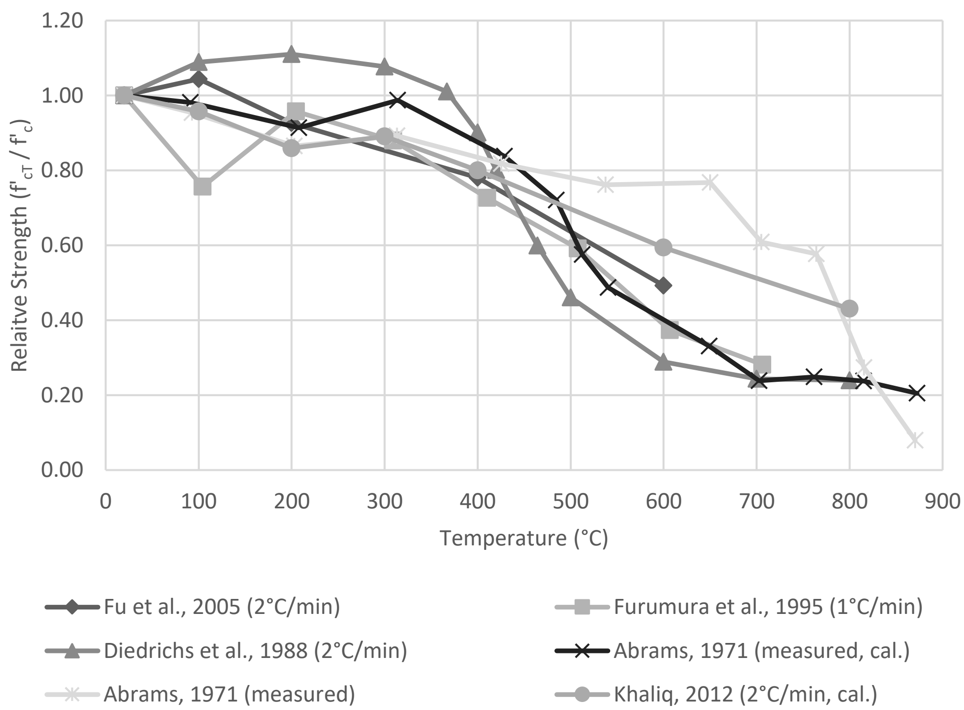

Fig. 2.7: Relative Hot Strength of Concrete after Exposure to Slow Rates of Heating and Natural Cooling

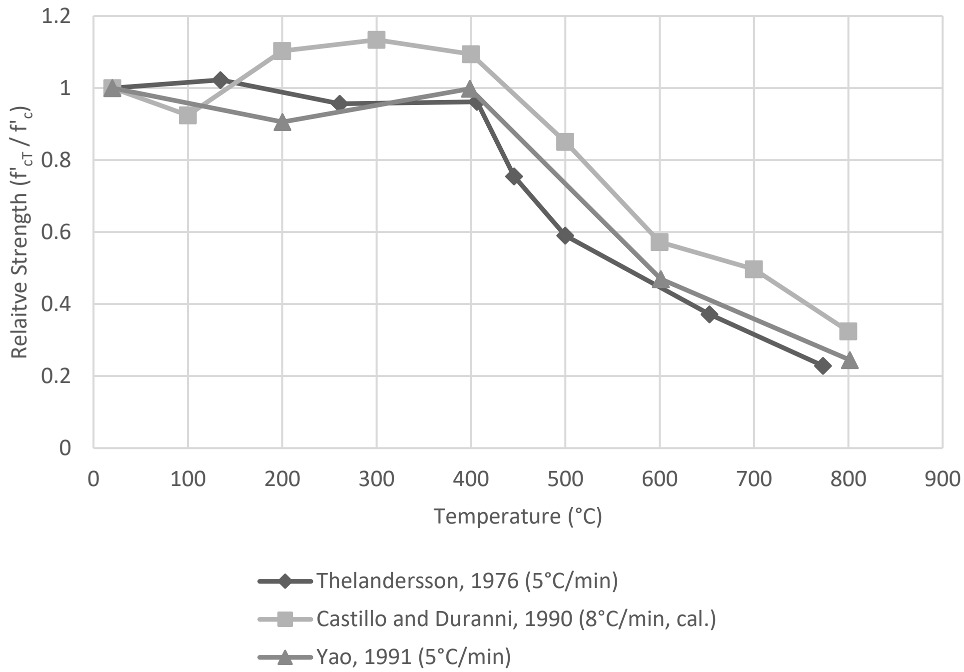

Fig. 2.8: Relative Hot Strength of Concrete after Exposure to Rapid Rates of Heating and Natural Cooling

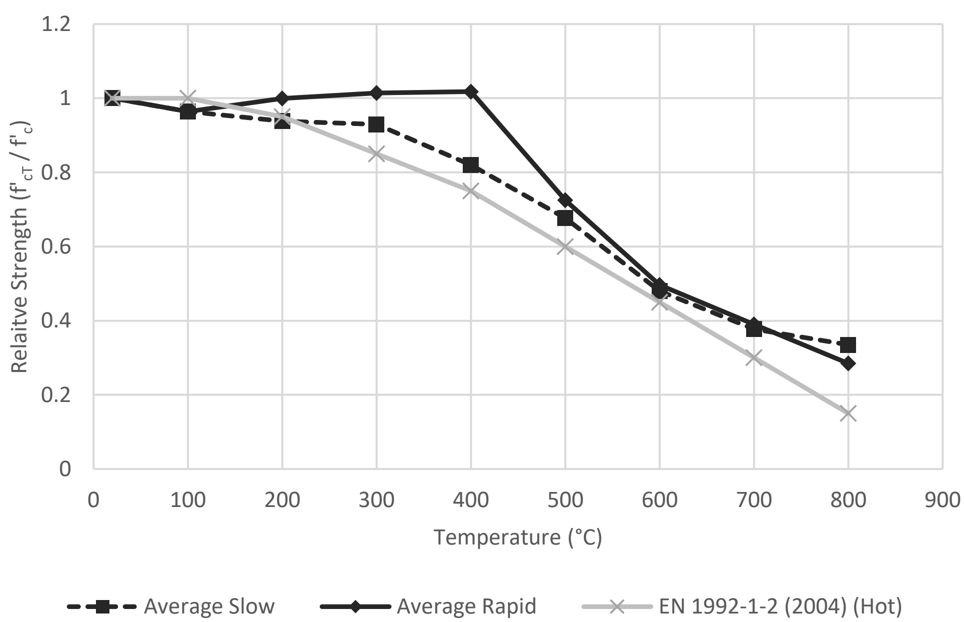

Fig. 2.9: Relative Average Hot Strength of Concrete after Exposure to Slow or Rapid Heating and Natural Cooling

Figures 2.10 and 2.11 display the relative strain ($\varepsilon_{cT/R}$) for hot and residual testing conditions. Under hot conditions, strain increases relatively linearly at all temperatures. A similar trend appears for residual samples up until about 400°C, at which point greater fluctuation emerges. Due to a shortage of applicable strain data, the development of slow and fast averages for both hot and residual was not feasible. Although many experimental studies have been carried out on concrete under varying heating rates, strain and/or stress-strain responses are very rarely reported in full detail. With the limited strain records available, no clear relationship emerges differentiating the effect of heating rate on strain.

Based on the observed literature, it can be concluded that heating rates have a minimal effect on the strength of concrete. On average, slow heated samples had slightly lower strengths than fast heated specimens. But at any given temperature, the effect of heating fluctuated, producing either higher or lower strength between the two heating regimes. A justification for the changing impact of heating rates has been proposed by Mohamidbai (1986). Slow heating rates apply temperatures over a longer duration, generating strength reduction by long term moisture loss. Alternatively, higher heating rates result in large thermal gradients causing strength reduction by micro cracking. These two phenomena result in similar degradation for slow rates as compared to faster rates.

It appears then that the main influence of heating rate is not on the stress-strain response, but on explosive spalling. Explosive spalling is a phenomenon in which exterior portions of a concrete specimen violently spall off during heating, greatly reducing the elements cross-section. The full mechanisms of explosive spalling are still not fully understood; however, heating rate is often cited as a major influencer in the spalling process (Jansson, 2013). Phan and Carino (2003), Castillo and Duranni (1990), and Diederichs et al. (1988) all reported notable explosive spalling in their HSC samples, but not in their NSC. Noumowe et al. (1996) even observed explosive spalling in HSC specimens at a heating rates as low as 1°C/min. It is well documented in the literature that NSC is often unaffected by spalling compared to HSC (Kodur, 2014). However, due to the severity of explosive spalling on RC, further consideration is recommended with regards to heating rate.

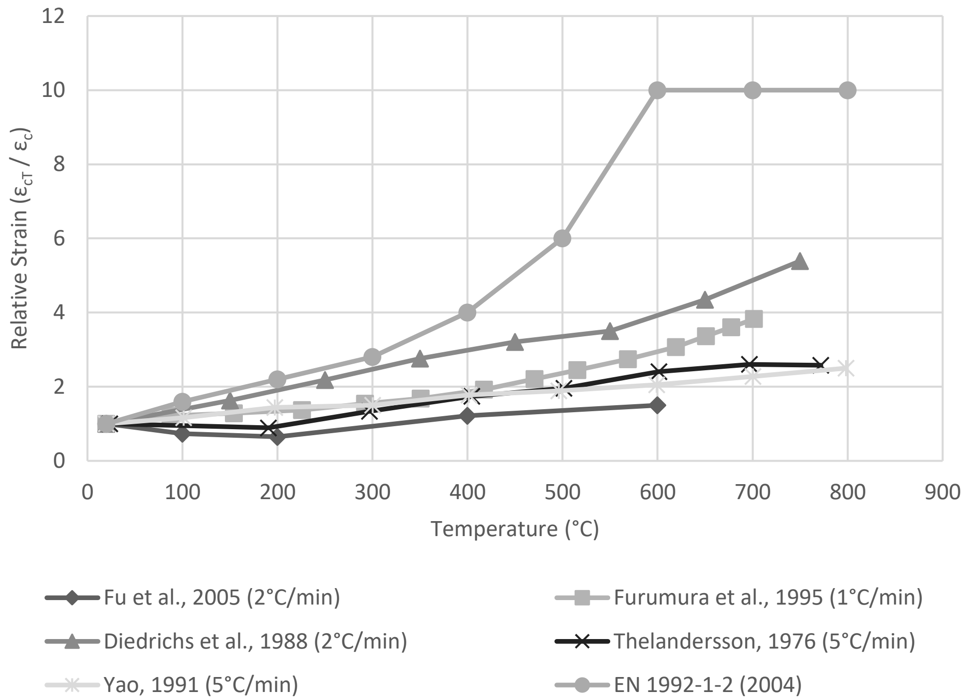

Fig. 2.10: Effect of Heating Rate on Relative Hot Strain of Concrete

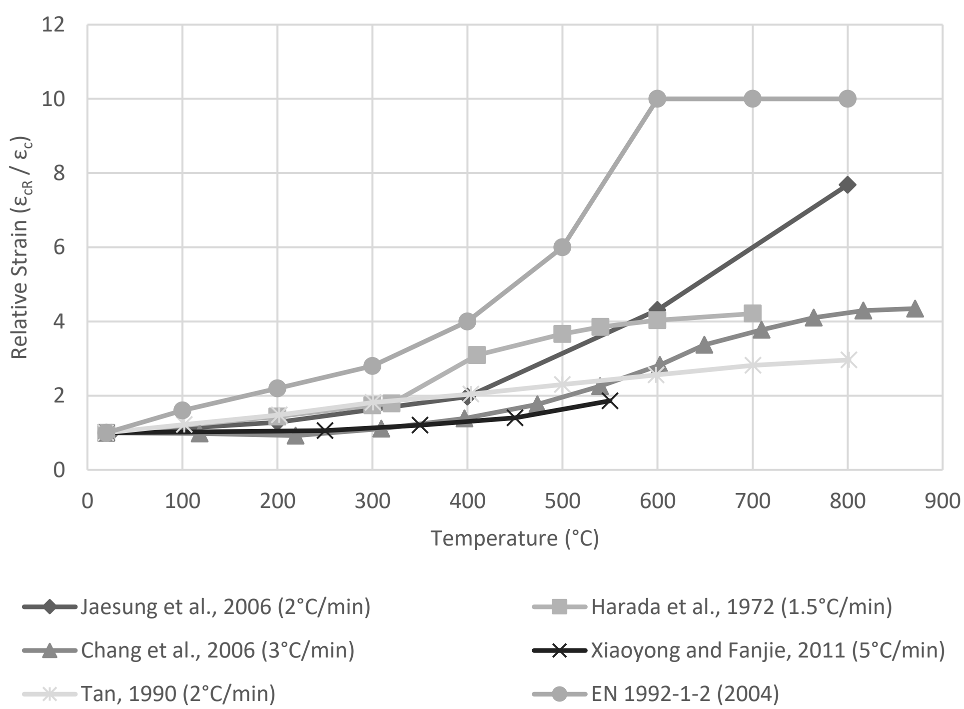

Fig. 2.11: Effect of Heating Rate on Relative Residual Strain of Concrete

2.4.2 Maximum Temperature

The effect of elevated temperatures on concrete is the most well documented of the four variabilities in the literature. General consensus regarding its impact has been covered extensively in the literature (Kodur, 2014). The averaged relative strength and strain based on the experiments evaluated in this chapter are presented in Figures 2.12 and 2.13. Considering relative strength, hot tested specimens observe minor decay in the lower temperature ranges up until 300-400°C. Some experimental work, such as by Diederichs et al. (1988) and Castillo and Duranni (1990), even observe minor strength gains in the 200°C range for hot tested specimens. This strength gain was identified by Castillo and Duranni (1990) to be a result of particle stiffening as moisture evaporates from the concrete. This response only occurs for specific concrete mixes. Residually tested specimens feature relatively linear decay, reaching comparable levels to the hot tested specimens past 400°C. Maximum strength loss of 70 % and 80 % is reached at 800°C for hot and residual specimens, respectively. This reduction illustrates the substantial impact that maximum temperature has on the stress-strain response of concrete.

Strain remains largely unaffected at lower temperatures below 400°C. Beyond this temperature, total strain increases exponentially reaching maximum strains at 700°C of 3.4 times that of the initial strain at ambient temperatures. Hot and residual conditions present comparable strain profiles and values across the entire temperature spectrum. The Eurocode approximation provides a highly conservative profile for strain response at elevated temperature. Shortages in the experimental literature have likely led to this adoption of a highly conservative profile. In contrast, strength reduction is much better represented by the Eurocode, with a reasonable agreement at all temperatures and test conditions.

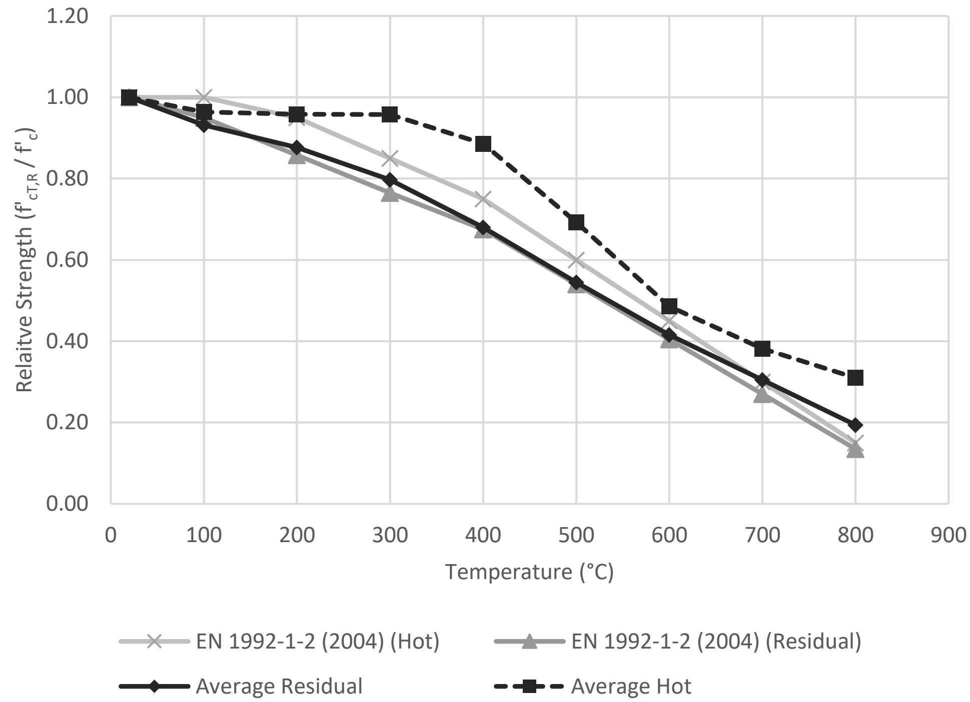

Fig. 2.12: Relative Strength of Concrete for Hot and Residual Conditions

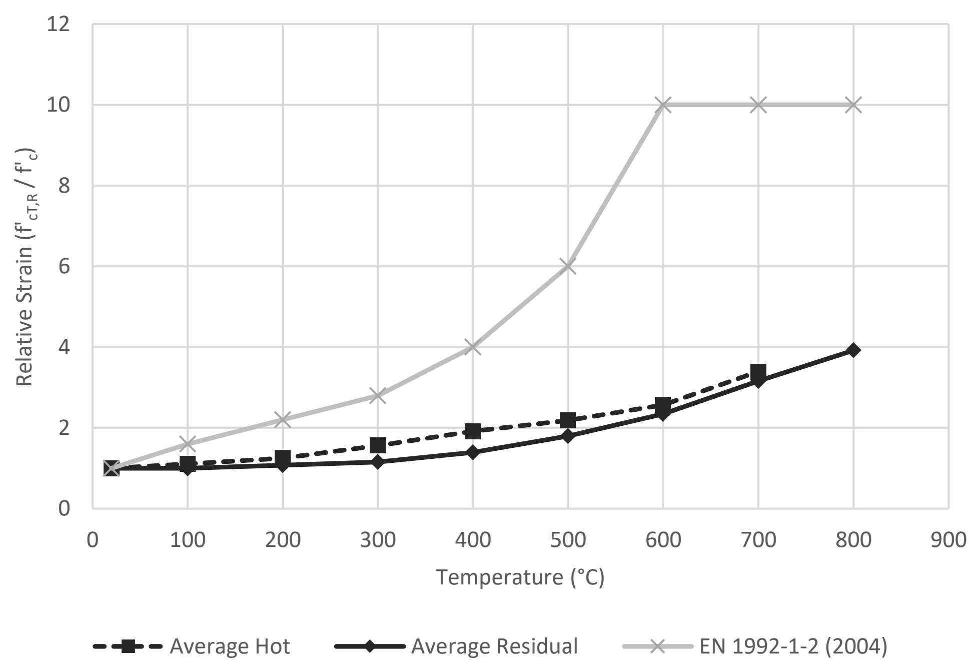

Fig. 2.13: Relative Strain of Concrete under Hot and Residual Conditions

2.4.3 Maximum Temperature Duration

Overall temperature duration is unique, as it influences every stage of natural fire exposure. Depending on the rate of heating and cooling, overall duration varies greatly. Therefore, maximum temperature duration is defined and reported in the experimental data as the period from when the compartment reaches maximum temperature (T_{max}), until compartment cooling begins. In a natural scenario, Harmathy (1993) defines maximum temperature duration as occurring from T_{max} until $0.8T_{max}$ on the cooling branch. In both cases, this duration represents the fully developed period of the fire wherein minimal to no external temperature variation takes place.

Due to a limitation in long term testing data, this section focuses on the work of Carette et al. (1982) and Mohamidbai (1987) with complimentary work interjected. Carette et al. undertook the residual evaluation of concrete after extreme long-term exposure periods. Calcareous samples were placed in a furnace for one and four months to determine the impact of long-term heating on concrete. Figure 2.14 presents these results compared with short-duration heating of one hour by Noumowee et al. (1996) and durations defining uniform internal temperature by Phan (2001).

At the lowest temperature of 75°C, strength reduction is relatively constant across all four duration periods. Phan (2001) noticed the largest reduction, but this is largely due to interpolation of recorded data. With increased temperature to 300°C and 450°C, strength reductions occurred as typically observed for concrete heated in these ranges. At both temperatures, results from Phan’s measured specimens present a similar reduction to the samples heated at the one-month and four-month duration. At 450°C, a strength reduction of 14.8 % is experienced between one hour and uniform, with only a further 0.5 % between uniform and four months. This trend indicates that once a uniform internal temperature is reached, negligible reduction occurs regardless of the duration of exposure beyond that point.

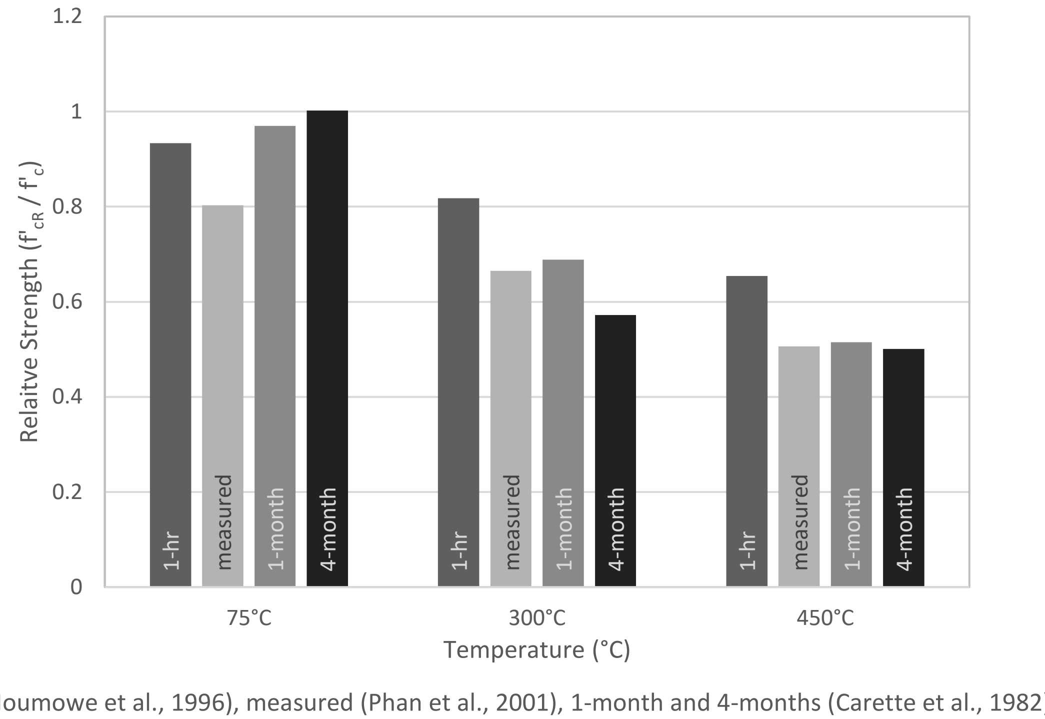

Fig. 2.14: Relative Strength of Concrete over Long Term Exposure Periods

To identify the impact of short duration heating, Mohamidbai (1987) evaluated the residual response of concrete after 1-hr heating increments. Figure 2.15 exhibits the relative strength reduction during the experiments. Results from similar experiments are provided by Savaa et al. (2005) for 2-hr exposure to maximum temperature and Li et al. (2004) for 0-hr duration. Li et al.'s results represent the minimum possible exposure duration, wherein all of the degradation occurs during the heating and cooling periods.

Similar to Figure 2.14, it can be seen that specimens exposed for a shorter duration exhibit higher relative strengths than those exposed for a longer duration. Significant strength loss is noted between the 1-hr and 2-hr exposed specimens. At the higher temperatures approaching 800°C; the 1-hr, 2-hr, and 3-hr exposed samples all begin to exhibit comparable strength loss. As such, it again appears that the majority of strength reduction occurs at a very short duration (within the first hours), with extended exposure only contributing to relatively minor reductions.

The presented experimentation in Figure 2.15 were undertaken on cubed specimens of 100 mm or 150 mm. For standard cylinder specimens, it is typically considered that a uniform internal temperature gradient is reached after 1-hr of exposure (Fu et al., 2005; Diederichs et al., 1988). Considering the smaller size of the cube specimens, it can be concluded that the limited strength reduction after the 1-hr and 2-hr exposure is due to the specimens reaching a uniform internal temperature. Once this temperature gradient becomes uniform, no identifiable strength reduction occurs at prolonged periods. The results also indicate the diminishing influence of duration as maximum temperature increases. At lower temperatures, the discrepancies between instantaneous, 1-hr, and 2-hr durations are significantly more pronounced than at 800°C.

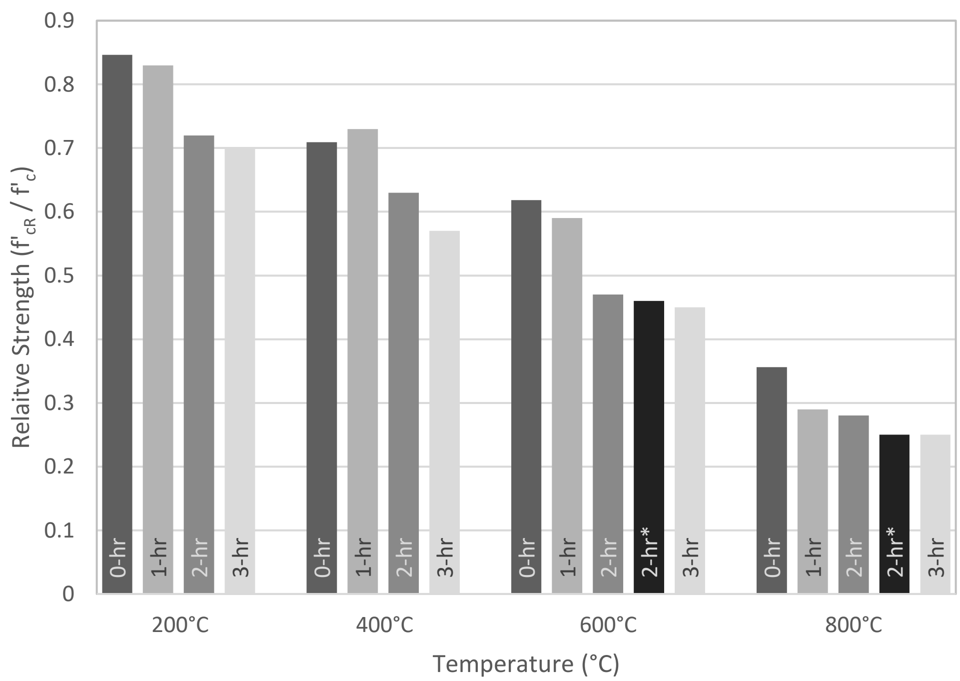

0-duration (Li et al., 2004); 2-hr* (Savaa et al., 2005); 1-hr, 2-hr, and 3-hr (Mohamidbai, 1987)

Fig. 2.15: Relative Ultimate Strength of Concrete over Short Term Exposure Periods

The impact of duration on strain at maximum strength is more difficult to determine. Although experimental work exists in the literature, significant discrepancies between testing conditions make meaningful comparisons impossible. To properly draw conclusions regarding the impact of temperature duration on strain, further testing is required.

2.4.4 Cooling Rate

As previously explored in this chapter, concrete exhibits notably greater strength during hot conditions versus residually after cooling. Considering the effects of a natural environment, variable rates of cooling can be present, ranging from slow cooling in a heated space to rapid cooling from firefighting events. Similar to the degradation caused during heating, thermal gradients also arise during cooling, which depending on the rate, generate greater or lesser internal thermal stresses. Therefore, the impact of cooling is of great importance to the overall stress-strain relationship.

To evaluate the effect of cooling, the experimental testing is divided into three categories: ambient cooling, rapid cooling, and slow cooling. Ambient cooling is defined as removing the specimen from its heated environment and allowing cooling to occur in ambient air (typically 20°C). From the perspective of a realistic fire, this scenario of ambient cooling is far less likely as opposed to rapid or slow cooling within the fire exposed compartment. However, due to experimental standardization, considerable data is reported for this scenario. Ambient cooling is typically identified as resulting in a cooling rate of circa 1°C/min (Morita et al., 1996).

Rapid cooling is achieved in experimental work either by exposing the specimen to water during the cooling stage. Quenching and spraying techniques are typically applied by submerging or spraying the specimen with ambient temperature water for a prolonged duration. In the specific case of 150 mm cubed specimens, Botte and Caspeele (2017) identified that from an elevated temperature of 600°C, quenching is equivalent to a cooling rate of 30-40°C/min. The results of this experiment demonstrate the magnitude of possible cooling rates that can occur during natural fire scenarios.

Slow cooling is defined as allowing the cooling of specimens to occur within the heating environment, typically a furnace or oven. This scenario is particularly likely to occur in a real-world scenario, as the slow cooling of concrete within its compartment is realistic for structural members. Culfik and Ozturan (2010) and Savaa et al (2005) observed that slow cooling resulted in a cooling rate of 0.3°C/min and 0.4°C/min respectively. Although the rate heavily depends on the specific compartment, a rate of less than 0.5°C/min can be generally adopted to define slow cooling.

Figures 2.16, 2.17, and 2.18 display the relative strength versus temperature of specimens exposed to ambient, rapid, and slow cooling. All presented tests feature siliceous aggregate. The overall profile of the experiments under each cooling method were found to be in good agreement with one another. To better compare the three methods, the results from each case were averaged as exhibited in Figure 2.19.

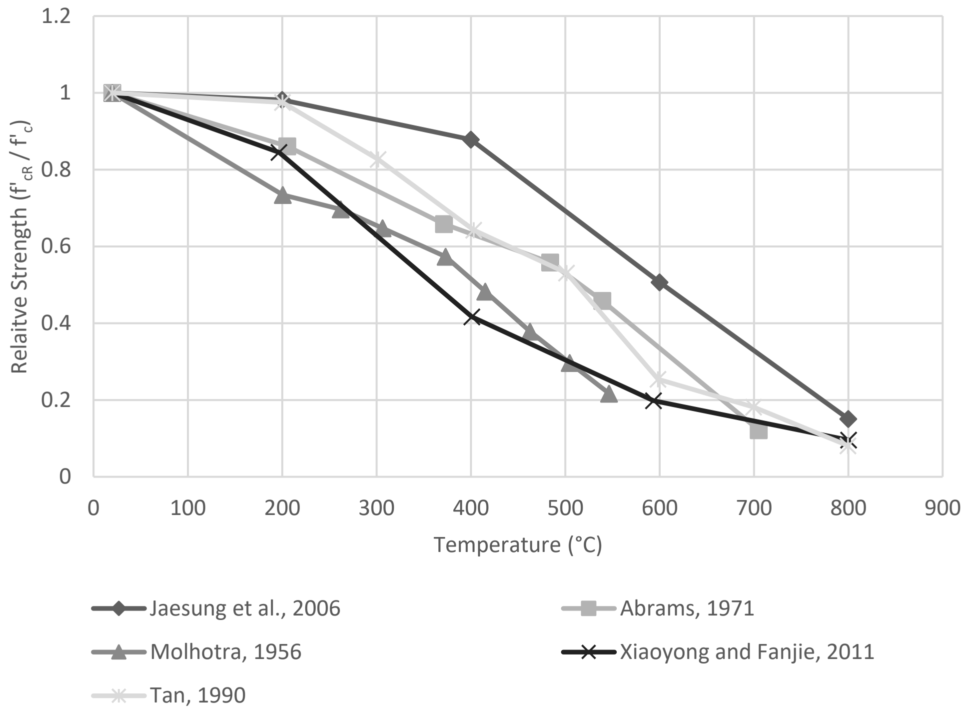

Fig. 2.16: Relative Strength of Concrete under Ambient Cooling

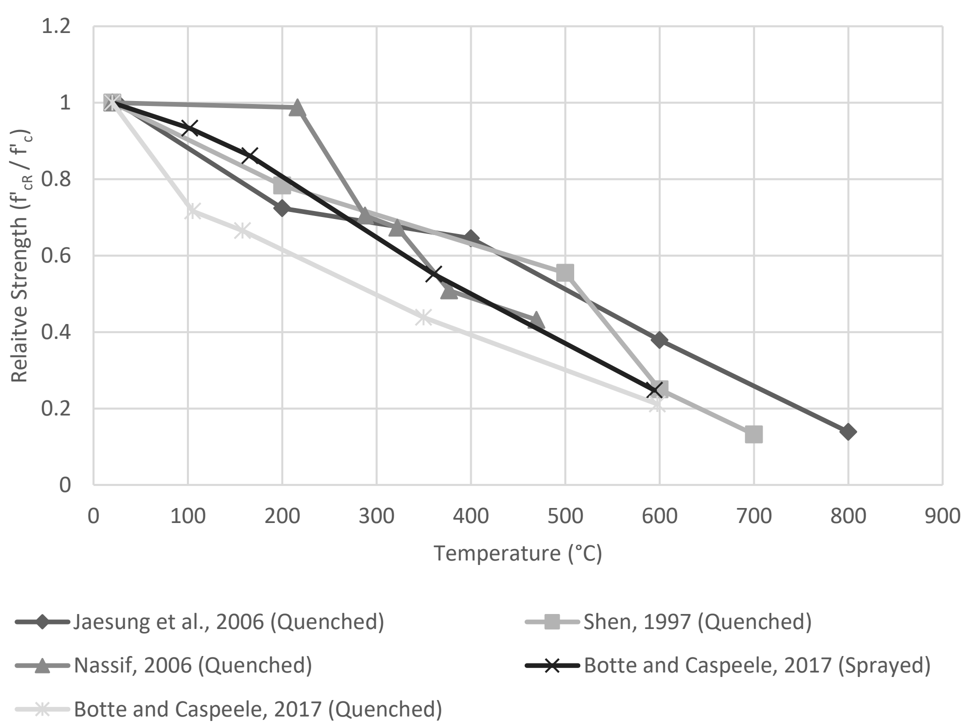

Fig. 2.17: Relative Strength of Concrete under Rapid Cooling

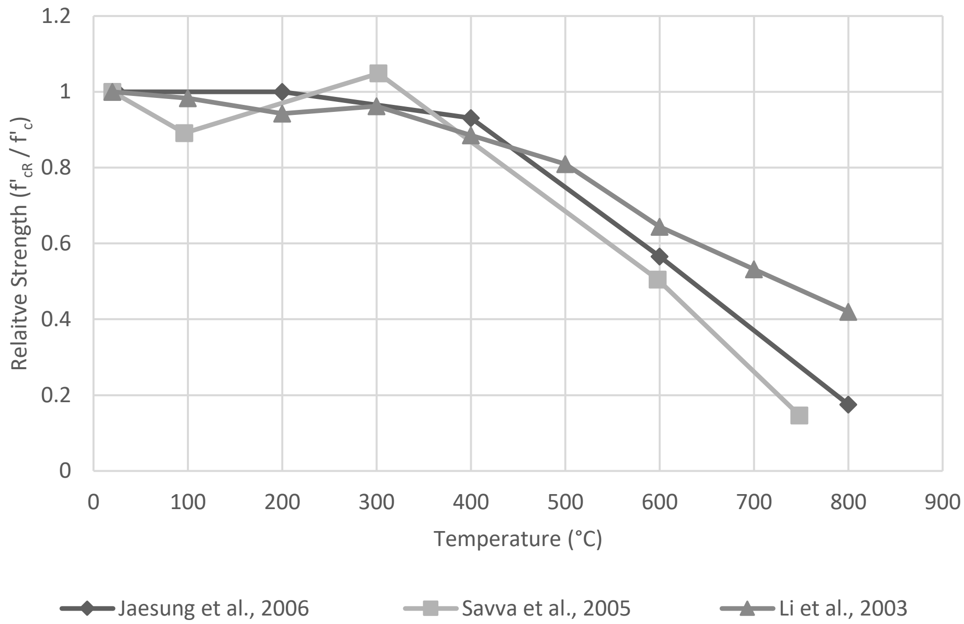

Fig. 2.18: Relative Strength of Concrete under Slow Cooling

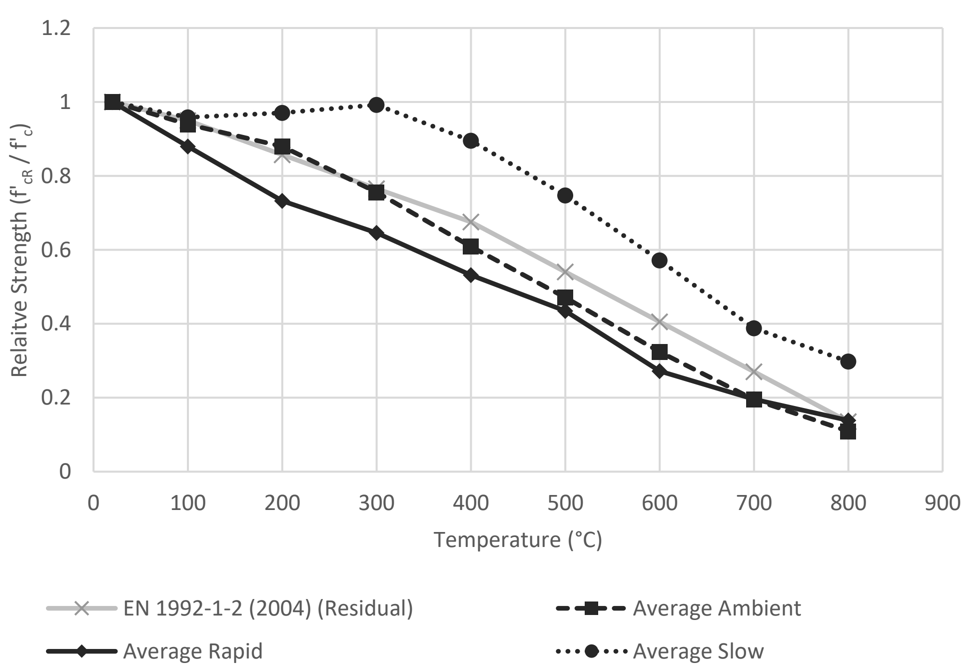

Fig. 2.19: Average Relative Strength of Concrete Considering Three Cooling Regimes

By observation of Figures 2.16 to 2.19, the following conclusions can be made about the influence of cooling rate on the concrete strength:

- Increased cooling rates result in a decline in the strength of the concrete. Between slow to rapid cooling, a further average strength reduction of 25 % is experienced.

- Cooling rate has the greatest effect on strength in the mid-temperature range of 200°C to 400 °C. At 400°C, changing the cooling rate from slow to rapid results in a further strength reduction of 36 %. This trend indicates the importance of considering cooling rates in low to medium temperature fire events.

- The impact of cooling rates on strength reduction diminishes with increasing cooling rate. It can be seen that a large strength reduction occurs from slow to natural (0.5°C/min to 1°C/min), but the further degradation from natural to rapid cooling (1°C/min, and 40°C/min) is much less. At 400 °C, changing the rate from ambient to rapid results in a further strength reduction of 7.6 %. At the same temperature, it was previously identified that slow to rapid resulted in a 36 % further reduction. It can be concluded that the impact of cooling is asymptotic, reaching a steady state with increasing cooling rates.

- All three cooling regimes converge with increasing temperature, reaching a minimum parity at 800°C. This trend is similarly seen with heating rate.

- Slower cooling methods are capable of retaining strength at lower temperatures. Until 300°C slow cooling retained the majority of the concrete's strength, before declining steeply. At the higher cooling rates of ambient and rapid, strength degradation begins at a very low temperature and decreases relatively linearly.

- Eurocode results were found to be in good agreement with the ambient cooling rate. Alternatively, slow cooling was very conservative approximated and rapid cooling was unconservative approximated; particularly in the mid-temperature range.

In addition to the aggregated figures, a number of unique conclusions about the effect of cooling on strength arise in specific papers. Botte and Caspeele (2017) investigated the influence of cooling regimes on the long-term residual stresses. Testing was conducted 56 days after heating had occurred to capture the full effect of strength reduction with time. An interesting discrepancy arose wherein specimens cooled by quenching, demonstrated a minor strength gain over comparably sprayed or ambiently cooled specimens. The authors proposed that the quenching process may have rehydrated cement particles resulting in the strength gain over long durations.

Abramowicz and Kowalski (2010) explored the concept of short duration water cooling on concrete. Their tests involved the quenching of samples for a ten second duration, followed by natural cooling. It was found that the short time immersion produced no significant effect on the specimens strength, producing very similar results to that of their baseline ambient cooling tests. These results validate the concept of using an average cooling rate for design purposes; because although cooling has significant effects, near instantaneous rapid cooling does not. It should be noted that what constitutes as short duration is entirely dependent on the geometry and properties of the concrete being exposed.

Bingöl and Gül (2008) and Cülfik and Özturan (2010) demonstrated the effect of cooling regimes on NSC with calcareous aggregate. Although a shortage of experimental data on calcareous specimens makes a larger comparison impossible, the findings of these two publications matched the trends of the siliceous aggregate discussed earlier in this Section. Ambient cooling to quenched cooling resulted in reduced strength with greatest influence in the 350°C range and converging at higher temperatures. Strain increased with faster cooling rates and maximum temperature.

Figure 2.20 displays strain at maximum compressive strength under various cooling rates, but only up until 500°C due to the limitation of available data. To see the full temperature range, Figure 2.21 exhibits results from only Jaesung et al. (2008) up to 800°C for all three cooling methods. From the comparison, it is observed that strain increases with increased rates of cooling. Below 400°C, the disparity between rates is fairly minimal. Beyond that point however, Jaesung et al. (2006) found that strain increases and diverges rapidly across all of the cooling regimes. Unlike strength, strain does not converge at high temperatures. Jaesung et al. (2006) recorded a maximum differential at 800°C of 47 % between slow and rapid cooling.

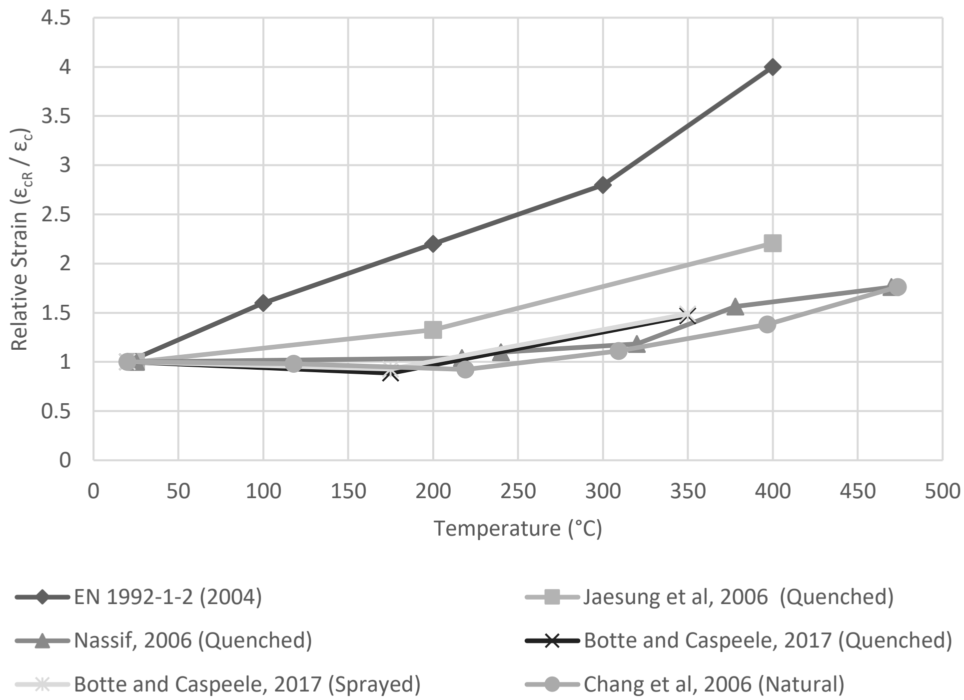

Fig. 2.20: Relative Strain of Concrete Experienced at Ultimate Strength under varied Cooling Regimes

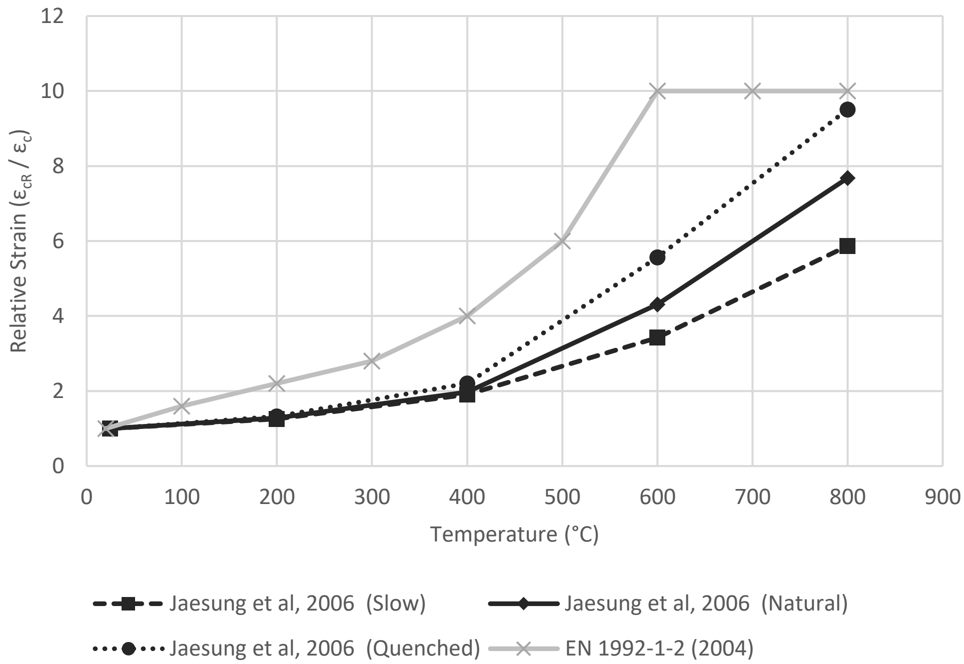

Fig. 2.21: Relative Strain of Concrete Experienced at Ultimate Strength by Jaesung et al. (2006)

2.5 Discussion

To compare the influence of each of the four natural fire variabilities, the recorded experimental data has been aggregated over the entire temperature spectrum. The relative strength findings are summarized in Figures 2.22 and 2.23 for residual and hot conditions. The profiles on the graphs represent the possible degradation of each fire variability when increased from a datum state as defined:

- Heating Rate — rapid (> 2°C/min) to slow (≤ 2°C/min)
- Maximum Temperature — ambient (20°C) to an elevated temperature
- Exposure Duration — 0-hr exposure to 3-hr exposure
- Cooling Rate — slow (≤ 1°C/min) to rapid (quenching)

The values for heating rate were taken from Figures 2.6 and 2.9; values for maximum temperature from Figure 2.12; values for exposure duration from Figure 2.15; and values for cooling rate from Figure 2.19. Due to a lack of data for exposure duration during the hot condition, the residual profile has been applied for the hot condition Figure 2.23. Although not accurate to the true response, it is likely conservative and provides a baseline for further analysis. Due to the scarcity of strain data, particularly for duration and heating rates, generation of similar profiles is not reasonably possible for strain response.

Figure 2.22 and 2.23 present a clear indication as to which fire variability has the greatest effect on concrete strength at each temperature range. In the low temperatures below 100°C, minimal degradation occurs with all four variabilities contributing relatively equally to strength loss. In the mid-range of 200°C to 500°C, cooling rate appears to be the most significant factor affecting degradation. Exposure duration also reaches its maximum influence during this range, with comparable effects to that of maximum temperature. Reaching temperatures in excess of 600°C, the effects of the maximum temperature dominate the response of the concrete. By 800°C, the influence of maximum temperature far out ways the effects of any of the other three variabilities.

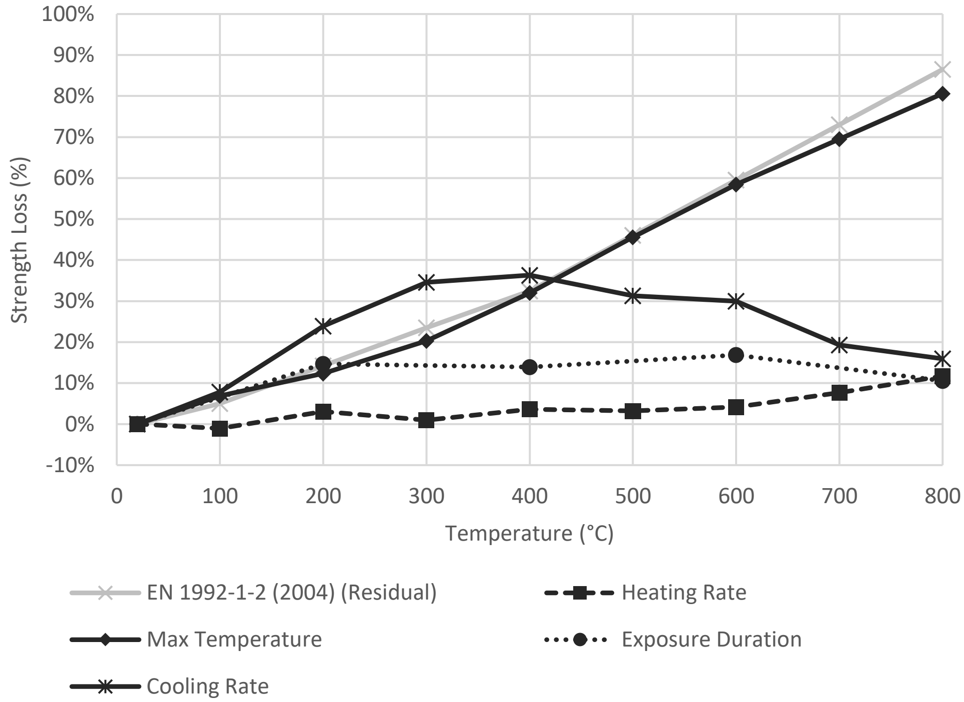

Fig. 2.22: Residual Condition Strength Loss of Concrete Under Various Influences from Specified Datum

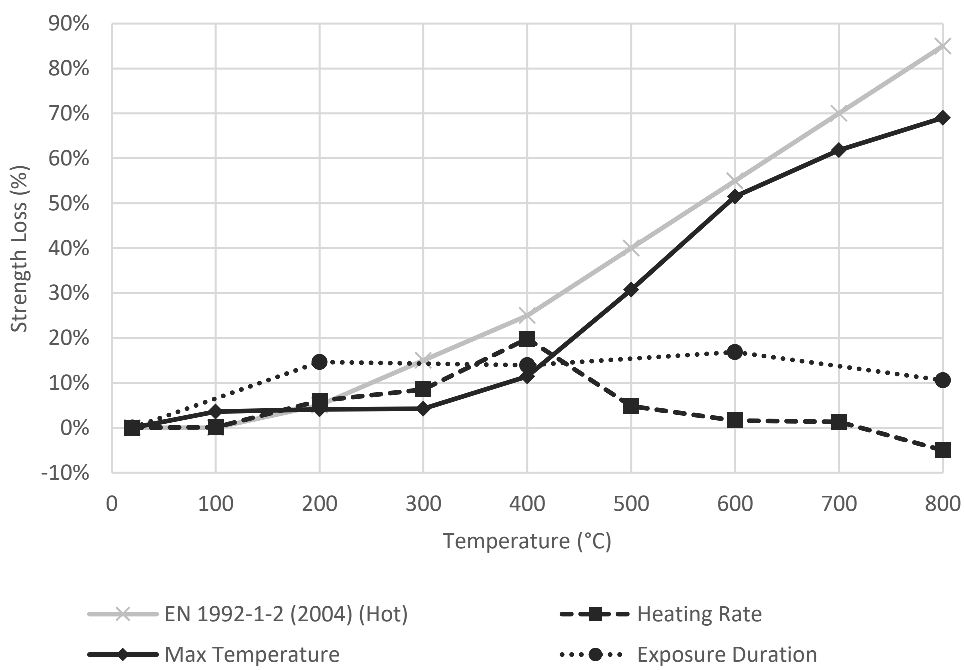

Fig. 2.23: Hot Condition Strength Loss of Concrete Under Various Influences from Specified Datum

2.6 Conclusion

Based on the reviewed literature, the following conclusions can be made regarding the impact of each variability on concretes stress-strain response:

1. Heating rates have a minimal impact on the strength of concrete. Slow heating (≤ 2°C/min) did present marginally higher average strength losses than rapid heating, but the findings were so close as to preclude any conclusive statements to this effect. As for the effect on strain, no clear trend emerges. Sometimes samples with faster rates result in slightly greater strains, and sometimes the reverse.

2. Maximum temperature causes the most significant impact to concrete. Major degradation begins at temperatures in excess of 300°C, with only minor losses present before this temperature. Residual tests displayed greater strength reduction compared with hot testing, featuring a further average strength reduction of 14 %. At the highest evaluated temperature of 800°C, the literature averages 70 % and 81 % strength loss for hot and residual specimens, respectively. Strain observed similar responses, incurring minor changes at temperatures less than 400°C, but increasing rapidly at higher temperature. By 800°C, strains reached on average 3.5 times that of the initial strain at ambient temperature. The difference between residual and hot testing had minimal impact on strains. However, at higher temperatures, residual did display slightly greater strains over hot specimens, but not significantly so. These findings are in line with many other publications on the effects of maximum temperature of concrete.

3. Maximum temperature duration is important in the early stages of fire events, particularly the first hours of exposure. Beyond this time, once the internal temperature gradient becomes uniform, negligible further degradation occurs regardless of extended exposure. Depending on the intensity of fire exposure and specimen dimensions, time to reach uniform temperature will vary greatly. Insufficient data is available to give any indication as to the impact of duration on strain.

4. Cooling rate was found to have a considerable effect on concrete strength between slow (< 1°C/min) to ambient cooling (≥ 1°C/min). The difference between ambient to rapid cooling was also noticeable at lower temperatures, but became negligible in excess of 400°C. This trend indicates that the impact of cooling decreases with increasing cooling rates, especially at higher temperatures. At 800 °C, all three cooling regimes converge to less than 15 % difference. Based on the limited data available, strain appears to increase with greater cooling rates and greater applied temperatures. However, more data regarding the influence on strain is preferred for a more conclusive result.

5. To expand the experimental work regarding the influence of natural fires on concrete's stress-strain relationship, additional experimental work needs to be completed, specifically addressing: mix proportions, water content, aggregate size, curing age, additives, and aggregate to cement ratio. Particular focus should be taken to account for strain results, specifically under variable exposure durations and cooling rates.

2.7 References

Abramowicz, M. and R. Kowalski. “The Influence of Short Time Water Cooling on the Mechanical Properties of Concrete Heated up to High Temperatures.” *Journal of Civil Engineering and Management*, vol. 6, no. 2, 2010, pp. 85-90.

Abrams, M.S. “Compressive Strength of Concrete at Temperatures to 1600F.” *ACI Special Publication*, SP. 25-2, 1971, pp. 33-58.

Anderberg, Y. and S. Thelandersson. *Stress and Deformation Characteristics of Concrete at High Temperatures: 2-Experimental Investigation and Material Behavior Model*. Bulletin 34 - Division of Structural Mechanics and Concrete Construction. Lund Institute of Technology, Lund, Sweden, 1976.

ASCE 7-16. *Minimum Design Loads and Associated Criteria for Building and Other Structures*. American Society of Civil Engineers. Reston, VA, USA. 2016.

ASTM E-119. *Standard Test Methods for Fire Tests of Building Construction and Materials*. American Society for Testing and Materials. West Conshohocken, PA, USA. 2018.

Bingöl, A.F. and R. Gül. “Effect of Elevated Temperatures and Cooling Regimes on Normal Strength Concrete.” *Fire and Materials*, vol. 33, no. 2, 2008, pp.79-88.

Botte, W. and R Caspeele. “Post Cooling Properties of Concrete Exposed to Fire.” *Fire Safety Journal*, vol. 92, no. 1, 2017, pp. 142-150.

Carette, G.G., K.E. Painter, and V.M. Malhotra. “Sustained High Temperature Effects on Concrete Made with Normal Portland Cement, Normal Portland Cement and Slag, or Normal Portland Cement and Fly Ash.” *Concrete International*, vol. 4, no. 4, 1982, pp. 41-51.

Castillo, C. and A.J. Durrani. “Effect of Transient High Temperature on High-Strength Concrete.” *ACI Materials Journal*, vol. 87, no. 1, 1990, pp. 47-53.

Chang, Y.F., Y.H. Chen, M.S. Sheu, G.C. Yao. “Residual Stress-Strain Relationship for Concrete after Exposure to High Temperatures.” *Cement and Concrete Research*, vol. 36, no. 10, 2006, pp. 1999-2005.

Cooper, L.Y. and K.D. Steckler. *Methodology for Developing and Implimenting Alternative Temperature-Time Curves for Testing the Fire Resistance of Barriers for Nuclear Power Plant Applications*. NUREG-1547, NISTIR 5842, Building and fire Research Laboratory. Gaithersburg, MD, USA, 1996.

Cülfik, M.S. and T. Özturan. “Mechanical Properties of Normal and High Strength Concretes Subjected to High Temperatures and Using Image Analysis to Detect Bond Deteriorations.” *Construction and Building Materials*, vol. 24, no. 8, 2010, pp. 1486-1493.

Diederichs, U., U. Jumppanen, and V. Penttala. “Material Properties of High Strength Concrete at elevated Temperatures.” *13th Congress of International Association for Bridge and Structural Engineering*, Helsinki, Finland, 1988. Published by ResearchGate, 2015.

EN 1991-1-2. *Eurocode 1: Actions on Structures - Part 1-2: Actions on structures Exposed to Fire*. European Committee for Standardization. Brussels, Belgium. 2002.

EN 1992-1-2. *Eurocode 2: Design of Concrete Structures - Part 1-2: General Rules – Structural fire Design*. European Committee for Standardization. Brussels, Belgium. 2004.

Fu, Y.F., Y.L. Wong, C.S. Poon, and C.A. Tang. “Stress-Strain Behaviour of High Strength Concrete at Elevated Temperatures.” *Magazine of Concrete Research*, vol. 57, no. 9, 2005, pp.535-544.

Furumura, F., T. Abe, and Y. Shinohara. “Mechanical Properties of High Strength Concrete at High Temperatures.” Translation Reported by L.T. Phan. *Fire Performance of High-Strength Concrete: A Report of the State-of-the-Art*. NISTIR 5934, Building and Fire Research Laboratory. Gaithersburg, MD, USA, 1996.

Harada, T., J. Takeda, S. Yamane, and F. Furumura. "Strength, Elasticity, and Thermal Properties of Concrete Subject to Elevated Temperatures." *ACI Special Publication*: *Concrete for Nuclear Reactors*, SP. 34-21, 1972, pp. 377-406

Harmathy, T.Z. *Fire Safety Design and Concrete*. Longman Scientific and Technical, 1993.

Implementation of Eurocodes. *Handbook 5 - Design of Buildings for the Fire Situation*. Leonardo Da Vinci Joint Research Project, 2005.

ISO 834. *Fire Resistance Tests – Elements of Building Construction*. International Organization for Standards. Geneva, Switzerland. 2014.

Jaesung, L. *Experimental Studies and Theoretical Modelling of Concrete Subjected to High Temperatures*. Diss. University of Colorado, 2006.

Jansson, R. *Fire Spalling of Concrete*. Diss. KTH Royal Institute of Technology, 2013.

Khaliq, W. *Performance Characterization of High Performance Concretes Under Fire Conditions*. Diss. Michigan State University, 2012.

Kodur, V. "Properties of Concrete at elevated Temperatures." *ISRN Civil Engineering*, vol. 2014, no. 468510, 2014, pp. 1-15.

Li, M., C.X. Qian, and W. Sun. "Mechanical Properties of High-Strength Concrete After Fire." *Cement and Concrete Research*, vol 34, no. 6, 2004, pp. 1001-1005.

Malhotra, H.L. "The Effect of Temperature on Compressive Strength of Concrete." *Magazine of Concrete Research*, vol. 8, no. 23, 1956, pp. 85-94.

Mohamedbhai, G.T.G. "Effect of Exposure Time and Rates of Heating and Cooling on Residual Strength of Heated Concrete." *Magazine of Concrete Research*, vol. 38, no. 136, 1986, pp. 151-158.

Morita, T., H. Saito, and H. Kumagai. "Residual Mechanical Properties of High Strength Members Exposed to High Temperature." Translation Reported by L.T. Phan. *Fire*

Performance of High-Strength Concrete: A Report of the State-of-the-Art. NISTIR 5934, Building and Fire Research Laboratory. Gaithersburg, MD, USA, 1996.

Nassif, A. "Postfire Full Stress-Strain Response of Fire Damaged Concrete." *Fire and Materials*, vol. 30, no. 5, 2005, pp. 323-332.

Naus, D.J. *The Effect of elevated Temperatures on Concrete Material and Structures – A Literature Review*. NRC FIN No. Y6741, US Nuclear Regulatory Commission. Oak Ridge, TN, USA, 2005.

Netinger, I., I. Kesegic, I. Guljas. "The Effect of High Temperatures on the Mechanical Properties of Concrete made with Different Types of Aggregates." *Fire Safety Journal*, vol. 46, no. 7, 2011, pp. 425-430.

Noumowe, A.N., P. Clastres, G. Debicki, J.-L. Costaz. "Transient Heating Effect on High Strength Concrete." *Nuclear Engineering and Design*, vol. 166, no. 1, 1996, pp. 99-108.

Phan, L.T. and N.J. Carino. "Code Provisions for High Strength Concrete Strength-Temperature Relationship at Elevated Temperatures." *Materials and Structures*, vol. 36, no. 2, 2003, pp. 91-98.

Phan, L.T. *Mechanical Properties of High-Strength Concrete at Elevated Temperatures*. NISTIR 6726, Building and Fire Research Laboratory. Gaithersburg, MD, USA, 2001.

Purkiss, J.A. *Fire Safety Engineering, Design of Structures*. Elsevier Ltd, 2007.

Savva, A, P. Manita, and K.K. Sideris. "Influence of Elevated Temperatures on the Mechanical Properties of Blended Cement Concretes Prepared with Limestone and Siliceous Aggregates." *Cement and Concrete Composites*, vol. 27, no. 2, 2005, pp. 239-248.

Shen, R., L.Y. Feng, and K. Rong. "Assessment of Mechanical Properties of Steel Bars After High Temperature." Translated by J. Xiao and G. König. "Study on Concrete at High Temperature in China – an Overview." *Fire Safety Journal*, vol. 39, no. 1, 2004, pp. 89-103.

Tan, W. “A Research on Reinforced Concrete Beams Subjected to High Temperature and Expert Systems.” Translated by J. Xiao and G. König. “Study on Concrete at High Temperature in China – an Overview.” *Fire Safety Journal*, vol. 39, no. 1, 2004, pp. 89-103.

Xiaoyong, L. and B. Fanjie. “Residual Strength for Concrete after Exposure to High Temperatures.” *Innovative Computing and Information International Conference*, Wuhan, China, 2011. Published by Springer, 2011, pp. 382-390.

Yao, Y.X. “Research on Fire Response of Reinforced Concrete Frames and Determination of Temperature Reached During a Fire.” Translated by J. Xiao and G. König. “Study on Concrete at High Temperature in China – an Overview.” *Fire Safety Journal*, vol. 39, no. 1, 2004, pp. 89-103.

Youssef, M.A. and M. Moftah. “General Stress-Strain Relationship for Concrete at Elevated Temperature.” *Engineering Structures*, vol. 29, no. 10, 2007, pp. 2618-2634.

Zhang, B., N. Bicanic, C.J. Pearce, and G. Balabanic. “Residual Fracture Properties of Normal and High Strength Concrete Subject to Elevated Temperatures.” *Magazine of Concrete Research*, vol. 52, no. 2, 2000, pp. 123-136.

Zhang, B., N. Bicanic, C.J. Pearce, G. Balabanic, and J.A. Purkiss. “Discussion on: Residual Fracture Properties of Normal and High Strength Concrete Subject to Elevated Temperature.” *Magazine of Concrete Research*, vol. 53, no. 3, 2001 pp. 221-224.

Chapter 3

3.0 Equivalent Standard Fire Duration to Evaluate Internal Temperatures in Natural Fire Exposed RC Beams

In the pursuit of undertaking performance-based fire design, accurately determining the severity of a fire event is an essential step. Historically, fire severity has been represented by standard temperature-time curves, as outlined in ASTM E119 (2018) and ISO 834 (2014). These curves form the basis of the existing prescriptive fire design methods. However, because standard fire curves fail to consider compartment specific parameters, they have no relationship with natural fire events, and thus, are not suitable for performance-based design. To model natural fires, several temperature-time curve alternatives, varying greatly in complexity and implementation, have been proposed in the literature (Cooper and Steckler, 1996). As a means of industry standardization, the fire severity generated by a natural fire needs to be related back to standard fires using time equivalency. The major benefit of defining time equivalents (t_e), is that existing data, testing, and computer programs utilizing standard fire curves, can be directly related to natural events for conducting structural fire design (Buchanan, 2001). Available methods to calculate the t_e duration have extensively focused on protected steel members, which deviate greatly from reinforced concrete (RC) sections because of their unique fire-related properties and expected internal thermal gradients. This chapter demonstrates the importance of internal thermal gradients in RC members, summarizes the existing time equivalent approaches, and proposes a new method to determine the t_e for rectangular RC beams while accounting for section dimensions.

3.1 RC Thermal Gradient

When exposed to fire, RC cross-sections develop large thermal gradients, as the temperature level slowly transfers from the surface to the inner core. To undertake performance-based design, the two-dimensional thermal gradients within an RC cross-section can be simplified to a one-dimensional average internal temperature profile

(AITP) (El-Fitiany and Youssef, 2009). The AITP describes the temperature as a function of the section depth, allowing for analysis of beams experiencing uniaxial bending. Figure 3.1 provides a qualitative representation of the AITP for an RC beam exposed to fire on three sides. The concrete section is first divided into a two-way mesh to conduct heat transfer analysis (Figure 3.1a). Throughout the entire fire exposure period, the maximum temperature experienced at each location in the mesh is recorded. The meshed units are subsequently grouped into horizontal layers (Figure 3.1b), and the average temperature for each layer is calculated. The AITP, shown in Figure 3.1c, represents the maximum temperature experienced by each layer throughout the fire event. For standard fires, because the temperature monotonically increases, the maximum temperature for each layer occurs at the end of the fire duration. For natural fires, thermal inertia at the beginning of the cooling phase results in a temperature lag, where some interior layers will reach their maximum temperature shortly after the fire begins to decay (Purkiss, 2007). As a result, the AITP does not represent a particular instance, but rather represents the most severe influence of the fire on the section. Suitability of AITPs in representing section temperature gradients for performance-based design has been proven by El-Fitiany and Youssef (2017), Alhadid (2017), Youssef et al. (2015), El-Fitiany and Youssef (2014), and El-Fitiany and Youssef (2009). The importance of evaluating internal thermal gradients during the performance-based design of RC members exposed to fire is highlighted by Wang et al. (2013) and Guo and Shi (2011).

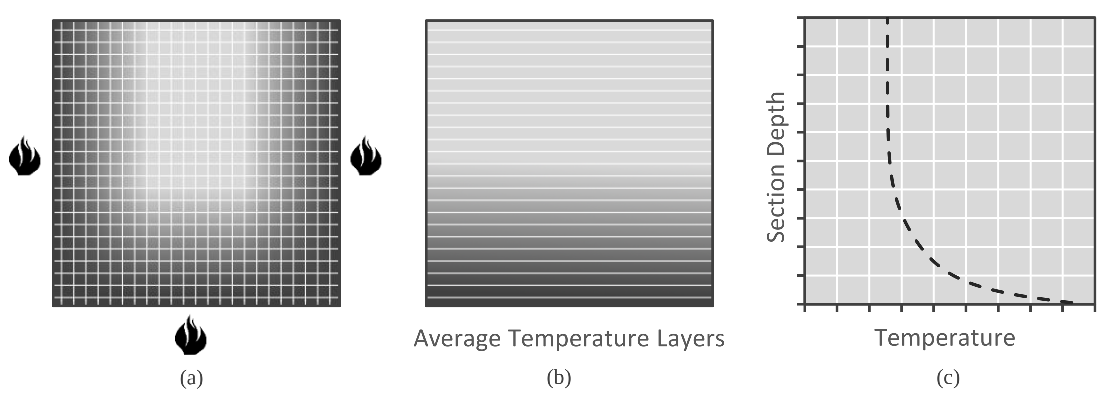

Fig. 3.1 Heat Transfer Modelling: (a) Heat Transfer Mesh, (b) Average Temperature Layers, and (c) AITP

3.2 Existing time equivalent Methods

Beginning in the early 1900's, time equivalent methods representing fire severity have been presented in the literature. Eurocode broadly divides these methods into two categories: thermal and mechanical (EN 1993-1-2, 2005). Thermal methods are based on the temperature or thermal energy experienced by an element exposed to fire, while mechanical methods are based on structural behavior. A brief summary of three thermal and two mechanical methods is provided below. Details about their implementation with worked examples are given by Wade et al. (2014).

3.2.1 Equal Area Method (Thermal)

Equal area method was the first widely recognized time equivalent theory, developed by Ingberg (1928). The t_e is identified when the area under the standard fire curve is equal to the area under a chosen design fire curve, as shown in Figure 3.2a. Although simple in implementation, by comparing the area under the curve, the relationship is not accurately accounting for the energy of the fire as it ignores the heating rate, maximum temperature, and cooling rate. Therefore, short hot fires and long cold fires, which have the same area, could be represented by the same t_e, despite having highly different heat distribution profiles (Thomas et al., 1997).

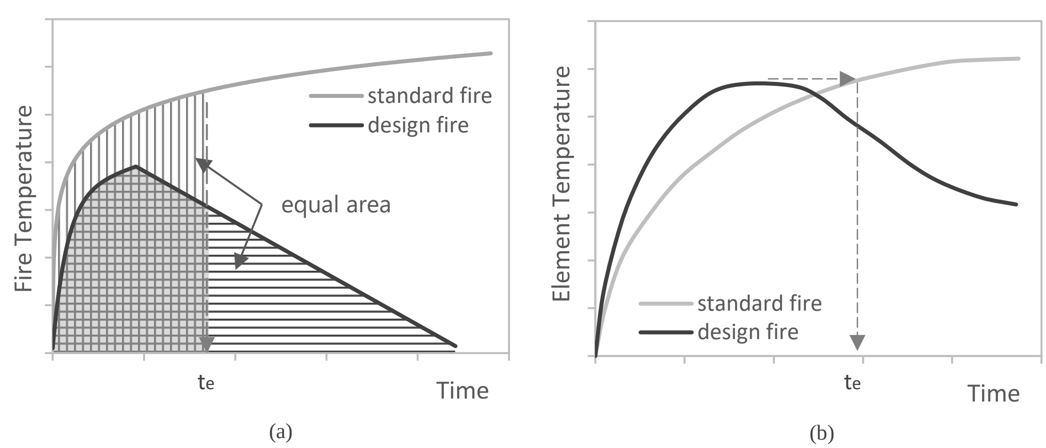

Fig. 3.2 Thermal Equivalent Time Methods: (a) Equal Area Method and (b) Maximum Temperature Method

3.2.2 Maximum Temperature Method (Thermal)

Maximum temperature method was most notably developed by Law (1971), Pettersson (1975) and Schneider et al. (1990). The t_e is defined as the exposure duration to the standard fire required to generate the same maximum temperature within an element as produced by the design fire (Figure 3.2b). The methods developed by Pettersson (1975) and Schneider et al. (1990) have subsequently been implemented in the design standards CIB (1986) and EN 1991-1-2 (2002) (Buchanan, 2001). Maximum temperature methods account for fuel load, compartment area, and ventilation; thus, providing far greater correlation to natural events than the equal area method. It is generally accepted that the Eurocode method is applicable for steel and concrete elements (Buchanan, 2001). However, Thomas et al. (1997) and Xie et al. (2017) found the Eurocode approach to consistently produce unreliable results for concrete members. Purkiss (2007) stated that the maximum temperature approach is only valid for sections that can be characterized by a single uniform temperature, which clearly excludes concrete cross-sections given the significant temperature gradients within them.

3.2.3 Energy Method (Thermal)

Energy methods are explored by Harmathy and Mehaffey (1987), Harada et al. (2000), Nyman (2002), and Kodur et al. (2010). The t_e occurs when accumulated thermal energy from the standard fire matches that from a selected design fire. Harmathy and Mehaffey (1987) estimated thermal energy based on normalized heat loads, Harada et al. (2000) considered the properties of compartment boundaries, Nyman (2002) used the thermal energy of a fire itself, and Kodur et al. (2010) focused on the cumulative energy transferred to an RC beam. Energy methods do not typically account for the specific energy input needed to develop the internal thermal gradients of RC sections. The only exception is Kodur et al.'s (2010) energy method, as it is based on a fire's ability to transfer energy specifically to an RC beam. It thus, results in a t_e which produces a close representation of the internal temperature gradients resulting from the design fire.

3.2.4 Load Capacity Concept (Mechanical)

The load capacity concept focuses on the mechanical response of an isolated fire exposed element (Xie, 2017). In this case, the t_e is the standard fire duration at which the capacity of an element matches its lowest capacity during exposure to a selected design fire (Figure 3.3a). This concept provides a high level of accuracy in representing the severity of a fire on load capacity. However, it requires significant experimental and/or computational effort for each specific section as capacity is greatly influenced by the cross-section details. It also prioritizes a single mode of failure as the basis for equivalency, leaving potentially large deviations in other load responses, deflections, and interactions at the system level. A general method to calculate the t_e based on load capacity was not found in the literature. The concept however has been used by Thomas et al. (1997) and Xie et al. (2017) to demonstrate that the Eurocode t_e (EN 1991-1-2, 2002) is unconservative for RC elements when assessing the load capacity as the primary response.

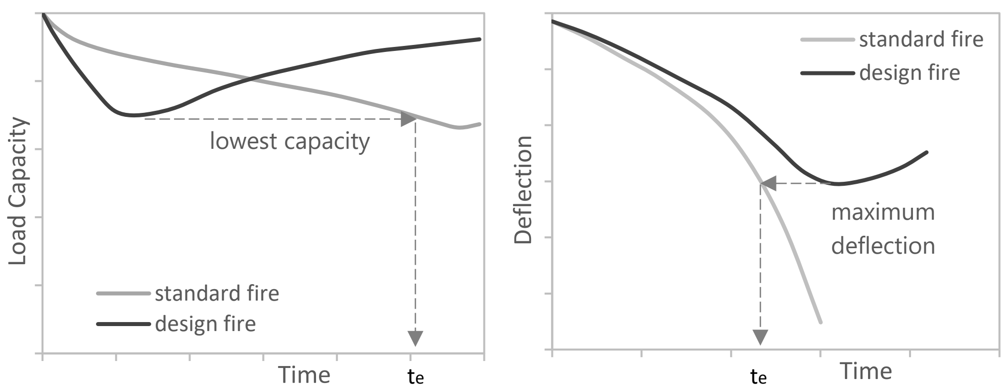

(a) (b)

Fig. 3.3 Mechanical Equivalent Time Methods: (a) Minimum Load Capacity Method and (b) Maximum Deflection Method

3.2.5 Maximum Deflection Method (Mechanical)

Maximum deflection method (MDM) uses the deflection serviceability of an isolated element as its basis for equivalence (Buchanan, 2001). The t_e for a specific element occurs when the deflection caused by a standard fire matches the maximum deflection caused by a selected design fire (Figure 3.3b). This method entails a great deal of complexity compared to thermal methods, but it does provide highly accurate deflection predictions, which can be used to satisfy serviceability limits. Similar to the load capacity concept, deflection accuracy comes at the expense of other mechanical responses. Kodur et al. (2010) used this method to computationally evaluate 72 RC beams under fire exposure, resulting in an empirical equation to determine the t_e for RC beams.

3.3 Research Significance

The existing time equivalent methods are based on specific maximum temperature, energy, load capacity, or deflection criteria. Although these methods have been successful in the case of steel members, the large cross-sections of RC members necessitate the consideration of internal thermal gradients. Of the existing methods, none directly consider the effects of internal gradients, nor account for the influence of cross-section dimensions.

In this paper, an average internal temperature profile method is proposed as an improved measure of fire severity for RC beams. The AITP method is based on the actual internal temperature gradients that develop within a concrete section, allowing for an accurate evaluation of the effect of fire on RC beams. Using this method, the t_e is defined as the duration of standard fire required to generate the same AITP in an RC section as experienced by a selected design fire. The following sections provide details about the conducted parametric studies, the proposed AITP t_e, and a recommended size adjustment factor.

3.4 Time Equivalent Parametric Study

3.4.1 Parameters

To examine the AITP t_e, the standard fire equation and design fire parameters are first defined. In North America, two standard fire curves are commonly used, as presented by Equations 3.1 and 3.2; where T_f is the fire temperature (°C), T_O is the initial temperature (°C), and t is the duration of fire exposure (hr). The first equation is prescribed by both EN 1991-1-2 (2002) and ISO 834 (2014); while the second was developed by Fackler (1959) to represent the temperature curve presented in tabular form in both ASTM E-119 (2018) and CAN/ULS-S101 (1982). The AITP time equivalent, proposed in this chapter is based on the ISO standard fire given by Equation 3.1; however, it should be noted that both equations result in almost identical temperatures with negligible difference in severity (Lie, 1992; Kodur, 2010).

$$T_f - T_O = 345\, log_{10}(480t + 1) \tag{3.1}$$

$$T_f - T_O = 750\left[1 - e^{(-3.79553\sqrt{t}\,)}\right] + 170.41\sqrt{t} \tag{3.2}$$

To develop a natural fire curve, the Eurocode provides a process based on a variety of parameters, from which, four key parameters can be identified. They are: floor area of the fire compartment (A_f), opening factor of the fire compartment (A_f), design fire load density as related to the floor area ($q_{f,d}$), and thermal absorptivity of the compartment enclosure (b) (EN 1991-1-2, 2002). A number of existing time equivalent methods are linked to these parameters, allowing them to be easily related to the Eurocode's natural fire definition. However, doing so limits the applicability of the time equivalent to only a small range of design fires developed using the Eurocode approach. Alternatively, a natural fire can be defined based on the key points of its fire curve. Figure 3.4 shows the temperature-time profile of a natural fire from the Cardington research tests (Lennon, 2014). This typical natural fire can be characterized by three key points: (i) the initial time at ambient temperature (T_o); (ii) the point of maximum temperature (T_{max}) and its corresponding time (t_{max}); and (iii) the final fire duration (t_{final}) upon cooling back to T_o. Given that T_o can be typically taken as 20°C, only t_{max}, t_{final}, *and* T_{max} are needed to define the curve.

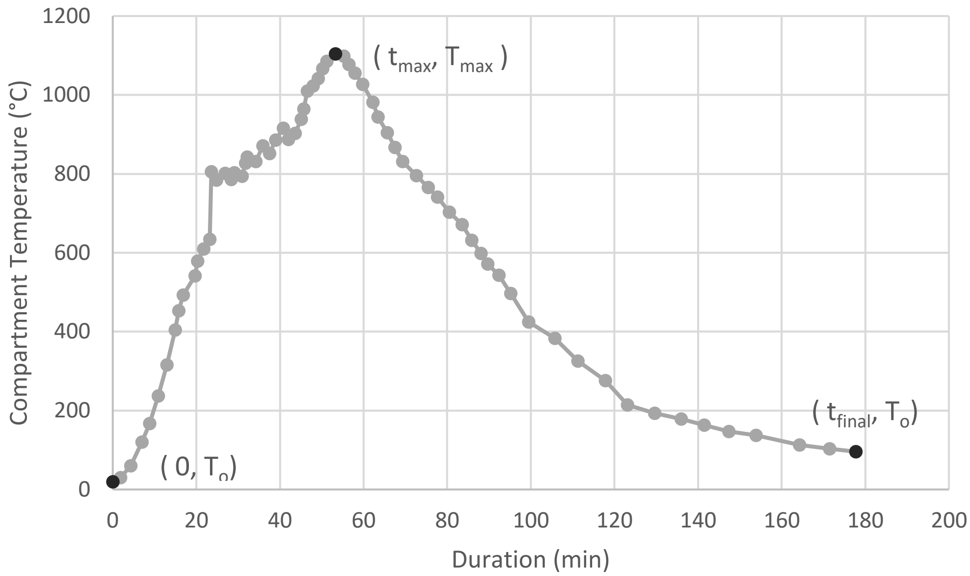

Fig. 3.4 Natural Temperature-Time Curve from Cardington Full Scale Testing (Lennon, 2014)

To demonstrate the limitation of the Eurocode parameters, 1470 design fires were developed following the Eurocode approach. Table 3.1 outlines the examined values for each of the used parameters. Values of A_f and O were chosen based on Equation A.2a of EN 1991-1-2 (2002); while $q_{f,d}$ and b were selected from the standard values given in Table E.4 of EN 1991-1-2 (2002) and Table 1.0 of Implementation of Eurocodes (2005). Additional factors were set consistent with the assumptions of no explosives in the fuel load and no on-site fire brigades or active firefighting measures. Compartment height was taken equal to 3.0 m.

Table 3.1 Eurocode Fire Parameters for Design Fires

A_f m^2	$q_{f,d}$ MJm^{-2}	b $Jm^{-2}s^{0.5}K$	O $m^{0.5}$
16	280	521	0.035
25	347	961	0.050
50	511	1341	0.070
75	730	1697	0.090
100	948	1918	0.110
300	1217		0.150
500			0.200

Based on the range of chosen parameters, it would seem reasonable to assume that a sufficient number of design fires have been produced to encompass every possible natural event. However, when the key parameters of t_{max}, t_{final}, *and* T_{max} are identified and plotted on a 3-dimensional grid (Figure 3.5a), it becomes clear that the resulting profiles ignore large amounts of possible combinations. As such, the suitability of any time equivalent based on the Eurocode parameters cannot be guaranteed for a wide variety of natural fires. To overcome this limitation, the parametric study and time equivalent presented in this chapter focus on the parameters of t_{max}, t_{final}, *and* T_{max}. The valid range of the three key parameters were determined based on the natural fires presented by Dembsey et al. (1995), Byström et al. (2012), Lennon (2004), Kirby et al. (1999), and Implementation of Eurocodes (2005). Within the valid ranges of 350°C $\leq T_{max} \leq$ 1200°C, 15 min $\leq t_{max} \leq$ 115 min, and 20 min $\leq t_{final} \leq$ 240 min; a sensitivity study was undertaken to determine the optimal intervals for each parameter such that the developed design fires are reasonably spaced. Values for t_{max} were chosen at 5-min intervals until 30 min, then at 17-min intervals until 115 min; values for t_{final} were chosen at 20-min intervals throughout; and T_{max} values were chosen starting from 350°C at 100°C intervals until 650°C, then at 50°C intervals until 1200°C. Any combination with $t_{max} \geq t_{final}$ was immediately excluded, resulting in a total of 1290 design fires for evaluation, resulting in a total of 1290 design fires for evaluation (Figure 3.5b).

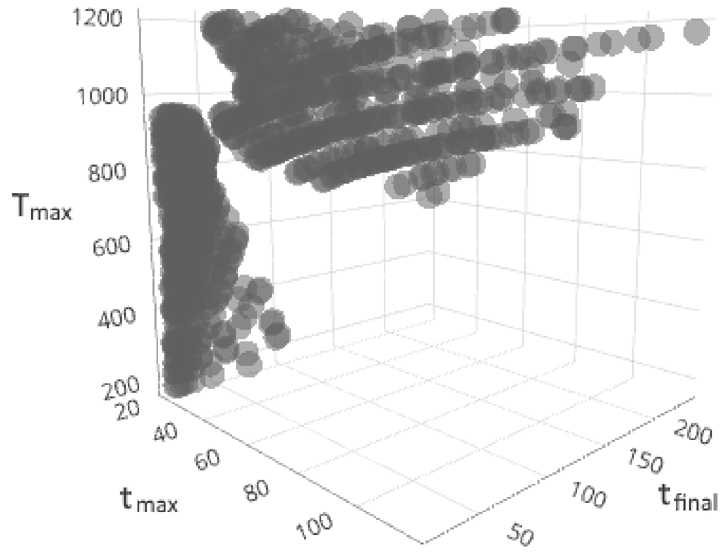

(a)

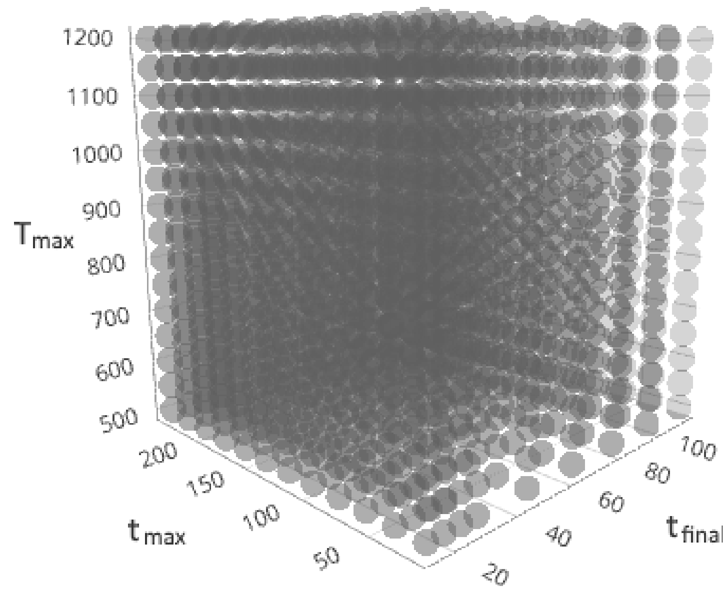

(b)

Fig. 3.5 Identification of Key Points using (a) Eurocode Parameters and (b) Proposed Parameters

Extrapolating the full design fire curve from the key points is a two-stage process. Firstly, for the heating stage, Equation 3.3 is adapted from the Eurocode method (EN 1991-1-2, 2002); where t is the time (min) and T_f is the fire corresponding temperature (°C). The equation is subsequently multiplied by a factor such that at $t = t_{max}$, $T_f = T_{max}$. Secondly, for the cooling stage, a linear profile is used connecting the point of maximum temperature to the end of the fire. This process was followed to assemble the temperature-time curve for each of the 1290 design fires used in this study.

$$T_f - T_O = 1325(1 - 0.324e^{(-0.2t^*)} - 0.204e^{(-1.7t^*)} - 0.472e^{(-19t^*)}) \quad (3.3)$$

To provide in-depth discussion about the effect of fire loading on the proposed time equivalent, six design fires have been selected. The fires were based on the Eurocode approach, their parameters are summarized in Table 3.2 and plotted in Figure 3.6. The six fires were developed using the Eurocode approach demonstrating a range of possible natural fire profiles similar to those presented in the literature. The design fires were broadly classified as: moderate, large, small, rapid hot, and long cool.

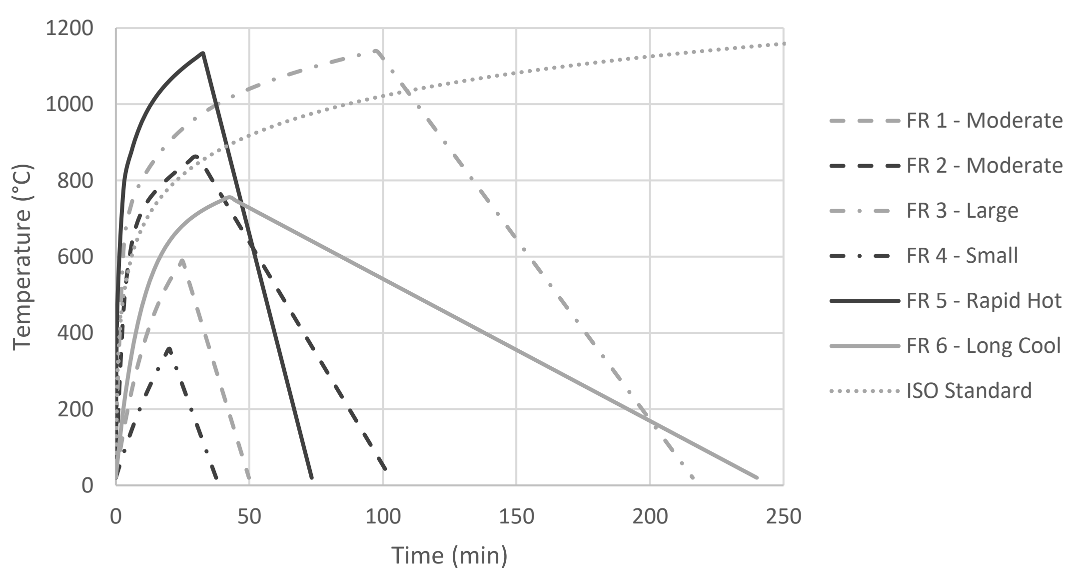

Fig. 3.6 Representative Design Fire Profiles

Table 3.2 Representative Design Fire Characteristics

Fire ID	Af	$q_{f,d}$	b	O	Class
	m^2	MJm^{-2}	$Jm^{-2}s^{0.5}K$	$m^{0.5}$	
FR 1	50	347	1341	0.070	moderate
FR 2	300	280	1341	0.050	moderate
FR 3	100	1217	961	0.050	large
FR 4	50	280	1918	0.090	small
FR 5	100	1217	1697	0.150	rapid hot
FR 6	40	511	1697	0.035	long cool

The cross-section of the theoretical concrete beam was taken as 250 x 500 mm. The effect of cross-section dimensions is examined in Section 6 of this chapter. Normal strength concrete (NSC) with siliceous aggregate was specified based on its standard usage in the industry. The thermal conductivity, density, and specific heat of siliceous aggregate were defined using the relationships provided by Lie (1991).

3.4.2 Methodology

Heat transfer analysis is completed for the full section using a finite difference method (FDM). A detailed description of the implemented FDM is given in Appendix A. The proposed AITP t_e is derived following the process summarized in Figure 3.7. AITPs are developed for a selected design fire (AITP-D) and a standard fire (AITP-S) with duration of t. Correlation between AITP-D and AITP-S is judged based on either mean or conservative criteria. Mean criterion compares the absolute percent difference between AITP-D and AITP-S at every layer of the profile and records the average percent difference for all of the layers. The duration t is incrementally increased until the lowest average percent difference is found. Conservative criterion ignores error differences; the duration t is incrementally increased until AITP-S has equal or larger temperatures at every layer when compared to AITP-D. Using the two criteria, a t_e can be found that provides either a best match or conservative value. The results of the two AITP criteria are given in Section 3.4.3.

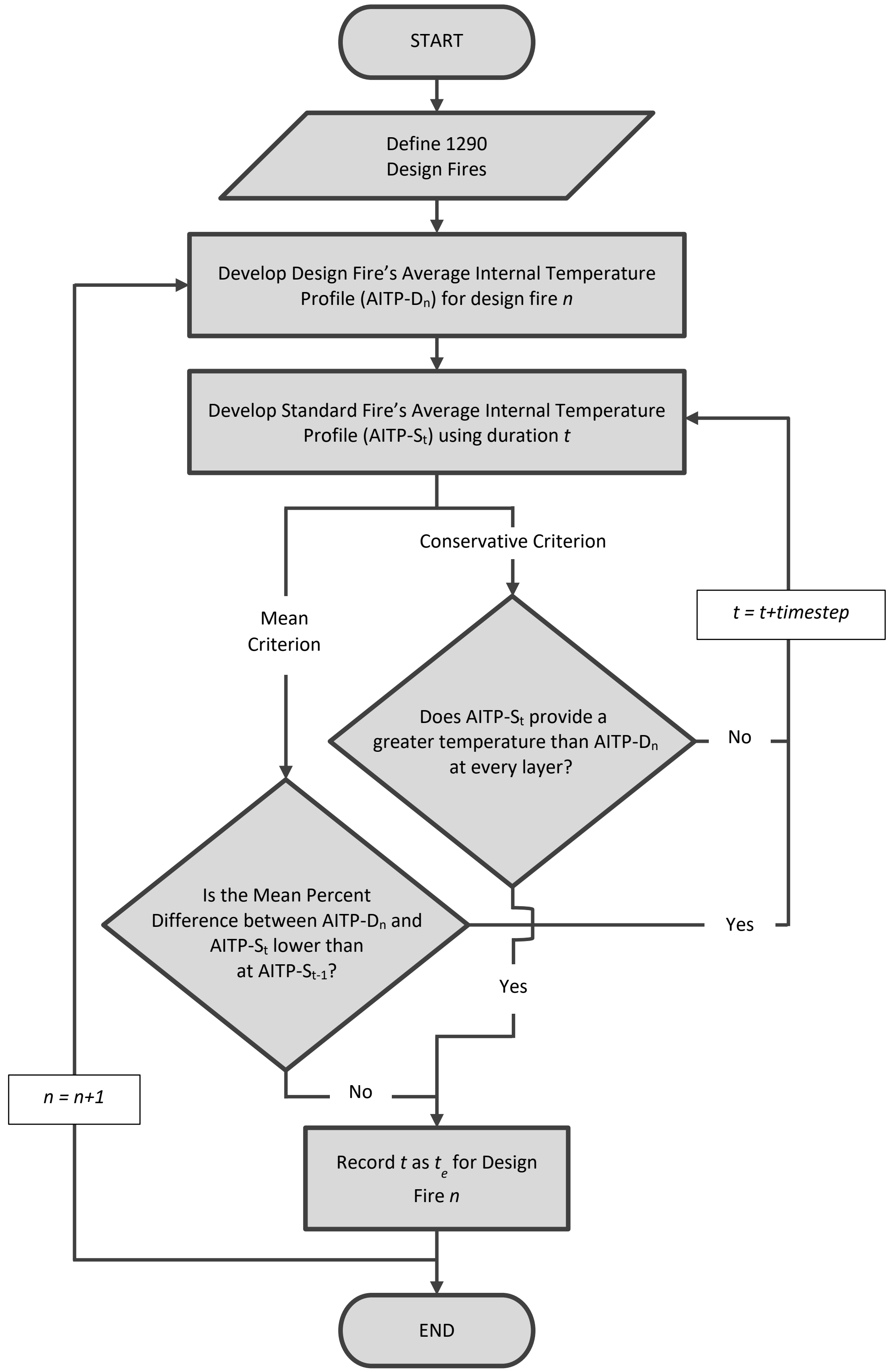

Fig. 3.7 Approach Followed to Calculate AITP Time Equivalents

3.4.3 AITP Time Equivalent Values

Figure 3.8 shows the AITP mean t_e versus the average and maximum error between the respective AITP-S and AITP-D. Of the 1290 evaluated cases, none recorded an average error in excess of 8.5 %. Maximum error is significantly greater for all considered cases, although the extent of the section affected by the high error is generally very small. Figure 3.9 displays a consolidation of the average error from the six design fires as function of section depth. Maximum deviation between AITP-S and AITP-D arises at the lower surface of the beam, where temperatures are highest. Moving away from the point of maximum difference, the discrepancy between AITP-S and AITP-D decreases rapidly. This trend can be defined by a highly-variable zone near the surface and a constant zone in the interior. At a distance of just 52.5 mm into the section, the error falls below 10 %. As such, even though the maximum error is large in value, its influence on the concrete section is relatively minor. A small uptick in the error is experienced around 35 mm due to the AITP-S and AITP-D crossing paths, which causes a divergence and subsequent re-convergence in this region. Depending on the design fire, the scale of divergence will differ. Cases with the largest average and maximum error are typically attributed to small fires, with low temperature over a short duration. Such fires are difficult to approximate given the intended purpose of the standard fire as a representation of a worst-case fire event. Considering that smaller fires are less likely to result in major structural damage, it is reasonable to accept higher errors for these types of fire events.

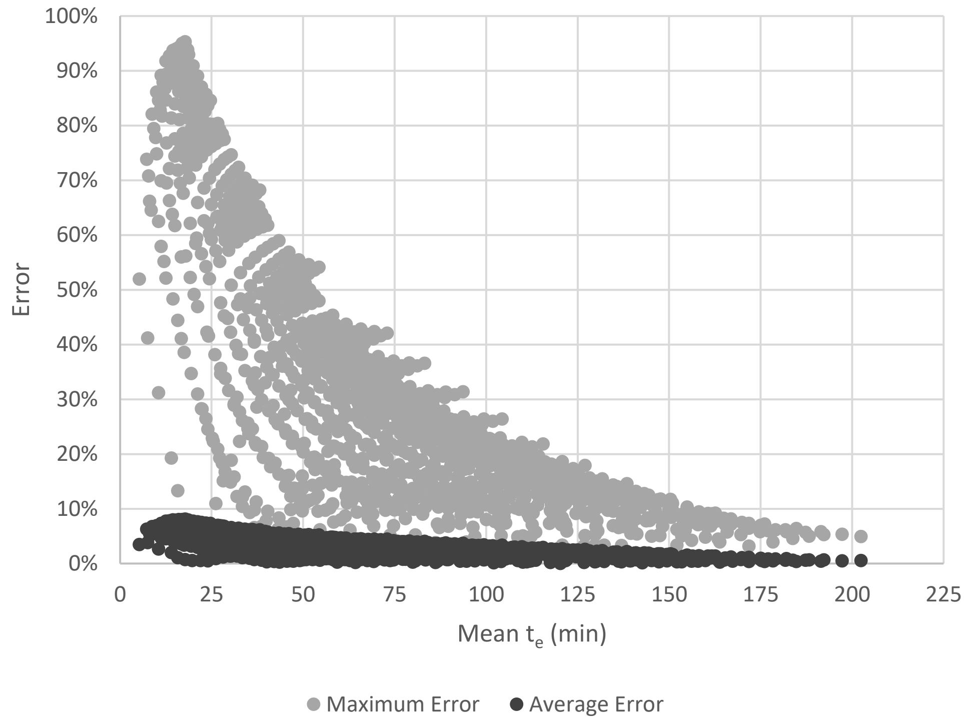

Fig. 3.8 Accuracy of AITP Mean Time Equivalent for Average Error and Maximum Error

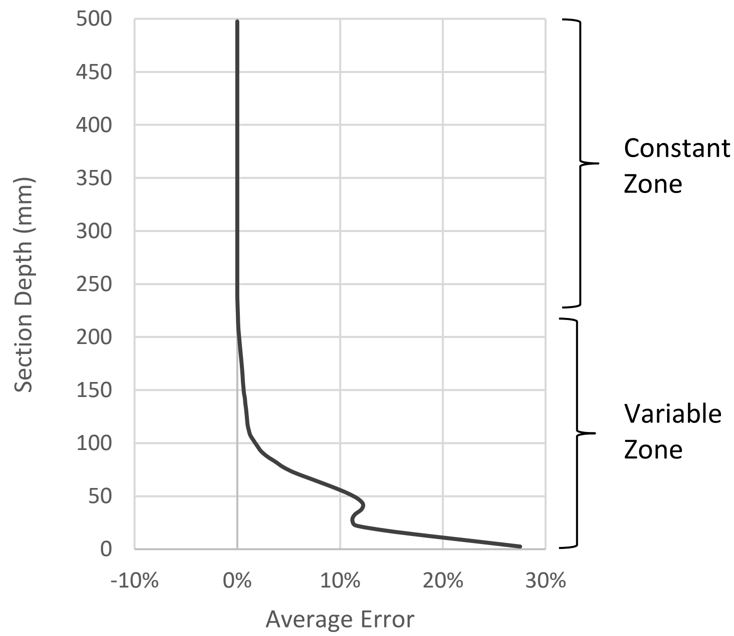

Fig. 3.9 Average Error as a Function of Section Depth

A calculation method for the mean and conservative t_e is proposed by the general Equation 3.4, with coefficients A through J given in Table 3.4. The equation and coefficients were determined using a least square regression analysis, common regression requirements of probability (p) < 0.001 and correlation (R^2_{adj}) > 95 % were maintained. In Equation 3.4, T_{max} is the maximum fire temperature (°C), t_{max} is the corresponding time (min), and t_{final} is the overall duration of the fire (min). Following Eurocode guidelines, the time variables t_{max} and t_{final} are measured from the point of flashover, and t_{final} is measured to the end of the decay phase, ignoring the relatively negligible impact of a fire's ignition and extinction periods.

$$t_e = A + Bt_{max} + Ct_{final} + DT_{max} + Et^2_{max} + Ft^2_{final} + GT^2_{max} \\ + Ht_{max}t_{final} + It_{max}T_{max} + Jt_{final}T_{max} \tag{3.4}$$

Table 3.3 Coefficients for Equation 3.4

		Mean Criterion	Conservative Criterion			
Valid Range	t_{max} (min)	15 - 115	15 - 115	15 - 115	15 - 115	15 - 115
	t_{final} (min)	20 – 240	20 – 240	20 – 240	20 – 240	20 – 240
	T_{max} (°C)	350 – 1100	350 - 750	750 - 950	950 - 1100	1100 - 1200
Coefficients	**A**	8.124	8.690	2.370	566.30	4404.0
	B	-0.153	-0.0829	-0.0893	-0.465	-5.745
	C	0.0384	0.0324	0.0446	1.188	1.039
	D	-0.0431	-0.0429	-0.0186	-1.332	-8.177
	E	-8.53×10^{-4}	-4.74×10^{-4}	-9.42×10^{-4}	-20.00×10^{-4}	-80.87×10^{-4}
	F	-6.46×10^{-4}	-4.16×10^{-4}	-7.39×10^{-4}	0.0	2.99×10^{-4}
	G	0.50×10^{-4}	0.66×10^{-4}	0.35×10^{-4}	7.95×10^{-4}	38.36×10^{-4}
	H	3.44×10^{-4}	1.57×10^{-4}	4.77×10^{-4}	-3.07×10^{-4}	-17.80×10^{-4}
	I	6.55×10^{-4}	5.33×10^{-4}	5.40×10^{-4}	12.05×10^{-4}	69.36×10^{-4}
	J	4.52×10^{-4}	3.70×10^{-4}	4.71×10^{-4}	-9.00×10^{-4}	-8.40×10^{-4}

* Equation 3.4 is only valid for sections of 250 x 500 mm in size

The valid ranges given in Table 3.4 are based on the extents of the parametric study. Fires outside of these valid ranges were not considered in this study. The equation is only valid for 250 x 500 mm concrete sections; variable dimensions are considered in Section 6. Due to the greater variability of the conservative t_e, four sets of coefficients are given, each is valid for the shown T_{max} range. These four ranges were determined by undertaking a sensitivity study to group design fires of similar severity. Figure 3.10 plots the t_e calculated numerically versus that evaluated using the mean and conservative equations to demonstrate their suitability.

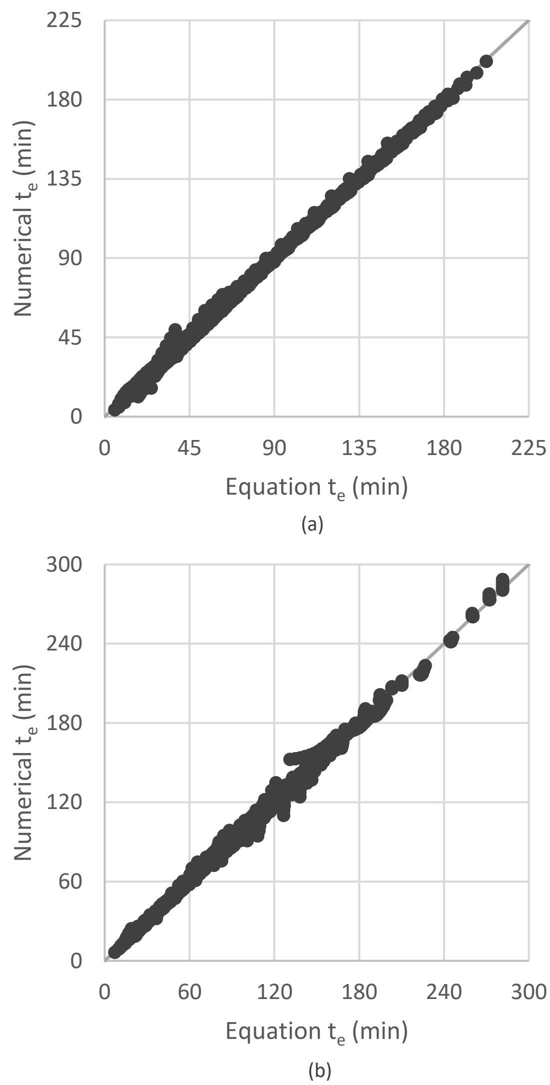

Fig. 3.10 Accuracy of Time Equivalent Equations: (a) Mean Criterion and (b) Conservative Criterion

3.5 Size adjustment Factor

3.5.1 Influence of Beam Width and Height

In this section, the effect of beam width (b_c) and height (h_c) on the AITP t_e is investigated. To the best of the author's knowledge, none of the existing time equivalent methods have considered section dimensions, despite its importance on defining the internal temperature gradients. Figure 3.11 displays the AITP of eight beams with b_c of 250, 400, 600, and 800 mm; and h_c of 500 and 800 mm. The sections were exposed on three sides to a 1-hr standard fire. Width variation significantly influences the AITP. Increasing the width from 250 to 800 mm reduces the temperature values by an average of 81 % for this sample fire. In contrast, height can be seen to have little to no impact on the AITP. The thermal profile recording the largest temperature values, corresponds to the beam with the smallest width. Wider elements, which have a larger interior to surface area ratio, experience a lower average internal temperature.

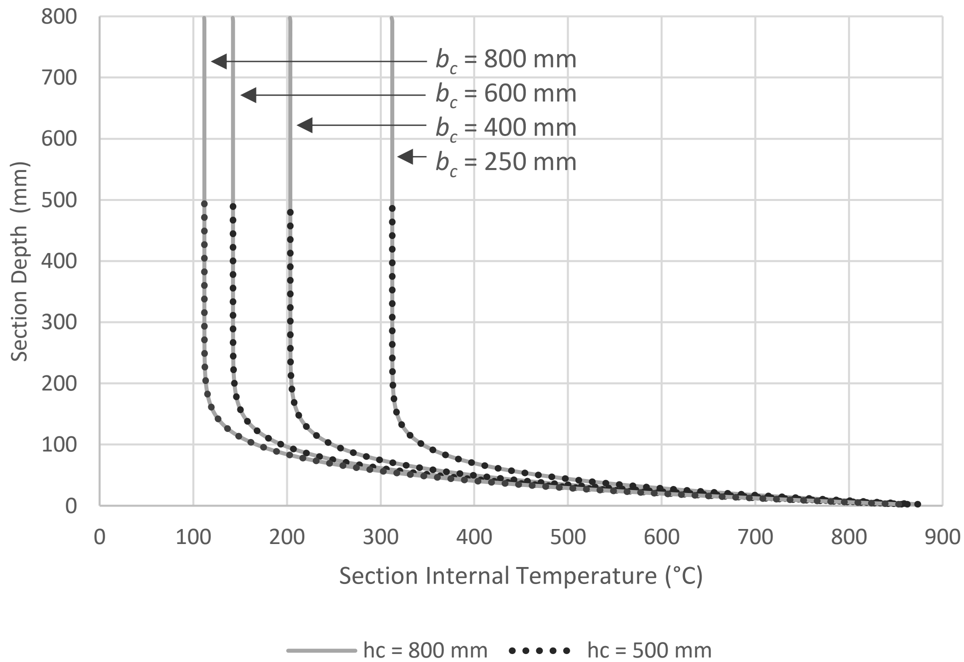

Fig. 3.11 Average Internal Temperature Profile due to 1-hr Standard Fire for Variable Cross-Sections

Figure 3.12 demonstrates the impact of section width on the AITP mean and conservative t_e for five beams with b_c of 250, 400, 600, and 800 mm; and an h_c of 500 mm. The sections are exposed to the six design fires defined in Section 5.1. The results indicate that as width increases, an equal or greater t_e is required for the larger and longer duration fires. Therefore, despite the average temperature becoming lower with increasing width, it is inaccurate and unconservative to represent a wider beam with the t_e derived for a smaller cross-section. The necessary increase in duration of the standard fire is highly dependent on the design fire. For instance, the smaller and shorter fires (FR 1, FR 4, and FR 5), are only capable of significantly heating the exterior layers of a beam, and only require minimal alteration to the t_e when width increases. Inversely, the larger and longer fires (FR 2, FR 3, and FR 6), require significant increases to the standard fire duration as these longer fires are able to slowly heat the entirety of a section.

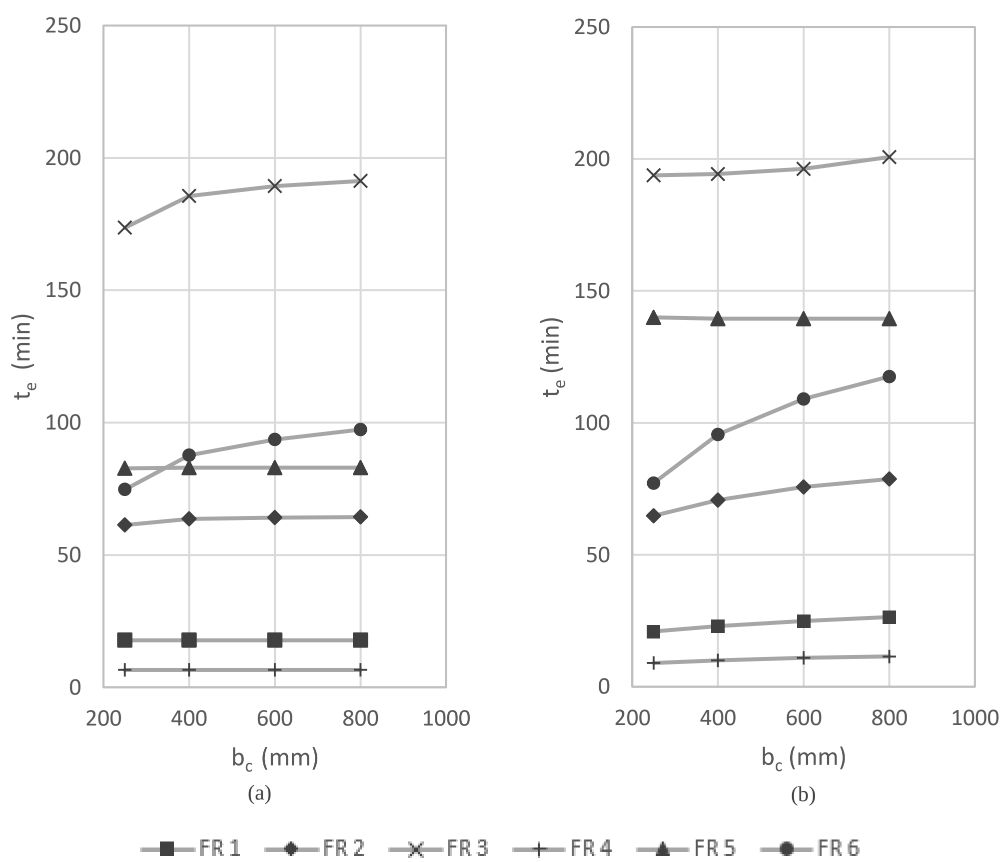

Fig. 3.12 Sensitivity of t_e to Section Width (a) Mean Criterion and (b) Conservative Criterion

A similar comparison was conducted studying the effect of variable heights on the AITP t_e. Sections were evaluated with h_c at 300, 400, 500, 700, and 800 mm; and b_c held constant at 250 mm. As previously determined, the height of RC beams had no impact on the mean or conservative t_e. Despite this, when the section height is compared against the error between AITP-D and AITP-S (Figure 3.13), a notable influence can be observed. As height increases, the correlation between the two profiles improves markedly. This trend can be explained by examining the two zones of the AITP profile. For taller beams, the constant zone dominates the average error calculation, while for shorter beams, the variable zone plays a more significant role. As the error values are low in the constant zone, the average error will seem to be affected by the section height. Thus, shorter beams will give higher error than taller beams, regardless of the fact that both have almost matching AITPs and identical t_e durations. In this section, a study of 5160 RC cross-sections of variable dimensions and design fire exposures is considered. It was found that the variable zone averages a height of 227 mm. In the previous evaluation of the t_e, the section height was taken constant at 500 mm, allowing the constant and variable zones to contribute equally to the error calculation. To account for different section heights, the errors can be normalized such that the constant and variable zones are having equal influence regardless of the section height. Equation 2 is used for normalization. The end of the variable zone was identified when the temperature difference between successive AITP layers was less than 1°C. The 0.45 factor in Equation 3.5 was selected such that the normalized average error will be equal to the actual average error, for the moderate fire FR 2 when section height is 500 mm.

$$Normalized_{\ Error} = Error \div \frac{Transient\ Zone\ Height}{0.45\ Section\ Height} \tag{3.5}$$

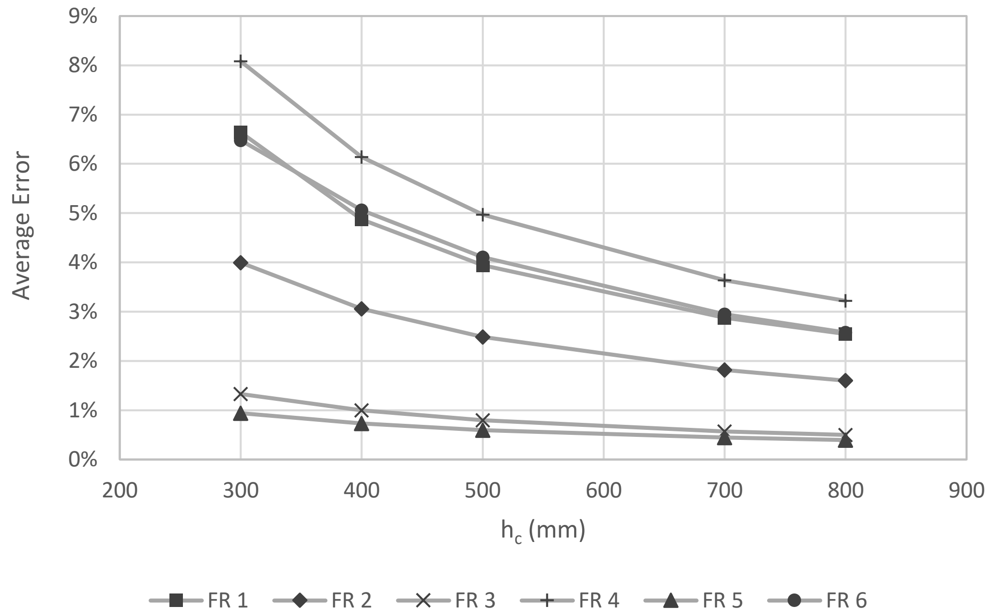

Fig. 3.13 Section Height versus Average Error for Mean Criterion

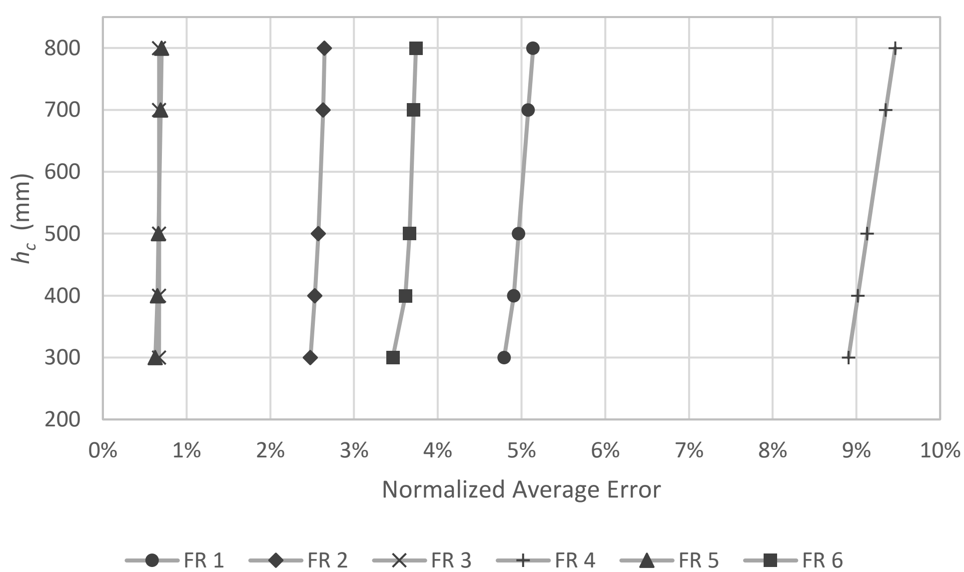

Fig. 3.14 Section Height versus Normalized Average Error for Mean Criterion

To develop a general equation to account for beam dimensions, a parametric study was undertaken on sections with b_c of 250, 400, 600, and 800 mm. Height was held constant throughout the study at 500 mm, with normalized results used to evaluate the mean criterion. The methodology presented in Section 3.4.2 was followed. Standard and design fires were assembled consistent with the process outlined in Section 3.4.1, resulting in 1290 cases per cross-section. In total, considering all 4 cross-sections, 5160 cases were analyzed in this section.

3.5.2 AITP Size Adjustment Factor

Figure 3.15 presents the mean t_e for the 5160 considered cases versus (a) the normalized average error and (b) the maximum error. Considering all four section widths, 322 out of the 5160 test cases resulted in an average error greater than 10 %. In determination of the size adjustment factor (ψ_{size}), all 5160 cases were utilized for the conservative criterion; while for the mean criterion, cases with error greater than 10 % were highlighted and manually excluded. The high error data points can be identified as belonging to fires with low temperature and duration. To eliminate these fires, the valid range of the data was altered to exclude fires with T_{max} < 600°C and fires with T_{max} < 750°C reached during a t_{max} < 60 min. The design fires passing and failing this new range are highlighted on Figure 3.15 in grey and black, respectively. Applying the condition completely eliminates the high error data points, but also eliminates a variety of passable data points, resulting in 4704 cases used in the determination of the mean ψ_{size}.

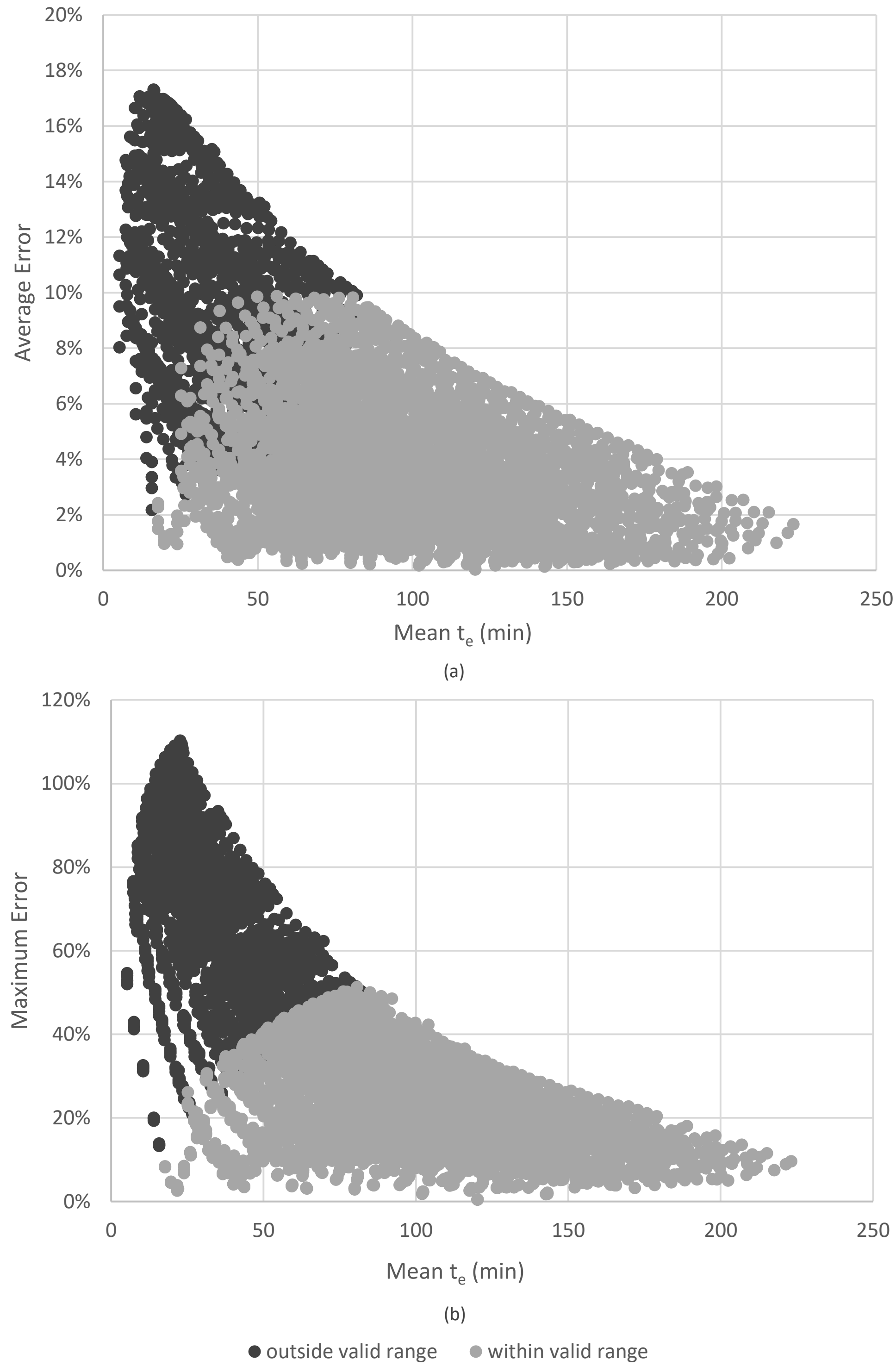

Fig. 3.15 AITP Mean Time Equivalent in Relation to (a) the Normalized Average Error and (b) the Maximum Error

The general equation for the ψ_{size} is presented in Equation 3.6; wherein b_c is the section width (m), T_{max} is the maximum fire temperature (°C), t_{max} is the time when maximum temperature occurs (min), and t_{final} is the overall duration of the fire (min). The coefficients for Equation 3.6 can be found in Table 3.5. Both the mean and conservative criteria were developed using regression analysis, maintaining the common requirements of probability (p) < 0.001 and correlation (R^2_{adj}) > 95 %. Valid ranges are prescribed based on the range of design fires for which the parametric study was undertaken.

$$\psi_{size} = \begin{cases} 1.0 \begin{cases} for\ bc < 300\ m \\ for\ conservative\ t_e\ when\ T_{max} > 1150℃ \\ for\ conservative\ t_e\ when\ t_e > 180\ min \end{cases} \\ \\ A + Bt_{max} + Ct_{final} + DT_{max} \\ \quad + b_c\left(E + Ft_{max} + Gt_{final} + HT_{max}\right) \ \geq 1.0 \end{cases} \tag{3.6}$$

Table 3.4 Coefficients for Equation 3.5

	Mean Criterion	Conservative Criterion
Valid Range	$200 \leq b_c \leq 800$ mm	$200 \leq b_c \leq 800$ mm
	$300 \leq h_c \leq 800$ mm	$300 \leq h_c \leq 800$ mm
	$15 \leq t_{max} \leq 115$ min	$15 \leq t_{max} \leq 115$ min
	$20 \leq t_{final} \leq 240$ min	$20 \leq t_{final} \leq 240$ min
	$600 \leq T_{max} \leq 1200$°C [1]	$350 \leq T_{max} \leq 1200$°C
A	1.022	0.819
B	-2.57×10^{-4}	3.78×10^{-4}
C	2.69×10^{-4}	-2.23×10^{-4}
D	-0.22×10^{-4}	1.82×10^{-4}
E	0.113	1.037
F	-8.23×10^{-4}	-27.00×10^{-4}
G	14.01×10^{-4}	27.15×10^{-4}
H	-1.93×10^{-4}	-10.75×10^{-4}

* Excluding T_{max} < 750 °C reached during t_{max} < 60 min

The value of the ψ_{size} is set equal to 1.0 for specific cases for the reasons given in this paragraph. Firstly, given the increasing nature of the t_e with b_c, the value of the ψ_{size} should never be taken less than one. Secondly, for small beams with b_c < 300 mm, Equation 3.4 is sufficient alone, and thus the value of the ψ_{size} is one. Lastly, a trend unique to the conservative t_e necessitates the addition of the final two constraints. When beams are narrow, heating from both sides causes the internal temperatures to rise significantly. In these cases, the critical point of the conservative t_e, where AITP-S is equal to AITP-D, is often at a height well away from the beams lower surface. As b_c increases, the effects of two-sided heating are diminished, reducing the internal temperatures, and causing the critical point to shift towards the lower surface. Once the critical point is at the surface, b_c has negligible influence on the t_e as the critical point is directly influenced by the surface temperature. In this case, the ψ_{size} remains at a value of 1.0 even as b_c increases. It is difficult to capture this constant value with the equation, therefore to alleviate the issue, condition terms (T_{max} > 1150°C and t_e > 180°C) were manually derived by an iterative process, for which the ψ_{size} is equal to one. Results for the mean t_e are presented in Figure 8, plotting the numerical versus equation-based t_e for results with and without the ψ_{size}. It can be seen that the t_e adjusted using the ψ_{size} exhibits far superior fit and significantly less deviation, especially on the unconservative side. A similar trend is noted for the conservative t_e. Applying these conditions significantly improves the accuracy of the equation in matching the analytical data. Figure 3.16 displays the numerical versus equation-based ψ_{size}, demonstrating a suitable representation for the general equation. Final results of the study are presented in Figure 3.17, plotting the numerical versus equation-based t_e for results with and without ψ_{size}. It can be seen that for both criteria, the t_e with ψ_{size} exhibits far superior fit, with significantly less deviation, especially on the unconservative side.

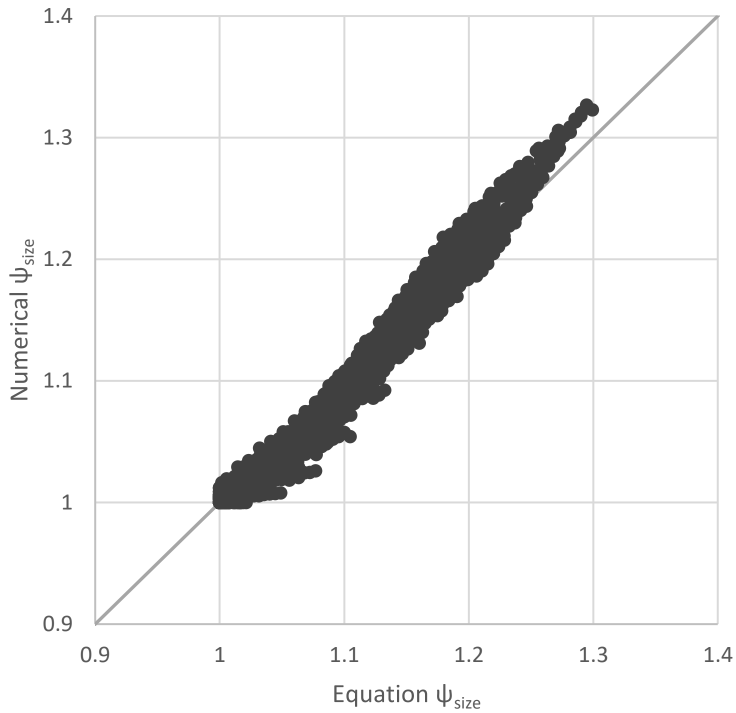

(a)

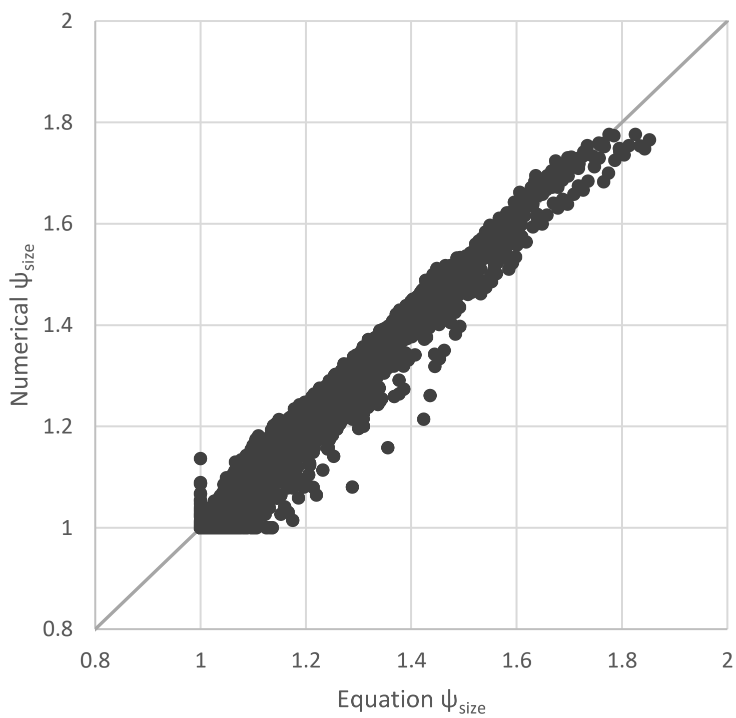

(b)

Fig. 3.16 Analytical vs. Equation ψ_{size} for: (a) Mean Criterion and (b) Conservative Criterion

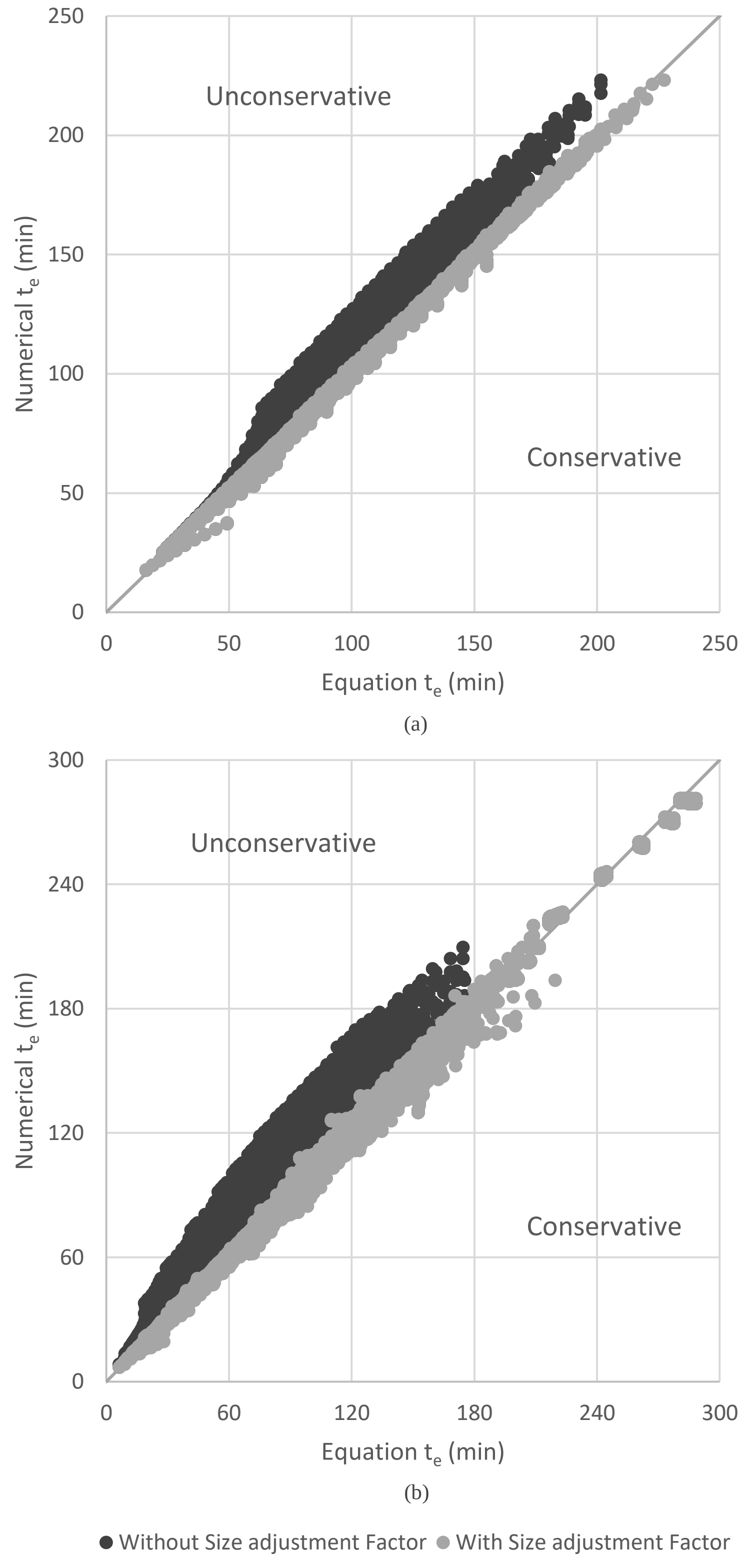

Fig. 3.17 Analytical vs. Equation t_e for: (a) Mean Criterion (b) Conservative Criterion with and without ψ_{size}

3.6 Comparison with Existing Methods

A comparison of existing methods is provided in Figures 3.18 to 3.23 for each of the six design fires. The referenced methods are sorted in pairs, featuring the early methods of Ingberg (1928) and Law (1971); the two code approaches of CIB (1986) and EN 1991-1-2 (2002); the RC Energy and MDM methods of Kodur et al. (2010); and the two AITP criteria. Each figure consists of three parts, displaying (a) the t_e, (b) the normalized average error for a 250 x 500 mm section, and (c) the normalized average error for an 800 x 500 mm section. For the AITP criteria, the t_e for the 800 x 500 mm section with ψ_{size} is indicated by the checkered bar. All t_e durations are calculated based on the ISO standard fire. It should be noted that the small fires FR 1 and FR 4 possess a $T_{max} < 600°C$, and therefore do not meet the conditions of the mean ψ_{size}. FR 1 and FR 4 do however meet all of the requirements of the conservative criterion.

A major trend is apparent between the methods tailored for RC elements (AITP mean criterion; Energy by Kodur et al., 2010; and MDM by Kodur et al., 2010) and those based on steel members or compartment boundaries (all others). The non-RC methods result in significantly greater error than the RC methods for all six design fires, indicating their poor ability in representing the internal temperature gradients. The only exception is Kodur et al.'s (2010) MDM, as it displays larger discrepancy for FR 1 and FR 4, this limitation for smaller fires is highlighted in the original publication. In the case of the moderate and larger fires of FR 2 and FR 3 (Figures 3.19 and 3.20), the non-RC methods result in a t_e almost half that of the AITP mean, producing significantly unconservative estimates. For the small fire FR 4 (Figure 3.21), the t_e of the non-RC approaches are more than double the AITP mean duration, resulting in massively conservative estimates of the fire's severity. As noted earlier, the conditions of the AITP mean criterion exclude its application for fire FR 4. Regardless, the mean criterion and the conservative criterion still exhibit far greater correlation between AITP-D and AITP-S than the existing methods. These discrepancies between the RC and non-RC methods highlight the importance of considering internal temperature profiles when developing and utilizing a time equivalent method for RC elements.

In comparison with the existing RC-methods by Kodur et al. (2010), AITP mean always results in the lowest error when representing the internal temperature profile. Additionally, Kodur et al.'s Energy and MDM methods alternate on which is more accurate depending on the design fire and the section size. This is most apparent when comparing differences between FR 1 and FR 2; and between 250 mm and 800 mm wide sections for FR 6. Using the AITP mean criterion, the most accurate representation of the internal profiles is reliably developed for every design fire and every section size. Some discrepancy in Kodur et al.'s (2010) results can be attributed to its development based on the ASTM standard fire, however this should play only a very minor role.

In Figure 3.22, the conservative t_e results in an average error far greater than the AITP mean and existing methods. The purpose of the conservative t_e is to produce equal or greater internal temperatures at every point in the section, which has been achieved for all cases. For the rapid hot fire FR 5, high temperatures are produced at the section's surface, but the internal temperatures are significantly lower due to the absence of a prolonged heating period. In order for the conservative t_e to match the high temperatures on the section's surface, it markedly over represents the internal temperatures, resulting in higher error. It should be noted that the AITP conservative is the only method capable of predicting these high surface temperatures in the case of rapid hot exposure.

The impact of the ψ_{size} is most noticeable for the longer duration fires of FR 2, FR 3, and FR 6. The long cool FR 6 demonstrates the most significant impact, as the conservative t_e is increased by almost 50 min between the 250 and 800 mm width sections (Figure 3.23). For FR 6, application of the ψ_{size} allows the mean AITP to remain more accurate than Kodur et al.'s methods and the conservative AITP to be more reasonably conservative than the non-RC methods. The ψ_{size} plays a crucial role in ensuring the accuracy and conservativeness of the AITP methods in comparison to the existing approaches.

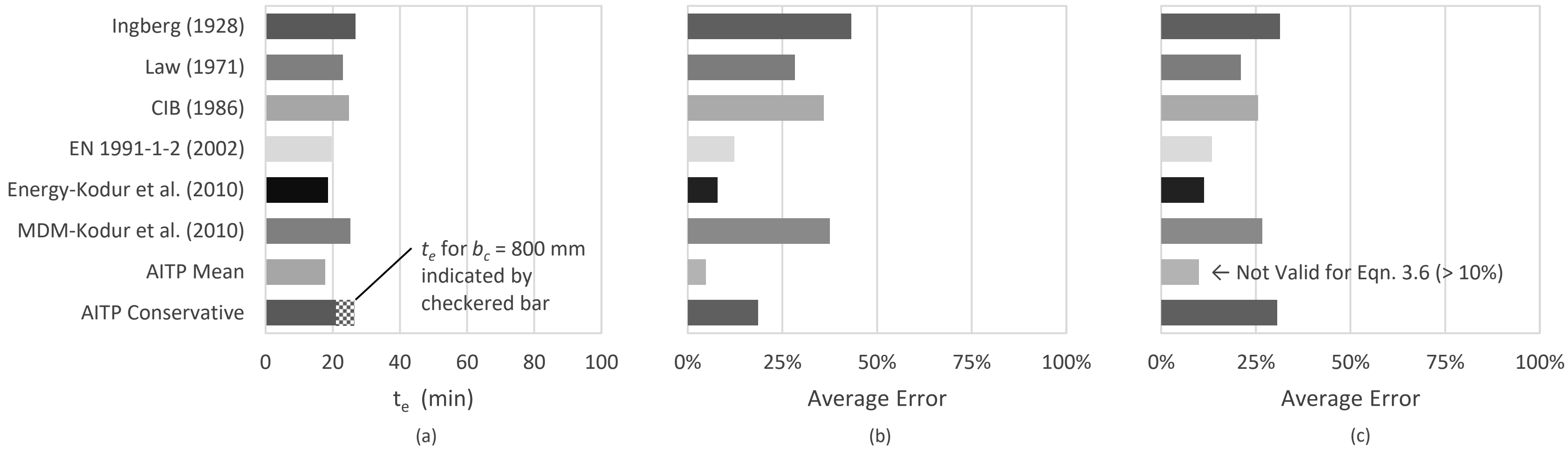

Fig. 3.18 Existing Methods for Moderate FR 1: (a) t_e, (b) Error for b_c 250 mm, and (c) Error for b_c 800 mm

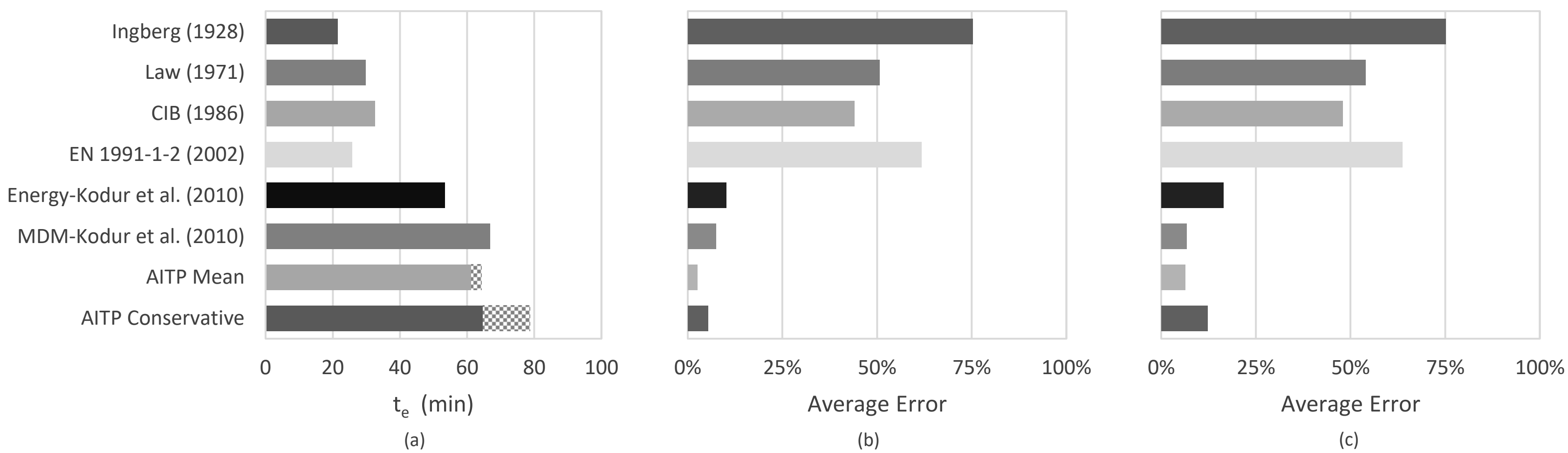

Fig. 3.19 Existing Methods for Moderate FR 2: (a) t_e, (b) Error for b_c 250 mm, and (c) Error for b_c 800 mm

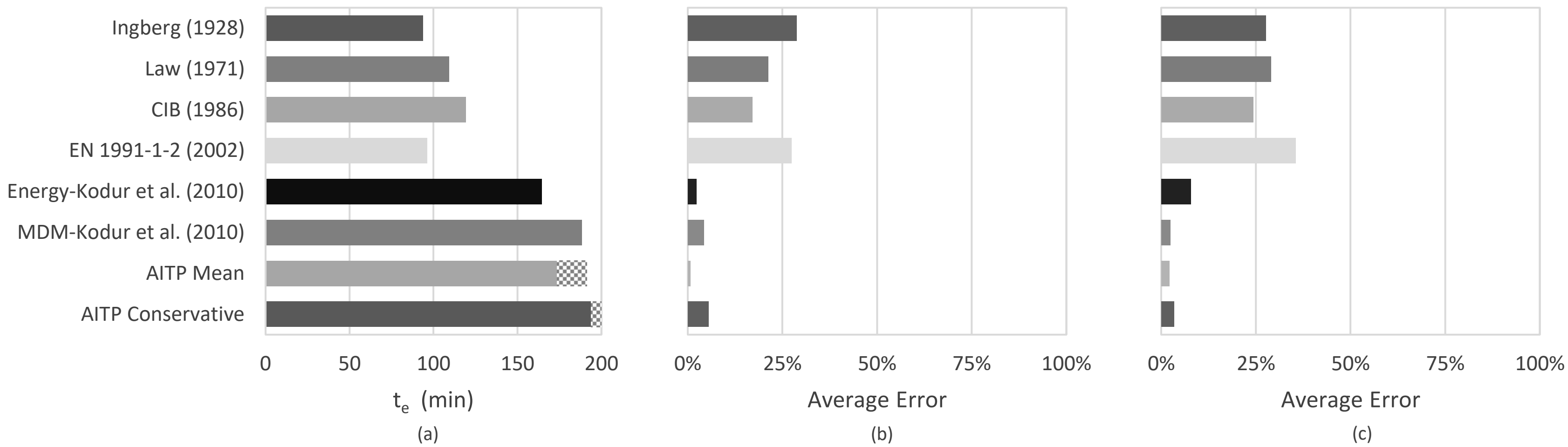

Fig. 3.20 Existing Methods for Large FR 3: (a) t_e, (b) Error for b_c 250 mm, and (c) Error for b_c 800 mm

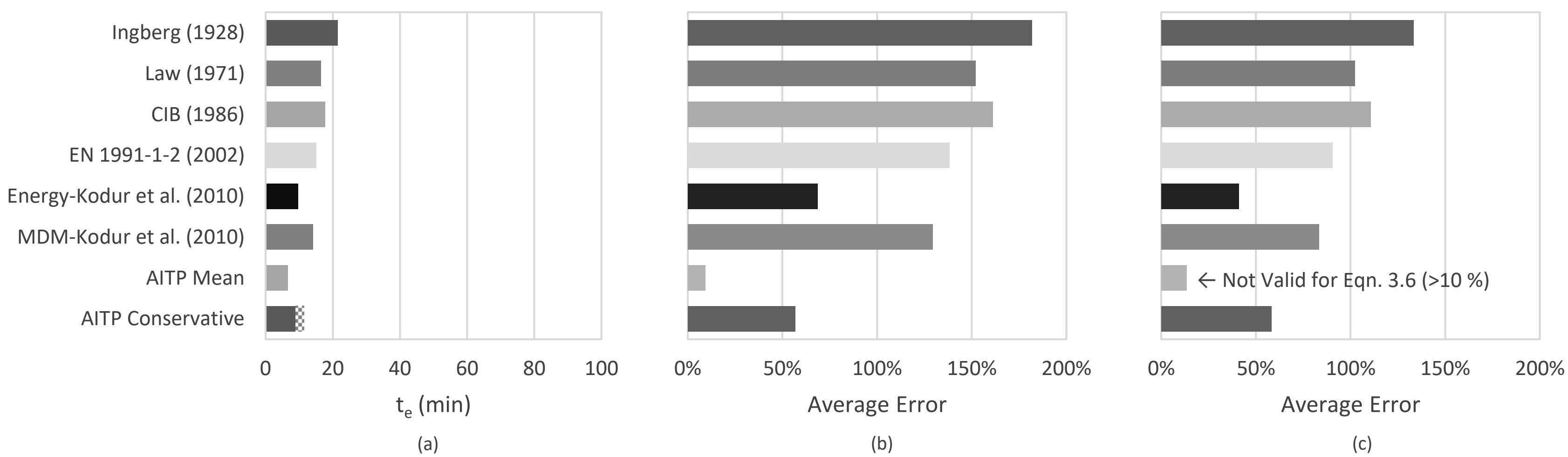

Fig. 3.21 Existing Methods for Small FR 4: (a) t_e, (b) Error for b_c 250 mm, and (c) Error for b_c 800 mm

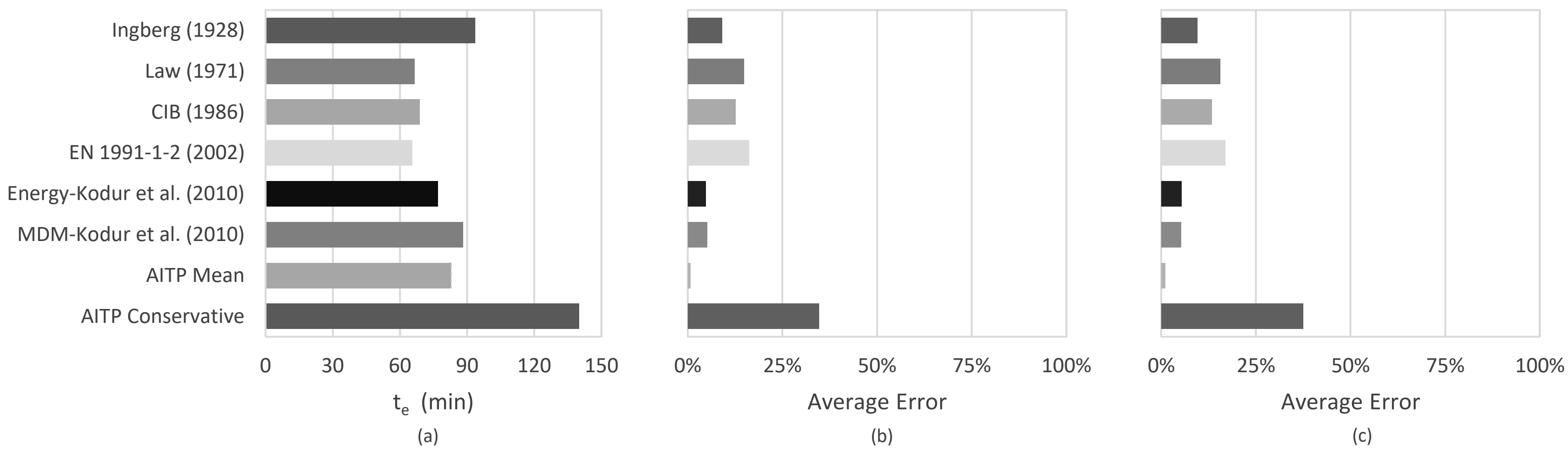

Fig 3.22. Existing Methods for Rapid Hot FR 5: (a) t_e, (b) Error for b_c 250 mm, and (c) Error for b_c 800 mm

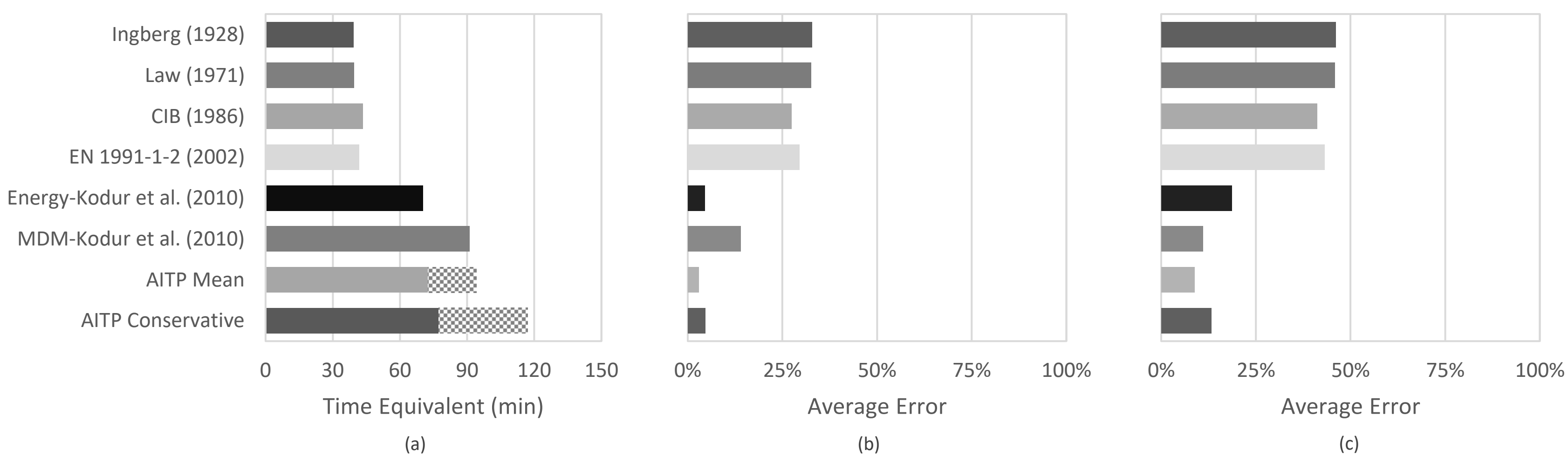

Fig 3.23. Existing Methods for Long Cool FR 6: (a) t_e, (b) Error for b_c 250 mm, and (c) Error for b_c 800 mm

3.7 Conclusion

To better facilitate performance-based design, time equivalent methods are needed to assess the severity of a natural fire in terms of the duration of a standard fire. Using a time equivalent, engineers can easily relate natural fires to the wealth of available data, testing, and computer programs based on standard fire curves. Existing time equivalent methods in the literature and design manuals have been proven to be largely inaccurate in representing the internal thermal gradient of RC elements exposed to fire. To better address time equivalency for RC elements, a new AITP method was introduced, which bases equivalency on the actual internal temperature profiles of RC beams.

To develop the AITP method, a parametric study was conducted on a 250 x 500 mm RC section exposed to 1290 design fires. Two equations were developed for the AITP method: mean and conservative. Mean criterion was based on accurately matching the internal temperature profiles of a design fire to that of a standard, while conservative criterion was based on selecting the shortest duration standard fire that produces equal or larger temperatures at every point in the section. Further evaluation regarding the influence of section dimensions on the t_e revealed the importance of accounting for section width. A size adjustment factor was proposed to be used in conjunction with the t_e. In comparison with existing methods, the AITP mean criterion displayed far greater accuracy in representing the internal temperature gradient, and the AITP conservative criterion the only method capable of consistently being conservative. The proposed t_e is valid for beams exposed to natural fire on three sides, within the ranges of 350°C $\leq T_{max} \leq$ 1200°C, 15 min $\leq t_{max} \leq$ 115 min, and 20 min $\leq t_{final} \leq$ 240 min. Using the proposed AITP method, designers can quickly relate the severity of a natural fire to an equivalent standard fire, allowing them to utilize existing standard fire resources.

3.8 References

Alhadid, M. *Behavior of Fire-Exposed RC Frames Before and After Jacketing*. Diss. Department of Civil and Environmental Engineering, Western University, 2017.

ASTM E-119. *Standard Test Methods for Fire Tests of Building Construction and Materials. American Society for Testing and Materials*. West Conshohocken, PA, USA. 2018.

Buchanan, A.H. *Structural Design for Fire Safety, 2nd ed*. Wiley, 2001.

Byström, A., X. Cheng, U. Wickström, and M. Veljkovic. "Measurement and Calculation of Adiabatic Surface Temperature in a Full-Scale Compartment Fire Experiment." *Journal of Fire Sciences*, vol. 31, no. 1, 2012, pp 35-50.

CAN/ULC-S101. *Standard Methods of Fire Endurance Tests of Building Construction and Materials*. Underwriters Laboratories of Canada. Toronto, Canada. 1982.

CIB. "Design Guide: Structural Fire Safety CIB W14 Workshop Report." Fire Safety Journal, vol. 10, no. 2, 1986, pp. 77-137.

Cooper, L.Y., and K.D Steckler. *Methodology for Developing and Implementing Alternative Temperature-Time Curves for Testing the Fire Resistance of Barriers for Nuclear Power Plant Applications.* no. 5842, National Institute of Standards and Technology, Gaithersburg, MD, USA. 1996.

Dembsey, N.A., P.J. Pagni, and R. B. Williamson. "Compartment Fire Experiments: Comparison with Models." *Fire Safety Journal*, vol. 25, no. 1, 1995, pp. 187-227.

El-Fitiany, S.F., and M.A. Youssef. "Assessing the Flexural and Axial Behaviour of Reinforced Concrete Members at Elevated Temperatures Using Sectional Analysis." *Fire Safety Journal*, vol. 44, no. 5, 2009, pp. 691-703.

El-Fitiany, S.F., and M.A. Youssef. "Fire Performance of Reinforced Concrete Frames Using Sectional Analysis." *Engineering Structures*, vol. 142, no. 1, 2017, pp. 165-181.

El-Fitiany, S.F., and M.A. Youssef. “Simplified Method to Analyze Continuous Reinforced Concrete Beams During Fire Exposure.” *ACI Structural Journal*, vol. 111, no. 1, 2014, pp. 145-156.

EN 1991-1-2. *Eurocode 1: Actions on Structures - Part 1-2: Actions on Structures Exposed to Fire*. European Committee for Standardization. Brussels, Belgium. 2002.

EN 1993-1-2. *Eurocode 3: Design of Steel Structures - Part 1-2: General Rules - Structural Fire Design*. European Committee for Standardization. Brussels, Belgium. 2005.

Guo, Z., and X. Shi. *Experiment and Calculation of Reinforce Concrete at Elevated Temperatures*. Elsevier Ltd, 2011.

Harada, K., R. Kogure, K. Matsuyama, and T. Wakamtsu. “Equivalent Fire Duration Based on Time-Heat Flux Area.” *4th Asia-Oceania Symposium on Fire Science and Technology*, Ottawa, Canada, 1994. Published by Fire Safety Science, 2000, pp. 513-524.

Harmathy, T.Z., and J.R. Mehaffey. “The Normalized Heat Load Concept and Its Use.” *Fire Safety Journal*, vol. 12, no. 1, 1987, pp. 75-81.

Implementation of Eurocodes. *Handbook 5 - Design of Buildings for the Fire Situation.* Leonardo Da Vinci Joint Research Project, 2005.

Ingberg, S. “Tests on the Severity of Building Fires.” *Quarterly of the National Fire Protection Association*, vol. 22, 1928, pp. 43-61.

ISO 834. *Fire Resistance Tests – Elements of Building Construction.* International Organization for Standards. Geneva, Switzerland. 2014.

Kirby, B.R., D.E. Wainman, L.N. Tomlinson, T.R. Kay, and B.N. Peacock. “Natural Fires in Large Scale Compartments.” *International Journal on Engineering Performance-Based Fire Codes*, vol. 1, no.2, 1999, pp. 43-58.

Kodur, V.K.R., P. Pakala, and M.B. Dwaikat. “Energy Based Time Equivalent Approach for Evaluating Fire resistance of Reinforced Concrete Beams.” *Fire Safety Journal*, vol. 45, no. 4, 2010, pp. 211-220.

Law, M. *A Relationship Between Fire Grading and Building Design and Contents*. no. 877, Building Research Establishment - Fire Research Note, UK, 1971.

Lennon, T. *Results and Observations from Full-Scale Fire Test at BRE Cardington*. no. 215-741, Building Research Establishment, Cardington, UK, 2004.

Lie, T.T. *Structural Fire Protection*. ASCE, 1992.

Nyman, J.F. *Equivalent Fire Resistance Ratings of Construction Elements Exposed to Realistic Fires*. MS. Department of Civil Engineering, University of Canterbury, 2002.

Pettersson, O. *The Connection Between a Real Fire Exposure and the Heating Conditions According to Standard Fire-Resistance Tests - With Special Application to Steel Structures*. Bulletin no. 39, Lund Institute of Technology - Division of Structural Mechanics and Concrete Construction, Lund, Sweden, 1975.

Purkiss, J.A. *Fire Safety Engineering, Design of Structures*. Elsevier Ltd, 2007.

Schneider, U., M. Kersken-Bradley, and U. Max. “Neuberechnung der Wärmeabzugs Faktoren für die DINV 18230: Teil 1 - Baulicher Brandschutz Industribau.” (In German). *Fraunhofer IRB Verlag*, Stuttgart, Germany, 1990.

Thomas, G.C., A.H. Buchanan, and C.M. Fleischmann. “Structural Fire Design: The Role of Time Equivalence.” *5th Asia-Oceania Symposium on Fire Science and Technology*, Melbourne, Australia, 1997. Published by Fire Safety Science, 1997, pp 607-618.

Wade, C.A., J.T. Gerlich, and A. Abu. “The Relationship Between Fire severity and Time-Equivalent.” *BRANZ Study Report*, no. SR 314. Building Research Levy, 2014.

Wang, Y.,I. Burgess, F. Wald, and M. Gillie. *Performance-Based Fire Engineering of Structures*. Spon Press, 2013.

Xie, P., A. Abu, and M. Spearpoint. “Comparison of Existing Time-Equivalent Methods and the Minimum Load Capacity Method.” 1*0th Asia-Oceania Symposium on Fire Science and Technology*, Tsukuba, Japan, 2015. Published by Fire Science and Technology, 2015, pp 263-271.

Youssef, M.A., and M. Moftah. “General Stress-Strain Relationship for Concrete at Elevated Temperatures.” *Engineering Structures*, vol. 29, no. 10, 2007, pp. 2618-2634.

Youssef, M.A., M.A. Diab, and S.F. El-Fitiany. “Shear Capacity of RC Beams at Elevated Temperatures.” *Magazine of Concrete Research*, vol. 67, no. 22, 2015, pp. 1190-1203.

Chapter 4

4.0 Assessing the Flexural Response of Fire-Exposed RC Beams using an Equivalent Standard Fire

Performance-based design requires the development of structural solutions to meet specific performance requirements. These performance requirements can be divided into serviceability and ultimate limit states; which are typically measured using deflection and load capacity (Purkiss, 2007). In the case of reinforced concrete (RC) beams, both of these requirements can be best represented by the sectional moment-curvature (M-φ) response.

A time equivalent (t_e) method was proposed in Chapter 3 to represent the severity of a natural fire using a standard fire duration. The method determines a t_e duration by comparing the average internal temperature profile (AITP) that develops within a concrete section during natural and standard fire exposure. The AITP t_e can be calculated using Equation 3.4 based on either mean or conservative criteria. A standard fire with a mean AITP t_e produces an internal temperature profile closely matching that of the design fire. While a standard fire with a conservative AITP t_e results in a profile with equal or larger temperatures at every layer. A size adjustment factor (ψ_{size}) was also proposed (Equation 3.6) to account for the influence of variable beam width (b_c) and height (h_c) on the AITP t_e duration. In the previous chapter, it was proven that the mean and conservative time equivalent equations are superior to the existing methods in predicting the internal average temperatures of concrete beam sections exposed to natural fire from three-sides. In this chapter, the use of the AITP method is examined for application in the performance-based fire design of RC beams. A study is presented for a selection of RC cross-sections and natural fires to assess the suitability of the time equivalent in representing the M-φ response. The following sections detail the analysis method to predict the M-φ relationship, outline the study methodology, and discusses the results.

In the final portion of this chapter, a case study is presented demonstrating a simplified approach to undertake performance-based flexural fire design for an RC beam. The case study highlights the three main steps in the design process: (i) determination of the natural fire severity using the AITP t_e, (ii) calculation of element internal temperatures, and (iii) sectional flexure analysis. The simplified analysis is validated with results from experimental testing and ABAQUS finite element (FE) modelling.

4.1 Flexural Analysis

A structural analysis program developed by El-Fitiany and Youssef (2009) was used in this chapter to produce the M-φ response of beams during fire exposure. The program has three main steps: (1) determine the internal thermal gradients of the section, (2) evaluate the concrete thermal and transient strains at elevated temperatures, and (3) complete a sectional flexure analysis. The section's internal thermal gradient is calculated using the finite difference method (FDM) presented by Lie (1992). Three-sided fire exposure is applied to the RC section from the two sides and lower face. Concrete thermal and transient strains are estimated using the equations recommended by Youssef and Moftah (2007). Sectional analysis is then carried out iteratively to determine the M-φ relationship. The program makes the following assumptions: (1) plane sections remain plane during fire exposure, as previously validated up to 1200°C by El-Fitiany and Youssef (2011); (2) perfect bond exists between steel and concrete; (3) normal strength concrete (NSC) is used, and thus, explosive spalling can be ignored; (4) influence of concrete tensile cracks on heat flow is ignored; and (5) geometrical nonlinearity is not considered.

4.1.1 Study Methodology

For a given RC section, the M-φ response is calculated for both natural and standard fire exposure. The natural fire curve is assembled based on experimentally recorded fire curves and theoretical profiles developed using the Eurocode approach (EN 1991-1-2, 2002). The standard fire curve is applied following the ISO profile (ISO 834, 2014) for a given mean or conservative AITP t_e duration. In total, each cross-section is evaluated for three fire events: the design fire, the AITP mean standard fire, and the AITP conservative standard fire. Comparison of the three *M*-*φ* profiles are presented to demonstrate the suitability of the AITP t_e in representing the natural fire. Due to the impracticality of displaying the full *M*-*φ* diagram for a large range of design fires and cross-sections, three key responses are identified for comparison. They are: the maximum moment at elevated temperature (M_{rT}), the initial curvature at elevated temperature (φ_{iT}), and the initial stiffness at elevated temperature (EI_{iT}). These three points are crucial to defining the *M*-*φ* relationship, and in turn, the serviceability and ultimate limit states needed for performance-based design.

4.1.2 Beam and Fire Parameters

Seven rectangular sections were selected to examine the *M*-*φ* response. Table 4.1 displays the section properties. The studied parameters are: concrete strength (f'_c), section width (b_c), section height (h_c), tension reinforcement ratio (ρ_s), and aggregate type (*agg.*) of either siliceous (*sil.*) or calcareous (*cal.*). Figure 4.1 exhibits general details of the studied cross-sections. At ambient conditions, the value of f'_c is specified as either 30 or 40 MPa, and the steel yield strength (F_y) is held constant at 400 MPa. Longitudinal steel area was equally split into 3 bars, spaced symmetrically about the centerline and with 55 mm of cover on all sides. Thermal properties for normal strength concrete (NSC) with siliceous and calcareous aggregate are applied from Lie (1992). The consideration of compression reinforcement and stirrup confinement was neglected for simplicity.

Table 4.1 Parametric Study Beam Properties

<table>
<tr><th>Beam #</th><th>F_y</th><th>f_c'</th><th>b_c</th><th>h_c</th><th>ρ_s</th><th>agg.</th><th>Studied Parameter</th></tr>
<tr><td></td><td>MPa</td><td>MPa</td><td>mm</td><td>mm</td><td>%</td><td>---</td><td></td></tr>
<tr><td>B1</td><td rowspan="7">400</td><td rowspan="4">30</td><td rowspan="5">250</td><td rowspan="5">500</td><td>1.0</td><td rowspan="3">sil.</td><td>p</td></tr>
<tr><td>B2</td><td>1.5</td><td>p</td></tr>
<tr><td>B3</td><td>2.0</td><td>p</td></tr>
<tr><td>B4</td><td>1.0</td><td>cal.</td><td>agg.</td></tr>
<tr><td>B5</td><td>40</td><td>1.0</td><td rowspan="3">sil.</td><td>f_c'</td></tr>
<tr><td>B6</td><td rowspan="2">30</td><td>400</td><td>800</td><td>1.0</td><td>b_c, h_c</td></tr>
<tr><td>B7</td><td>600</td><td>800</td><td>1.0</td><td>b_c, h_c</td></tr>
</table>

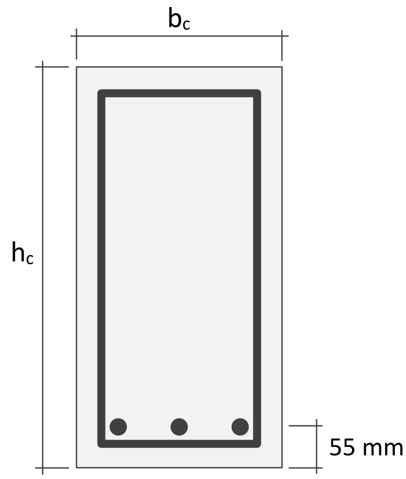

Fig. 4.1 Cross Section of Parametric Study RC Beam

Seven design fires are specified for the study (Figure 4.2). The first five were developed using the Eurocode approach to demonstrate a range of possible natural fire events. They can be broadly categorized as moderate, large, small, rapid hot, and long cool. The remaining two fires were taken from the experimental literature presented by Kirby et al. (1994) and Lennon (2014). Kirby et al. (1999) conducted testing in a 23 x 6 m concrete compartment filled with wood cribs. The large compartment, high density of fuel load, low emissivity boundaries, and good ventilation resulted in a large fire event. Lennon (2014) presents a fire curve from the Cardington Fire Tests completed by the Building Research Establishment (BRE) on a full-scale composite steel structure. The compartment spanned 11 x 7 m with fire resistant plasterboard walls, concrete floors, and uniformly spaced wood cribs for the fuel load. The two experimental programs provide a good representation of typical natural fires that can occur in a concrete structure.

The critical points of the fire curve needed to calculate the AITP t_e can be interpreted graphically from Figure 4.2. When determining the critical fire durations, it is important to neglect the initial ignition and final exhaustion periods of the fire. The low temperatures of these periods result in little influence on the surrounding concrete elements, but if the durations are included in the AITP t_e equation, they can have a significant impact on the t_e. The resulting values for the AITP t_e using the size adjustment factor (ψ_{size}) for each fire and beam width are presented in Table 4.2. In total, the study consists of 147 test cases using the seven cross-sections, seven design fires, seven AITP mean standard fires, and seven AITP conservative standard fires. It should be noted, that B6 and B7 possess a b_c greater than 350 mm, and therefore do not meet the condition of the mean ψ_{size} in the case of FR 4, when T_{max} is less than 600°C. These two non-valid cases were excluded from the study for the mean t_e.

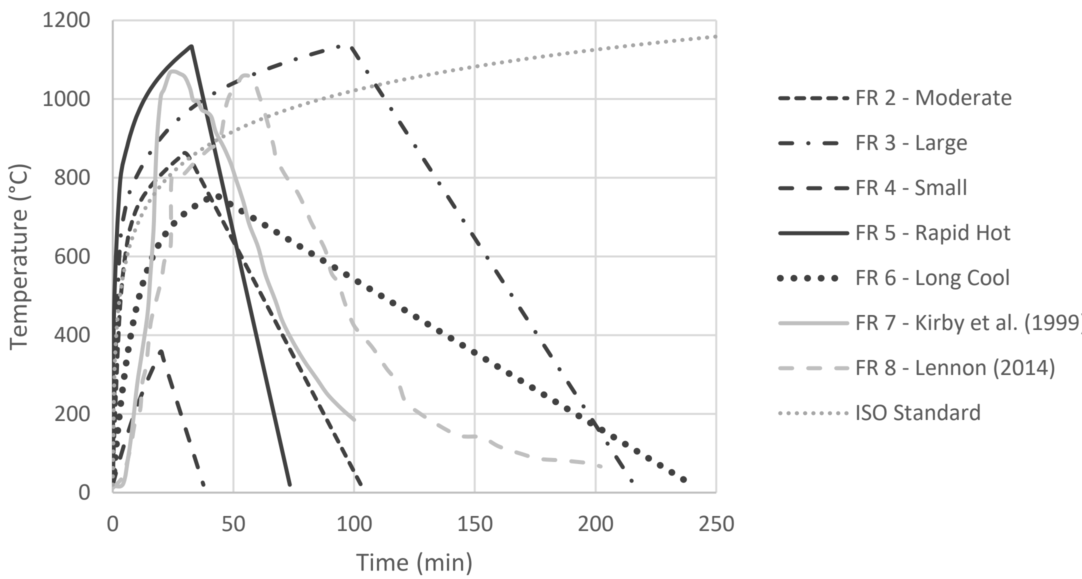

Fig. 4.2 Representative Design Fire Profiles

Table 4.2 AITP t_e durations for the Seven Specified Design Fires

	AITP Mean t_e *(min)*			**AITP Conservative t_e** *(min)*		
b_c =	*250 mm*	*400 mm*	*600 mm*	*250 mm*	*400 mm*	*600 mm*
FR 2	58.63	61.44	62.20	63.41	68.89	72.72
FR 3	170.49	183.37	187.28	195.47	195.47	195.47
FR 4	7.27	Not Valid		9.51	11.07	12.39
FR 5	79.62	79.62	79.62	128.43	128.43	128.43
FR 6	74.65	87.03	91.03	78.63	96.21	108.17
FR 7	78.30	81.11	81.69	89.99	93.93	96.04
FR 8	98.42	101.54	102.23	109.45	113.76	115.68

4.2 Flexural Assessment

Figure 4.3 and 4.4 display the full *M-φ* diagrams for B1 during the various fire exposure regimes. The ambient temperature profile is also provided as a baseline. All of the fire events led to the expected response of lowering the moment capacities and increasing the curvatures. The small fire (FR 4) results in only minimal thermal gradients within the section, and as such, virtually no visible change occurs to the *M-φ* diagram during fire exposure. For all seven fire events, the mean t_e presents a good fit with the design response. The highest deviation occurs for the large fire (FR 3), but the accuracy of the moment capacity remains at most within 6.7% of the actual. The conservative t_e produced a conservative profile, with lower moment capacity and larger curvatures for all seven design fires. For the rapid hot fire (FR 5), the conservative t_e is significantly longer in duration than the mean t_e, allowing it to capture the high surface temperatures that occur during rapid hot events. The *M-φ* response of FR 5 reflects this fact, showing a very conservative estimate for the conservative t_e. The experimental design fires of FR 7 and FR 8 likewise correlate well with the AIT t_e approximations.

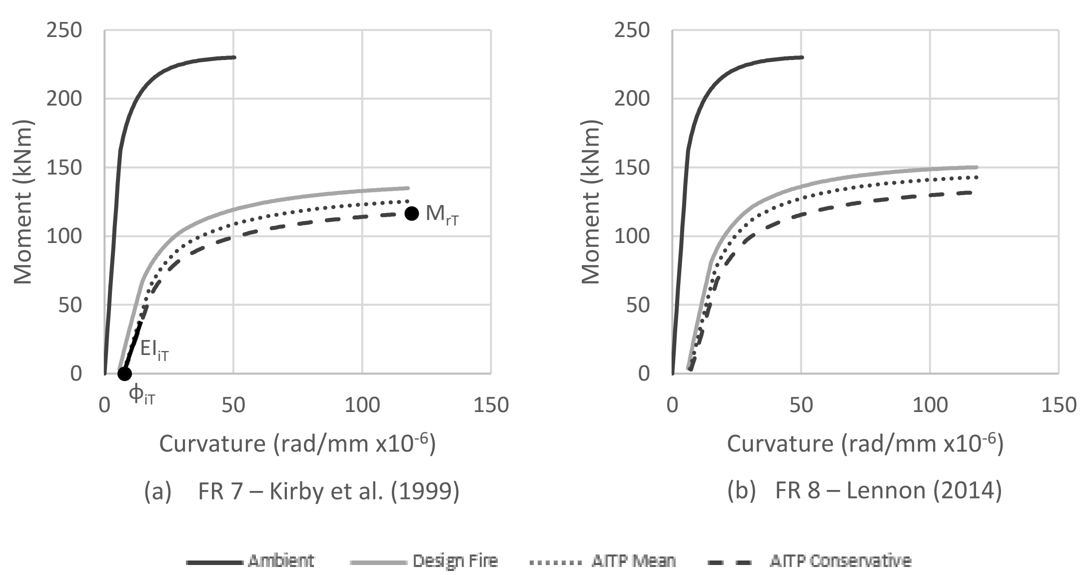

Fig. 4.3 Moment-Curvature Diagrams for B1 using Experimental Design Fires

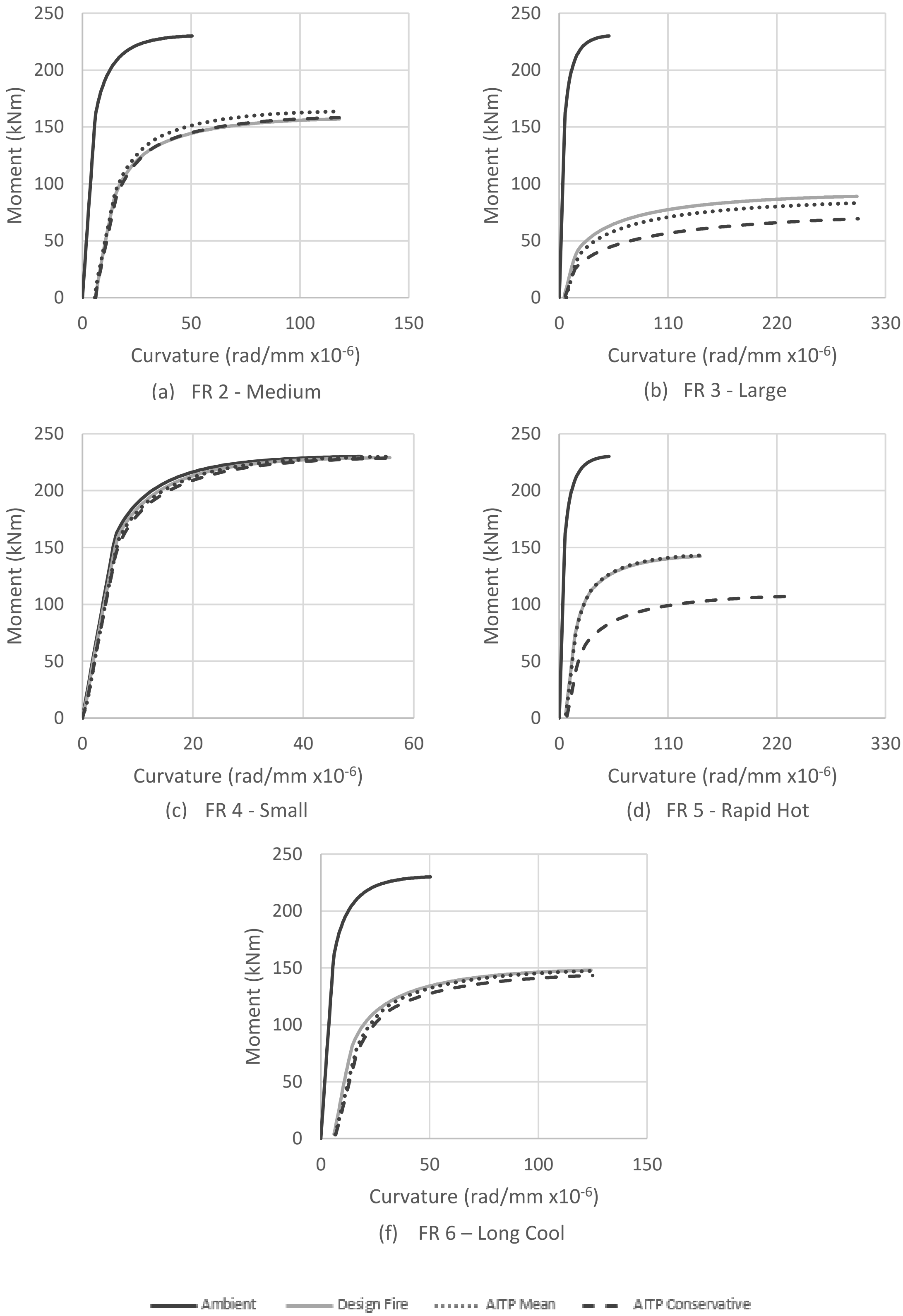

Fig. 4.4 Moment-Curvature Diagrams for B1 using Eurocode Design Fires

Comparison of the remaining test cases is conducted based on the M_{rT}, φ_{iT}, and EI_{iT} (graphically depicted on Figure 4.3a). Figure 4.5 displays the results of the design fire predictions versus the time equivalent fire predictions. The conservative criterion achieves its intended objective, resulting in conservative approximations for every test case. The mean criterion presents a reasonable fit along the line of equality. The M_{rT} is captured with a high degree of accuracy by the mean t_e, with error less than 10 % for every section and design fire. The φ_{iT} and EI_{iT} generally fall within 10 % error; however, because both responses are highly sensitive to small changes in thermal strains, some outliers yield much higher errors. Furthermore, in contrast with moment capacity, curvature and stiffness calculations at ambient and elevated temperatures are far more approximate. Given the approximate and sensitive nature of the calculations, it is difficult for the AITP t_e to provide highly accurate predictions for φ_{iT} and EI_{iT}. It should be noted however, that the higher error predictions of φ_{iT} and EI_{iT} associated with the mean t_e are on the conservative side. The maximum error for the unconservative mean t_e predictions are within 10 %.

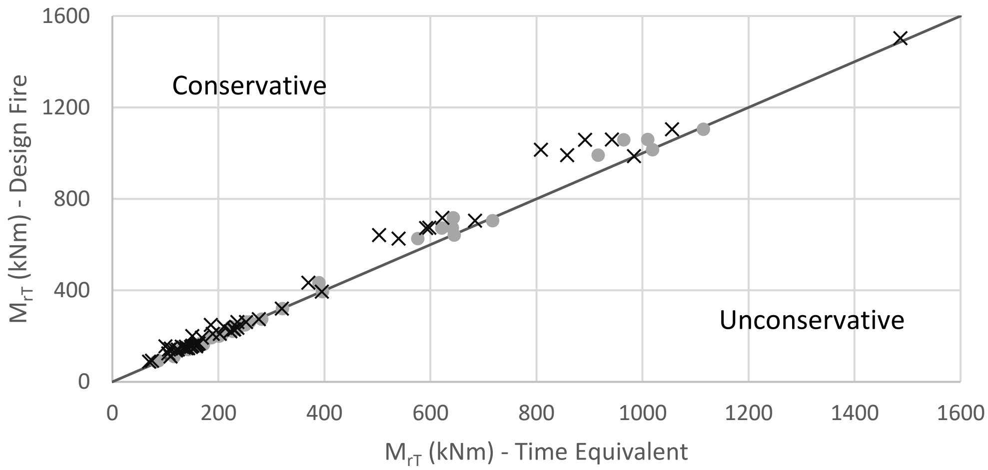

(a)

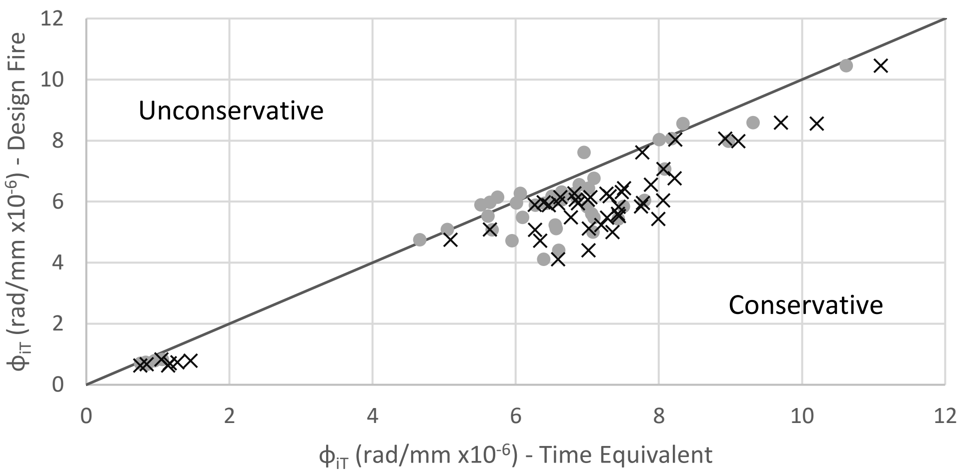

(b)

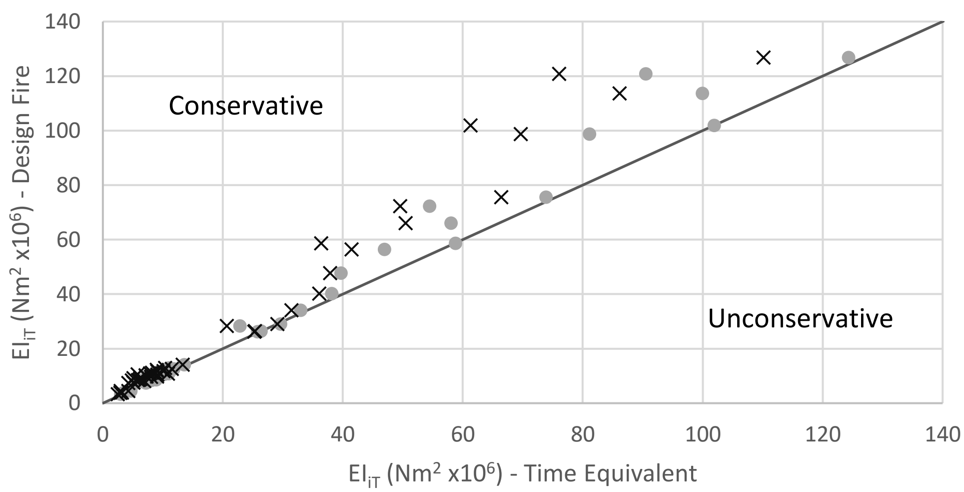

(c)

AITP Mean   AITP Conservative

Fig. 4.5 Design vs. AITP t_e Response for: (a) M_{rT}, (b) ϕ_{iT}, and (c) EI_{iT}

4.3 Comparison with Existing Methods

There are two existing time equivalent methods that are specifically applicable for RC beams. The first is presented in the Eurocode (EN 1991-1-2, 2002) and the second by Kodur et al. (2010). The Eurocode method was derived using the maximum temperature method for steel sections. As such, its applicability to evaluate the load capacity of RC elements has been disputed by Thomas et al. (1997) and Xie et al. (2017). Regardless, given the Eurocode's clear statement of applicability for concrete elements and its prominent standing as a design standard, it serves as a solid method for comparison. Kodur et al.'s (2010) method was derived based on the energy transfer of a natural fire to an RC beam. Kodur's results were found in Chapter 3 to be reasonably accurate in representing section internal temperatures; moment-curvature comparison will provide greater insight about the accuracy of the method.

Figure 4.6 shows the comparison between the mean AITP t_e, EN 1991-1-2 (2002), and Kodur et al. (2010). The comparison is made based on the moment-curvature responses of M_{rT}, φ_{iT}, and EI_{iT}. The three responses are recorded as a percent error from the value calculated using the design fire. A positive error indicates the time equivalent results in a conservative estimate of the actual design fire response, and a negative error indicates the opposite. The evaluation was undertaken for the beam section B2. Fire exposure was applied consistent with the seven design fires in Figure 4.2, allowing for assessment of the methods over a range of possible natural fire events.

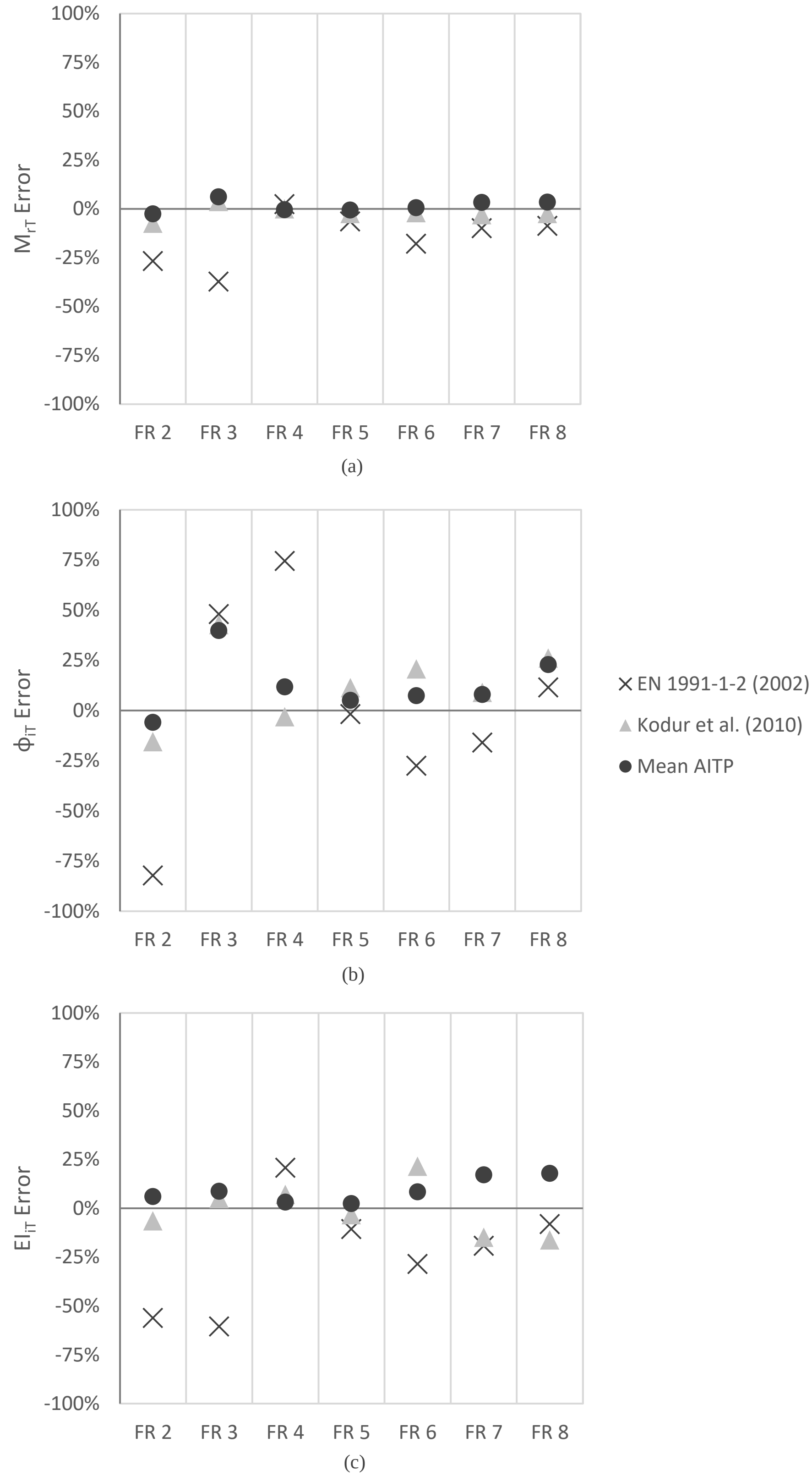

Fig. 4.6 Flexural Response of B2 for Existing Time Equivalent Methods

From Figure 4.6, the mean AITP t_e represents a high degree of accuracy in comparison with the existing methods. The Eurocode approach produces significantly deviant results across all three responses. The φ_{iT} in particular is poorly approximated by the Eurocode, with results ranging from 82 % unconservative for FR 1, to 74 % conservative for FR 4. Considering the inaccuracy of the Eurocode, it is evident that the consideration of internal concrete temperatures is critical to the determination of a t_e for RC elements.

Kodur's method presents a good level of accuracy, often producing comparable results to those developed by the AITP t_e. Although, in general, the AITP t_e produces slightly more accurate results. It should also be noted that the AITP t_e is often conservative when compared to Kodur's results. This is most evident for the EI_{iT} approximation during exposure to the experimental fires of FR 7 and FR 8. In this case, both methods record errors greater than 10 %, but the predictions of the AITP t_e are conservative, while those of Kodur's method are unconservative.

The conservative AITP t_e is not displayed on the figures. However, it should be noted, that given the same testing parameters, the conservative AITP t_e is the only method that consistently records conservative results for all responses and fire exposures.

4.4 Performance-Based Design of RC Beams Exposed to Natural Fire: A Case study

In this section, a case study is presented demonstrating a simplified approach to undertake performance-based flexural fire design of RC beams. The methodology proceeds in three sequential steps. Firstly, the severity of the fire event is determined by developing a natural temperature-time curve for a given compartment. The AITP t_e method is used to find an equivalent standard fire to define the severity of the natural fire event for an RC beam. Next, using a simple thermal model presented by Wickström (1986) and the equivalent standard fire from the previous step, the two-dimensional thermal gradients that develop within a RC section are determined. Lastly, flexural analysis is preformed to satisfy concrete equilibrium for both sagging and hogging conditions. The end result of the simplified analysis is the calculation of the sectional moment capacity (M_{rT}) during fire exposure. Application of the case study is performed on a section previously tested by Ellingwood and Lin (1991). The simplified analysis is validated using experimental results and an ABAQUS finite element (FE) model.

4.4.1 Severity of the fire event

Severity of a fire event is best represented by a temperature-time curve, which records a fire's temperature rise with time. The Eurocode provides a simple and well-documented approach to calculate a natural temperature-time curve based on a variety of compartment specific parameters (EN 1991-1-2, 2002). For smaller compartments, the Eurocode approach provides a reasonable and simple representation of fire severity (Buchanan, 2001). When considering larger floor areas, more numerous openings, or increased fuel loads; it is necessary to evaluate the effects of travelling fires (Dai et al., 2017).

In view of the fact that natural temperature-time curves are compartment specific, a time equivalent is used to relate the natural fire to the industry standard fire. By defining an equivalent standard fire duration, the wealth of experimental testing and material models derived using the standard fire, can be applied to a specific compartment. For RC beams, time equivalency can be determined using the AITP t_e proposed in Chapter 3. Although there are several existing time equivalent methods, the AITP method is tailored specifically for RC beams, and to the best of the author's knowledge, it is the only method that accounts for RC section dimensions (φ_{size}). Equation 3.4 and 3.6 can be used to calculate the AITP t_e and φ_{size}.

4.4.2 RC Internal Thermal Model

The simplest and best documented thermal model is provided by Wickström (1986). Using Equation 4.1, the temperature rise (T) can be calculated at any location (x, y) within a concrete beam exposed to a standard fire. It should be noted that this version of the equation is only valid for three-sided heating from the bottom and two sides. A more comprehensive version for 4-sided heating is presented by El-Fitiany (2013).

$$T = T_f\left[\eta_w\left(\eta_x + \eta_y - 2\eta_x\eta_y\right) + \eta_x\eta_y\right] \tag{4.1a}$$

$$\eta_w = 1 - 0.616\left(\frac{1550}{\sqrt{kc\rho}}\,t_e\right)^{-0.88} \geq 0 \tag{4.1b}$$

$$\eta_x = -2.18 + 0.23ln\left[\left(\frac{k}{c\rho a_c}\,t_e\right)^2 \frac{1}{x^2(b_c - x)^2}\right] \geq 0 \tag{4.1c}$$

$$\eta_y = 0.23ln\left[\left(\frac{k}{c\rho a_c}\,\frac{t_e}{y^2}\right) - 1.09\right] \geq 0 \tag{4.1d}$$

Where T_f is the standard fire temperature (ISO 834, 2014) of the compartment (°C) at duration t_e (hr), b_c is the beam width (mm), x is the distance of the point under consideration to the left or right face (mm), and y is the distance from the bottom side (mm). The dimensionless terms η_w, η_x, and η_y are the ratios of the beam's surface temperature to that of the fire temperature, the temperature at interior point x, and the temperature at interior point y, respectively. To account for variable concrete properties: k is the thermal conductivity ($Wm^{-1}K^{-1}$), p is the concrete density (kgm^{-3}), c_s is the specific heat of concrete ($Jkg^{-1}K^{-1}$), and a_c is the thermal diffusivity of concrete (m^2s^{-1}).

4.4.3 Sectional Flexure analysis

Fire induced strains consist of three terms (Equation 4.2): stress-related strain (ε_{fT}), free-thermal strain (ε_{th}), and transient strain (ε_{tr}) (Youssef and Moftah, 2007). Concrete's stress-related strain is a function of the applied stress and temperature. For ambient conditions, a stress-related strain (ε_f) of 0.0035 defines the ultimate compressive strain (ε_{cu}) at failure (CSA A23.3, 2014). For elevated temperatures, El-Fitiany (2013) found it reasonable to predict the ultimate compressive strain (ε_{cuT}) at a value of 0.0035 + ε_{tr}. Free-thermal strains define the expansion of concrete and steel when exposed to elevated temperatures. Simple equations to determine ε_{th} of siliceous and calcareous aggregate are presented in Equation 4.3 (Youssef and Moftah, 2007). For steel, the ε_{th} can be determined using the reinforcement temperature and the steel coefficient of thermal expansion (α_s). Equation 4.4 displays a relationship for α_s taken from Lie (1992). Transient strain develops during first heating of the concrete.

$$\varepsilon = \varepsilon_f + \varepsilon_{tr} + \varepsilon_{th} \tag{4.2}$$

Siliceous Aggregate:

$$\varepsilon_{th} = -1.8 \times 10^{-4} + 9 \times 10^{-6}(T-20) + 2.3 \times 10^{-11}(T-20)^3 \leq 14 \times 10^{-3} \tag{4.3a}$$

Calcareous Aggregate:

$$\varepsilon_{th} = -1.2 \times 10^{-4} + 6 \times 10^{-6}(T-20) + 1.4 \times 10^{-11}(T-20)^3 \leq 12 \times 10^{-3} \tag{4.3b}$$

$$\propto_s = 0.004T + 12 \times 10^{-6} \qquad T < 1000°\mathrm{C} \tag{4.4a}$$

$$\propto_s = 16 \times 10^{-6} \qquad T \geq 1000°\mathrm{C} \tag{4.4b}$$

$$\varepsilon_{tr} = \varepsilon_{0.3} \left(0.032 + 3.226 \frac{f_c}{f_c'}\right) \frac{V_a}{0.65} \tag{4.5a}$$

$$\begin{aligned} \varepsilon_{0.3} = &-43.87 \times 10^{-6} + 2.73 \times 10^{-8}\, T + 6.35 \times 10^{-8}\, T^2 \\ &-2.19 \times 10^{-10}\, T^3 + 2.77 \times 10^{-13}\, T^4 \end{aligned} \tag{4.5b}$$

For the above equations: T is the element temperature (°C); V_a is the volume fraction of aggregate, which can be taken as 0.65 (Purkiss, 2007); $\varepsilon_{0.3}$ is the transient strain for an initial stress of $0.3f'_c$, given in Equation 4.5b; and f_c / f'_c is the ratio of current to maximum concrete stress, at the point of failure this relationship can be simplified as $f_c / f'_c = 1.0$.

Three material models are needed in the proposed simplified analysis: concrete compressive strength at elevated temperature (f'_{cT}), steel yield strength at elevated temperature (F_{yT}), and the steel stress-strain relationship at elevated temperature (F_{sT}). A relationship for f'_{cT} developed by Hertz (2005) is presented in Equation 4.6, where: T is the concrete temperature (°C) and f'_c is the concrete strength at ambient temperature (MPa). The coefficients for siliceous aggregate are T_1 = 15,000, T_2 = 800, T_8 = 570, and T_{64} = 100,000; and for calcareous aggregate are T_1 = 100,000, T_2 = 1080, T_8 = 690, and T_{64} = 1000. When concrete is loaded prior to fire, f'_{cT} can be increased by 25 %, to a maximum of f'_c.

$$f'_{cT} = f'_c \left[\frac{1}{1 + \frac{T}{T_1} + \left(\frac{T}{T_2}\right)^2 + \left(\frac{T}{T_8}\right)^8 + \left(\frac{T}{T_{64}}\right)^{64}} \right] \tag{4.6}$$

Equations 4.7 and 4.8 display the F_{yT} *and* F_{sT} (Lie, 1992). In these equations: T is the steel temperature (°C), F_y is the steel yield strength at ambient temperature (MPa), ε_{sT} is the steel total strain, and ε_p is the ambient yield strength (MPa) divided by 25 x 10^4 MPa.

$$F_{yT} = \left[1 + \frac{T}{900\ ln\left(\frac{T}{1750}\right)}\right] F_y \qquad 0 < T \ \leq 600\ ℃ \tag{4.7a}$$

$$F_{yT} = \left[\frac{340 - 0.34T}{T - 240}\right] F_y \qquad 600 < T \ \leq 1000\ ℃ \tag{4.7b}$$

$$F_{sT} = \frac{f(T, 0.001)}{0.001}\varepsilon_{sT} \qquad \varepsilon_{sT} \leq \varepsilon_p \tag{4.8a}$$

$$F_{sT} = \frac{f(T, 0.001)}{0.001}\varepsilon_p + f\left[T, \left(\varepsilon_s - \varepsilon_p + 0.001\right)\right] - f(T, 0.001) \qquad \varepsilon_{sT} > \varepsilon_p \tag{4.8b}$$

$$where\ f(T, \lambda) = (50 - 0.04T) \times \left[1 - \left(e^{-30+0.03T}\sqrt{\lambda}\ \right)\right] \times 6.9 \tag{4.8c}$$

At ambient temperatures, flexural equilibrium conditions can be easily satisfied using the equivalent stress-block parameters (α_1 and β_1). This concept can also be applied to RC beams at elevated temperatures. El-Fitiany and Youssef (2011) proposed Equations 4.9 and 4.10 to calculate α_{1T} and β_{1T} for sagging and hogging conditions at elevated temperatures. In Equation 4.9 and 4.10: t_e is the duration of the ISO-standard fire (hr), p_s is the reinforcement ratio, and F_{agg} accounts for aggregate type wherein siliceous aggregate should be taken as zero and calcareous aggregate should be taken as 1.0.

Sagging Condition:

$$\alpha_{1T} = \alpha_1 - 1.533 \times 10^{-2} + 24.397 \times 10^{-3}t_e + 15.758 \times 10^{-4}f_c' - 10.089 \times 10^{-5}b_c \tag{4.9a}$$

$$\beta_{1T} = \beta_1 - 2.907 \times 10^{-2} + 20.734 \times 10^{-3}t_e^2 - 94.794 \times 10^{-3}t - 75.057 \times 10^{-5}f_c' + 15.413 \times 10^{-5}b_c \tag{4.9b}$$

Hogging Condition:

$$\alpha_{1T} = \alpha_1 - 2.735 \times 10^{-2} - 1.497 \times 10^{-1}t_e + 7.579 \times 10^{-2}F_{agg} \tag{4.10a}$$

$$\beta_{1T} = \beta_1 - 1.965 \times 10^{-1} - 4.054 \times 10^{-2}\left(\frac{t_e}{\rho}\right)^2 + 2.448 \times 10^{-1}\left(\frac{t_e}{\rho}\right) - 3.456 \times 10^{-2}F_{agg} + 3.687 \times 10^{-3}f_c' + 2.342 \times 10^{-4}b_c \tag{4.10b}$$

Equation 4.11 displays the equilibrium equations, which are identical in form to the ambient, but substituted with the material stresses and stress-block parameters at elevated temperature. Sectional moment capacity at elevated temperature can likewise be solved for by resolving the moment induced by the internal forces (Equation 4.12).

$$C_{cT} = \alpha_{1T} \times f'_{cT} \times \beta_{1T} \times c \times b_c \tag{4.11a}$$

$$T_{sT} = F_{sT} \times A_s \tag{4.11b}$$

$$C_{cT} = T_{sT} \tag{4.11c}$$

$$M_{rT} = \sum T_{sT} \left(d - \frac{\beta_{1T} \times c}{2} \right) \tag{4.12}$$

Where: C_{cT} is the compression force in the concrete at elevated temperature, c is the depth of the neutral axis, b_c is the width of the compression zone, T_{sT} is the tension force in the steel at elevated temperature, A_s is the area of steel, and d is the effective depth of the tension force element.

4.4.4 Ellingwood and Lin (1991)

The case study is undertaken for a cross-section and natural fire matching the work of Ellingwood and Lin (1991). Their work focused on section internal temperatures during exposure. Failure was not induced during testing, and as such, no ultimate capacity was recorded. To the best of the author’s knowledge, no testing has been published recording RC beams tested to capacity failure during exposure to natural fire. Therefore, the results from Ellingwood and Lin (1991) are used to validate the internal temperature approximations, while validation of the flexural capacity is done using ABAQUS FEM.

Figure 4.7 shows the section details of the experimental beam, measuring 228 x 533 mm in cross-section. Concrete mix design stipulated the use of NSC with Type I Portland cement and calcareous gravel aggregate. Lower longitudinal reinforcement consists of 4-22 mm bars, while upper reinforcement consists of 4-25 mm bars. In the analysis, only lower reinforcement will be considered for the sagging condition, and only upper reinforcement for the hogging condition; therefore, ignoring the effect of compression steel. Shear reinforcement is provided by 10 mm stirrups spaced at 215 mm intervals. Concrete cover to traverse reinforcement stirrups is 38 mm. Ambient material properties specified a f'_c of 33.7 MPa and F_y of 420 MPa.

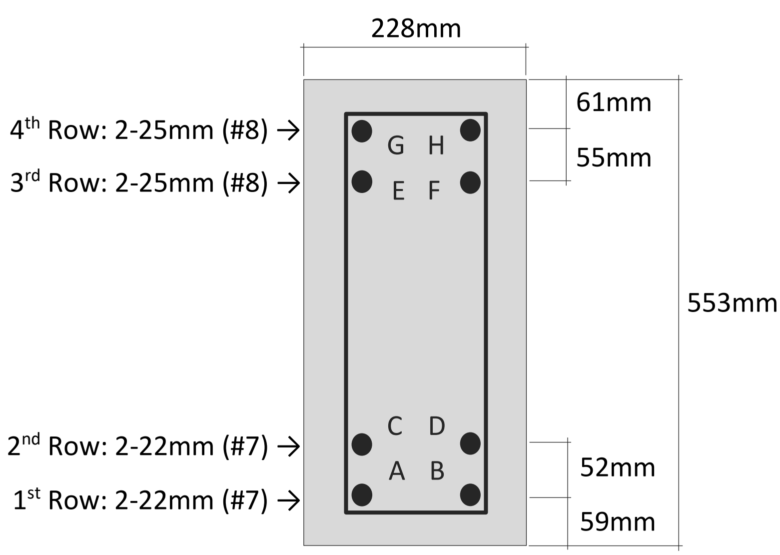

Fig. 4.7 Ellingwood and Lin (1991) Beam Cross-Section

4.4.5 Simplified Performance-Based Analysis

Severity of the fire event is represented as a temperature-time relationship. For a compartment fire this can be done using the Eurocode method, but in the case of Ellingwood and Lin (1991), the design fire was experimentally recorded (Figure 4.8). The key points for the AITP t_e are identified on the figure as: T_{max} = 1011°C, t_{max} = 37.4 min, and t_{final} = 145 min. The final duration (t_{final}) is found by linearly extending the cooling branch, ignoring the long cool-down period. Using Equation 3.4, the AITP conservative t_e is found to be 96 min (1.60 hr) and the AITP mean t_e 93 min (1.56 hr). There is only a small change between the mean and conservative durations, however, it should be noted that this is not generally the case and should not be inferred as such. Due to the similarity between the two, worked examples and figures are only shown for the conservative t_e, with final results presented in text for both the mean and conservative t_e. The width of the section is less than 350 mm, and therefore the φ_{size} does not need to be applied to the t_e.

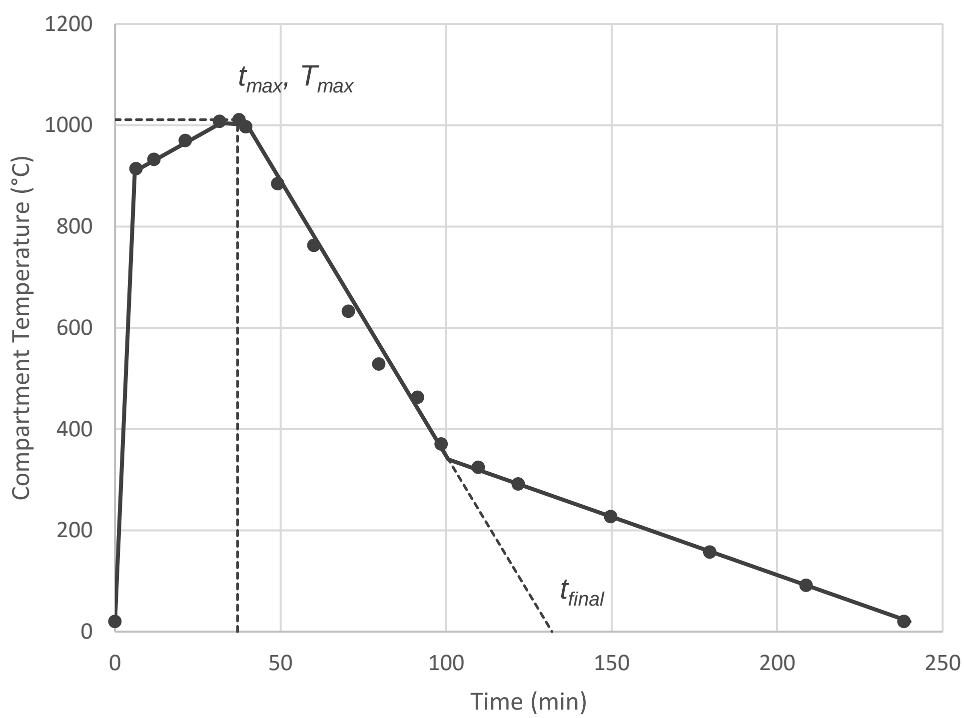

Fig. 4.8 Ellingwood and Lin (1991) Applied Design Fire

Section internal temperatures are calculated using Equation 4.1. Considering the selected NSC with calcareous aggregate, the values for the concrete thermal properties are taken as: k = 1.0 $Wm^{-1}K^{-1}$, p = 2400 kgm^{-3}, c_s = 1000 $Jkg^{-1}K^{-1}$, and a_c = 417x10^{-9} m^2s^{-1} (Lie, 1992). Depending on the mix design and aggregate, these values can vary greatly.

For the steel bars, temperature is found within the section at the x and y locations of the reinforcement. Because heating is assumed to occur evenly from the two sides, both the left and right bars in a given row exhibit the same temperature. The bar temperatures for the conservative t_e are as follows: row 1, 528°C; row 2, 331°C; row 3, 297°C; and row 4, 297°C. For the mean t_e, the bar temperatures are only slightly lower at: row 1, 518°C; row 2, 320°C; row 3, 290°C; and row 4, 290°C. Wickström's (1986) method assumes that temperature gradients will become linear at some height, hence rows 3 and 4 having the same temperature.

Determining the concrete temperature is less straight forward than the reinforcement, as it varies significantly throughout the section. Material and strain models however require a single input temperature. El-Fitiany and Youssef (2017) have proven that the thermal effects of a fire can be estimated with sufficient accuracy using a concrete average temperature (T_{av}). For the sagging scenario, T_{av} can be found by taking the temperature average along the section's width at a given depth. At the depth of the compression zone, the temperature gradient becomes almost constant with height since heat flow in that region is governed by the two vertical sides. Therefore, by taking the T_{av} within the compression zone, a single concrete temperature can be identified. Using Equation 4.1, T_{av} was calculated by sampling internal temperatures along the section's width at a constant height. Samples were taken at 12 width increments and a height of $0.8h_c$. The selected height represents a location where the thermal distribution is assumed to be constant. Taking a weighted average of the samples finds T_{av} as 412°C for the conservative t_e and 405°C for the mean t_e.

For the hogging condition, temperature gradients at the bottom face vary greatly and do not exhibit the same constant profile experienced near the upper face. As such, calculation of a single T_{av} can not be achieved for a simplified analysis. The resulting equilibrium calculation for hogging is entirely based on steel temperature and does not require a concrete temperature. The effect of non-linear concrete temperature is implicitly included in the stress-block parameters.

Flexural analysis is laid out for the sagging load in Tables 4.3 and 4.4. For simplicity, the tension capacity of concrete, effects of concrete confinement, and compression reinforcement are omitted. Results in the tables are only displayed based on the conservative t_e temperatures. Material properties and fire induced strains are first calculated for the concrete section based on T_{av}. Assuming the c value as 102.2 mm, the force in the compression block is found as 441 kN. Based on a linear strain distribution, Equation 4.13 provides the geometric relationship needed to interpolate the concrete strain at the height of the reinforcing rows. Fire-induced strains and steel stresses at elevated temperatures are likewise calculated for each layer of steel reinforcement. The c value is iterated until equilibrium between the concrete and steel occurs.

$$\varepsilon_{tots} = \frac{d}{c}\varepsilon_{cuT} - \varepsilon_{totc} \tag{4.13}$$

Hogging analysis is presented in Table 4.5. Because a T_{av} could not be determined, concrete strains, and subsequently steel strains, are not required. Steel yield stress is used in place to find the tension force at each row of reinforcement. The assumed c value is iterated until equilibrium is satisfied at 146.2 mm. For both sagging and hogging scenarios, Equation 4.12 finds the maximum M_{rT} based on the conservative t_e exposure to be 178.5 kNm and 257.6 kNm, respectively. By the same approach, the mean t_e finds sagging M_{rT} as 181.0 kNm and hogging M_r as 259.9 kNm.

Table 4.3 Sagging Flexure Analysis for Concrete

(1)	(2)	(3)	(4)	(5)	(6)	(7)	(8)	(9)	(10)
T_{av}	f'_{cT}	α_{1T}	β_{1T}	ε_{tr}	ε_{cuT}	ε_{th}	ε_{totc}	c	C_c
(Eq.4.1)	(Eq.4.6)	(Eq.4.9a)	(Eq.4.9b)	(Eq.4.5)	(5)+0.0035	(Eq.4.3)	(6)-(7)	assume	(Eq.4.11a)
°C	MPa	---	---	x 10^{-3}	x 10^{-3}	x 10^{-3}	x 10^{-3}	mm	kN
412	28.9	0.85	0.77	11.11	14.61	3.33	11.28	102.2	441

Table 4.4 Sagging Flexure Analysis for Steel

(1)	(2)	(3)	(4)	(5)	(6)	(7)	(8)	(9)
ID	T	A_s	α_s	ε_{tots}	ε_{th}	ε_{sT}	F_{sT}	T_s
---	(Eq.4.1)	---	(Eq.4.4)	(Eq.4.13)	(2)x(4)	(5)-(6)	(Eq.4.8)	(3)x(8)
---	°C	mm^2	x 10^{-5}	x 10^{-3}	x 10^{-3}	x 10^{-3}	MPa	kN
A, B	528	387	1.42	56.49	7.45	49.04	239	93
C, D	331	387	1.33	49.05	4.42	44.64	331	128

Table 4.5 Hogging Flexure Analysis for Concrete and Steel

(1)	(2)	(3)	(4)
α_{1T}	β_{1T}	c	C_c
(Eq.4.10a)	(Eq.4.10b)	assume	(Eq.4.11a)[1]
---	---	mm	kN
0.61	1.02	146.2	696

(1)	(2)	(3)	(4)	(5)
ID	T	A_s	F_{yT}	T_s
---	(Eq.4.1)	---	(Eq.4.7)	(3)x(4)
---	°C	mm^2	MPa	kN
E, F, G, H	297	509	342	174

[1] *In lieu of f'_{cT}, f'_c for ambient temperatures should be used during hogging analysis*

4.4.6 FE Modelling

An ABAQUS FE model is used to validate the flexural capacity and compliment the experimental temperature results from Ellingwood and Lin (1991). A detailed description of the ABAQUS model is provided in Appendix B. The beam was modelled using solid elements to facilitate the heat transfer analysis, which is not possible using the wire reinforcement approach. To ensure flexural failure, the section outlined in Figure 4.8 was given an arbitrary length of 6 m to ensure flexural failure. Simple support conditions were specified at the ends. Heat transfer was applied based on the given design fire with material properties specified for NSC calcareous aggregate by Lie (1992). Evaluating the fire event as an uncoupled load, the heat transfer profile of the beam was input into the strength analysis as a predefined condition. Uniform loading was applied at various intervals until failure was observed based on strain non-convergence in ABAQUS.

4.4.7 Case Study Evaluation

Comparing the simplified analysis with the experimental and ABAQUS results demonstrates the accuracy of the proposed methodology. Figure 4.9 presents the internal temperatures for the section based on natural fire (Figure 4.9a) and conservative t_e fire exposure (Figure 4.9b). The general isotherm profiles were developed using ABAQUS. Labelled reinforcement temperatures are based on Ellingwood and Lin's (1991) experimental results for the natural fire (Figure 4.9a) and based on Wickström's (1986) method for the conservative t_e fire (Figure 4.9b).

The conservative t_e records moderately conservative temperatures at just about every location within the section. The only exception occurs in the lower middle region, where the time equivalent results in a maximum negative differential of 56°C. This formation is due to the natural fire, with its long duration, being able to slowly heat the internals of the section. The time equivalent fire is not able to match this slow heating effect, and therefore small deviations will always arise in the lower middle region. Wickström's method found the reinforcement temperatures with a reasonable degree of accuracy. The largest error from the experimental results occurred in row 1 at 32 %. Despite the error, the simplified analysis resulted in a conservative temperature estimate for the reinforcement. Using the natural fire profile from ABAQUS, calculation of T_{av} at a height of $0.8h_c$ yields 325°C. The simplified analysis using the conservative t_e found T_{av} as 412°C, representing a 27 % conservative result to the FEM.

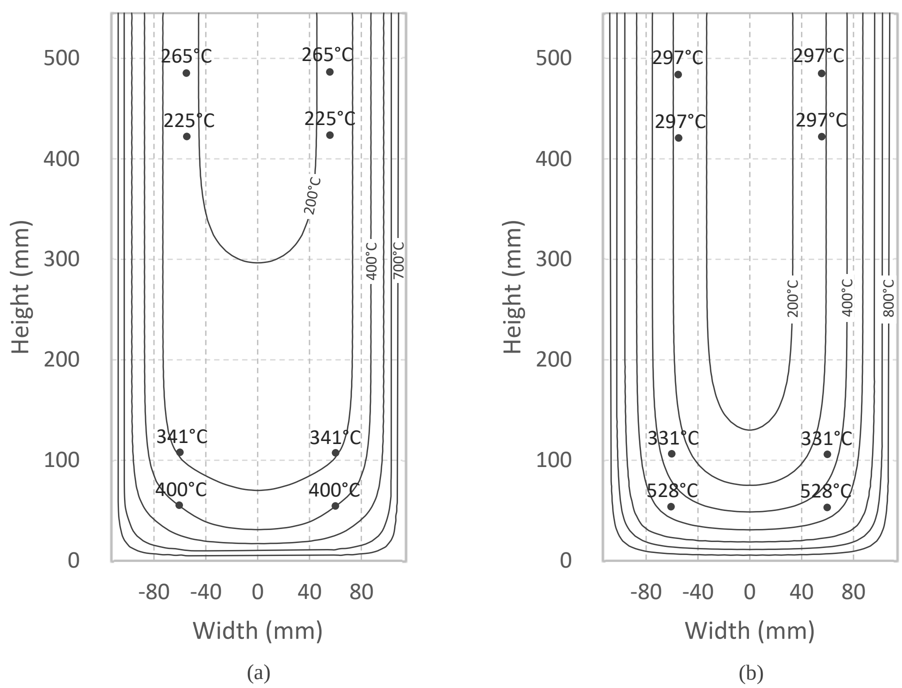

Fig. 4.9 Thermal Gradients due to (a) Natural Fire and (b) Conservative Time Equivalent Fire Exposure

Figure 4.10 presents the AITPs of the section during exposure to the experimental design fire and the time equivalent standard fires. The AITP profiles were developed using the methodology of Section 3.2. The mean t_e profile indicates a good correlation with the design fire, and the conservative t_e generates higher temperatures throughout.

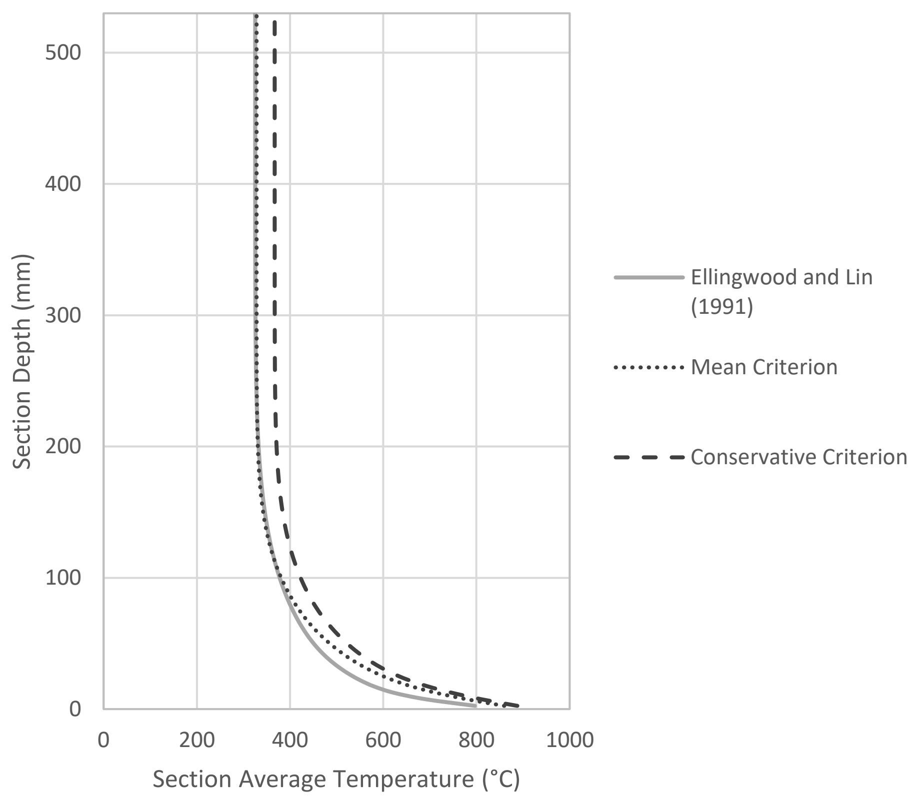

Fig. 4.10 AITP for Case Study Beam Based on Given Exposure Fires

The final moment capacities calculated by the simplified analysis and using ABAQUS are recorded in Table 4.6. For all cases, the simplified analysis records a lower, and thus conservative capacity to the FE analysis. The capacity found using the mean t_e is within 10 % for both the sagging and hogging conditions. Considering the similarity of the mean and conservative t_e durations, the two criterions result in only minor capacity differences. However, it should once again be noted that this minor difference is not generally the case, and will vary depending on section details and fire exposure.

Table 4.6 Moment Capacity Results

ABAQUS Analysis	Simplified Analysis	Absolute Difference
Conservative t_e Sagging		
198 kNm	179 kNm	10 %
Conservative t_e Hogging		
284 kNm	258 kNm	9 %
Mean t_e Sagging		
198 kNm	181 kNm	8 %
Mean t_e Hogging		
284 kNm	260 kNm	8 %

At ambient temperatures, standard sectional analysis finds the sagging capacity of the section to be 263 kNm and the hogging capacity as 328 kNm. In comparison with the moment capacities of the fire exposed section found by ABAQUS, this represents a 27 % and 14 % capacity reduction for the sagging and hogging conditions respectively. The marked change in moment capacity from ambient to fire exposed, strongly demonstrates the impact of fire events on RC beams and the necessity of undertaking a simplified analysis as proposed here.

4.5 Conclusion

The AITP t_e method, introduced in Chapter 3 of this thesis, was assessed based on the flexural response of beam sections. Using finite difference software developed by Youssef and El-Fitiany (2007), the M-φ relationship of RC beams during fire exposure was developed. A parametric study was undertaken to compare the M-φ response of beams exposed to a range of design fires and standard fires with an AITP t_e duration. To assess the AITP method for a larger number of cases, three key responses from the M-φ relationship were selected for evaluation: maximum moment, initial curvature, and initial stiffness. Evaluation of the key responses displayed good correlation between the AITP mean t_e and the design fire. Additionally, the conservative time equivalent produced a M-φ

profile with lesser moments and larger curvatures for every test case. Further comparison was undertaken with relation to existing time equivalent methods. The study demonstrated the improved accuracy of the AITP te in approximating the flexural response of RC beams.

The section concluded with a case study to present the application of the AITP t_e in performance-based design. For a given compartment, fire severity is determined as a temperature-time relationship and related using the AITP t_e to the standard fire. In leu of complex computational programs, a simple thermal model is used to determine the internal temperature at critical locations within the exposed RC element. Substituting material and strain models for RC at elevated temperatures, the equilibrium condition is resolved using the equivalent-stress block method. Internal temperatures and flexural capacity were found to be in good agreement with validation based on experimental and computational analysis.

4.6 References

Buchanan, A.H. *Structural Design for Fire Safety*. 2nd ed. Wiley, 2001.

CSA A23.3. *Design of Concrete Structures, 6th ed*. Canadian Standards Association. Mississauga, Canada. 2014.

Dai, X., S. Welch, A. Usmani. “A Critical Review of Travelling Fire Scenarios for Performance-Based Structural Engineering.” *Fire Safety Journal*, vol. 91, no. 1, 2017, pp. 568-578.

Dembsey, N.A., P.J. Pagni, and R.B. Williamson. “Compartment Fire Experiments: Comparison with Models.” *Fire Safety Journal*, vol. 25, no. 1, 1995, pp. 187-227.

El-Fitiany, S.F. and M.A. Youssef. “Fire Performance of Reinforced Concrete Frames Using Sectional Analysis.” *Engineering Structures*, vol. 142, no. 1. 2017, pp. 165-181.

El-Fitiany, S.F. and M.A. Youssef. “Stress-Block Parameters for Reinforced Concrete Beams during Fire Events.” *ACI Special Publication: Innovations in Fire Design of concrete Structures*, SP-279, 2011, pp. 1-40.

El-Fitiany, S.F. *Simplified Tools for Performance-Based Design of reinforced Concrete Frames Exposed to Fire*. Diss. University of Western Ontario, 2013.

El-Fitiany, S.F., and M.A. Youssef. "Assessing the Flexural and Axial Behaviour of Reinforced Concrete Members at Elevated Temperatures Using Sectional Analysis." *Fire Safety Journal*, vol. 44, no. 5, 2009, pp. 691-703.

Ellingwood, B. and T.D. Lin. "Flexure and Shear Behaviour of Concrete Beams During Fires." *Journal of Structural Engineering*, vol. 117, no. 2, 1991, pp. 440-458.

EN 1991-1-2. *Eurocode 1: Actions on Structures - Part 1-2: Actions on structures Exposed to Fire*. European Committee for Standardization. Brussels, Belgium. 2002.

Hertz, K.D. "Concrete Strength for Fire Safety Design." *Magazine of Concrete Research*, vol. 57, no. 8, 2005, pp. 445-453.

Implementation of Eurocodes. *Handbook 5 - Design of Buildings for the Fire Situation*. Leonardo Da Vinci Joint Research Project, 2005.

ISO 834. *Fire Resistance Tests – Elements of Building Construction*. International Organization for Standards. Geneva, Switzerland. 2014.

Kirby, B.R., D.E. Wainman, L.N. Tomlinson, T.R. Kay, and B.N. Peacock. "Natural Fires in Large Scale Compartments." *International Journal on Engineering Performance-Based Fire Codes*, vol. 1, no.2, 1999, pp. 43-58.

Kodur, V.K.R., P. Pakala, and M.B. Dwaikat. "Energy Based Time Equivalent Approach for Evaluating Fire resistance of Reinforced Concrete Beams." *Fire Safety Journal*, vol. 45, no. 4, 2010, pp. 211-220.

Lennon, T. *Results and Observations from Full-Scale Fire Test at BRE Cardington*. no. 215-741, Building Research Establishment, Cardington, UK, 2004.

Lie, T.T. *Structural Fire Protection*. ASCE, 1992.

Purkiss, J.A. *Fire Safety Engineering, Design of Structures*. Elsevier Ltd, 2007.

Terro, M.J. “Numerical Modeling of the Behaviour of concrete Structures.” *ACI Structural Journal*, no. 95-S18, 1998, pp. 183-192.

Wickström, U. *A Very Simple Method for Estimating Temperature in fire Exposed Concrete Structures*. Technical Report SP-RAPP 1986:46, Swedish National Testing Institute, Boras, Sweden, 1986.

Youssef, M.A. and M. Moftah. “General Stress-Strain Relationship for Concrete at Elevated Temperatures.” *Engineering Structures*, vol. 29, no. 10, 2007, pp. 2618-2634.

Chapter 5

5.0 Equivalent Standard Fire Duration to Evaluate Internal Temperatures in Natural Fire Exposed RC Columns

In Chapter 3 and 4 of this thesis, a time equivalent method was proposed for the application of reinforced concrete (RC) beams. This chapter presents a continuation of that work, focusing on the development of a time equivalent (t_e) for RC columns. The average internal temperature profile (AITP) t_e is derived by comparing the actual internal temperatures that develop in a concrete section exposed to natural and standard fire. During fire exposure, a typical beam undergoes heating from three sides, while a typical column undergoes heating on all four faces. Although a seemingly minor difference, the interaction of 4-sided heating has a significant effect on the internal temperature gradients, and in turn the section behaviour. Existing time equivalent methods have failed to make the distinction between the different heating scenarios, and to the best of the author's knowledge, no general method is available to evaluate the time equivalent for RC columns undergoing 4-sided natural fire exposure. In this chapter, the suitability of the proposed AITP t_e is assessed for the application of 4-sided heating by examining section internal temperatures and mechanical responses.

5.1 Application of the AITP for RC Columns

The application of AITPs was first proposed by El-Fitiany and Youssef (2009) as a simplified technique to evaluate the two-dimensional thermal gradients that develop within RC cross-sections during fire exposure. An AITP describes a section's internal temperatures as a function of depth, allowing for the analysis of RC elements resisting axial loading and uniaxial bending. To develop an AITP, a concrete section is first divided into a fine two-way mesh. Heat transfer is conducted using any acceptable method such as the finite difference method provided by Lie (1992). Throughout the heat transfer process, the maximum temperature experienced in each mesh block is recorded. At the end of the fire exposure, the meshed units are grouped into horizontal layers of equal height, and the average temperature for each layer is calculated. Subsequently, the AITP represents the maximum temperature experienced by each layer throughout the fire event. Figure 5.1 displays an example of the AITP developed for a 400 x 400 mm column and a 400 x 400 mm beam during exposure to a 1-hr ISO standard fire (ISO 834, 2014). Column 4-sided heating and beam 3-sided heating is undertaken consistent with Figure 5.1a and 5.1b. The AITP consists of two zones: highly-variable (non-linear) zones near the surface where temperatures are rapidly changing, and a constant zone (linear) near the core where temperatures are relatively consistent. For columns, the presence of heating along the top surface of the element creates a profile with two variable zones. As a result, the AITP for columns deviates markedly from that of beams.

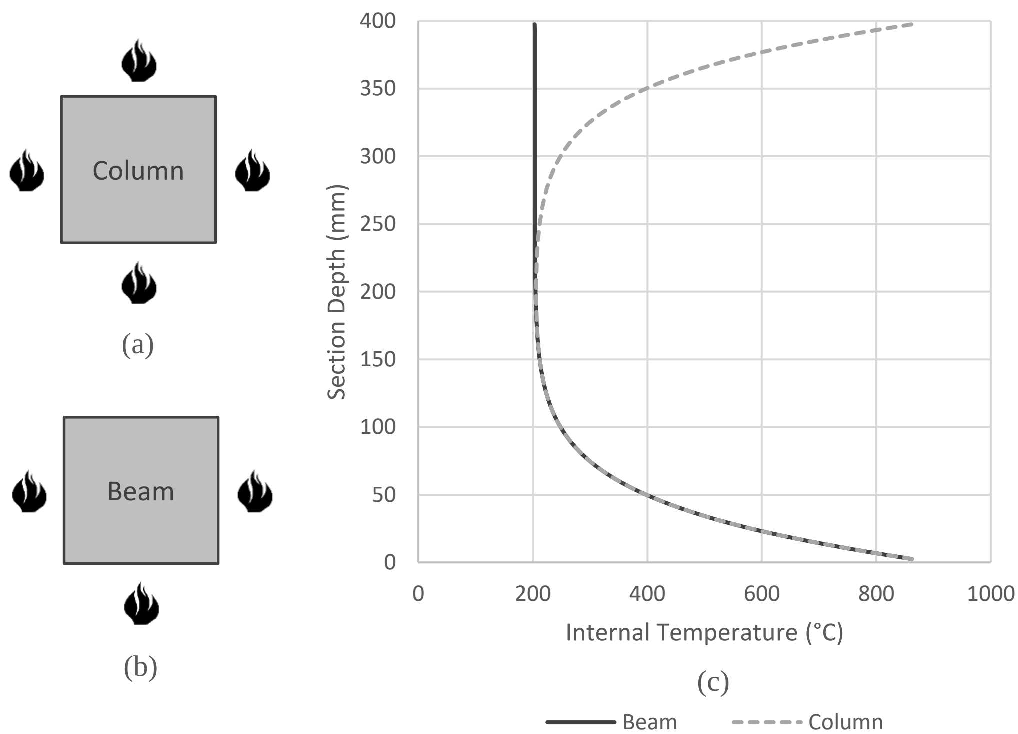

Fig. 5.1 (a) 4-Sided Heating, (b) 3-Sided Heating, and (c) AITP of Column and Beam for 1-hr ISO Standard Fire

5.2 Review of the AITP Time Equivalent

The AITP t_e is derived based on the correlation of the AITP developed by a selected design fire (AITP-D) and a standard fire with a specific duration (AITP-S). There are two criteria for correlation, mean and conservative. The mean criterion compares the percent difference between AITP-D and AITP-S at every layer of the profile and records the average percent difference for all of the layers. The duration of the standard fire is incrementally increased until the lowest absolute average percent difference is found. The conservative criterion ignores error differences, iterating the duration of the standard fire until the AITP-S has equal or larger temperatures at every layer when compared to AITP-D. Using the two criteria, the AITP t_e can be found to accurately or conservatively represent the severity of a fire event on an RC section.

Using the AITP methodology, Equation 5.1 was derived in Chapter 3 to evaluate the AITP t_e for 3-sided fire exposure. The maximum fire temperature, T_{max} (°C); the corresponding time, t_{max} (min); and the overall duration of the fire, t_{final} (min); were selected to define the general equation. The valid range and coefficients for Equation 5.1 are presented in Table 5.1. Equation 5.1 is only valid for concrete sections with width (b_c) of 250 mm and height (h_c) of 500 mm. To account for other section dimensions, the calculated t_e shall be multiplied by a size adjustment factor (ψ_{size}) given by Equation 5.2. The valid range for application of the ψ_{size} is detailed in Table 5.2 along with the coefficients of Equation 5.2.

$$\begin{aligned} t_e &= A + Bt_{max} + Ct_{final} + DT_{max} + Et_{max}^2 + Ft_{final}^2 + GT_{max}^2 \\ &\quad + Ht_{max}t_{final} + It_{max}T_{max} + Jt_{final}T_{max} \end{aligned} \tag{5.1}$$

$$\psi_{size} = \begin{cases} 1.0 \begin{cases} for\ bc < 300\ m \\ for\ conservative\ t_e\ when\ T_{max} > 1150℃ \\ for\ conservative\ t_e\ when\ t_e > 180\ min \end{cases} \\ \\ A + Bt_{max} + Ct_{final} + DT_{max} \\ \quad + b_c\left(E + Ft_{max} + Gt_{final} + HT_{max}\right) \geq 1.0 \end{cases} \tag{5.1}$$

Table 5.1 Coefficients for Equation 5.1

		Mean Criterion	Conservative Criterion			
Valid Range	t_{max} (*min*)	15 - 115	15 - 115	15 - 115	15 - 115	15 - 115
	t_{final} (*min*)	20 – 240	20 – 240	20 – 240	20 – 240	20 – 240
	T_{max} (°C)	350 – 1100	350 - 750	750 - 950	950 - 1100	1100 - 1200
Coefficients	**A**	8.124	8.690	2.370	566.30	4404.0
	B	-0.153	-0.0829	-0.0893	-0.465	-5.745
	C	0.0384	0.0324	0.0446	1.188	1.039
	D	-0.0431	-0.0429	-0.0186	-1.332	-8.177
	E	-8.53×10^{-4}	-4.74×10^{-4}	-9.42×10^{-4}	-20.00×10^{-4}	-80.87×10^{-4}
	F	-6.46×10^{-4}	-4.16×10^{-4}	-7.39×10^{-4}	0.0	2.99×10^{-4}
	G	0.50×10^{-4}	0.66×10^{-4}	0.35×10^{-4}	7.95×10^{-4}	38.36×10^{-4}
	H	3.44×10^{-4}	1.57×10^{-4}	4.77×10^{-4}	-3.07×10^{-4}	-17.80×10^{-4}
	I	6.55×10^{-4}	5.33×10^{-4}	5.40×10^{-4}	12.05×10^{-4}	69.36×10^{-4}
	J	4.52×10^{-4}	3.70×10^{-4}	4.71×10^{-4}	-9.00×10^{-4}	-8.40×10^{-4}

* Equation 5.1 is only valid for sections of 250 x 500 mm in size

Table 5.2 Coefficients for Equation 5.2

	Mean Criterion	Conservative Criterion
Valid Range	$200 \le b_c \le 800$ mm	$200 \le b_c \le 800$ mm
	$300 \le h_c \le 800$ mm	$300 \le h_c \le 800$ mm
	$15 \le t_{max} \le 115$ min	$15 \le t_{max} \le 115$ min
	$20 \le t_{final} \le 240$ min	$20 \le t_{final} \le 240$ min
	$600 \le T_{max} \le 1200$°C [1]	$350 \le T_{max} \le 1200$°C
A	1.022	0.819
B	-2.57×10^{-4}	3.78×10^{-4}
C	2.69×10^{-4}	-2.23×10^{-4}
D	-0.22×10^{-4}	1.82×10^{-4}
E	0.113	1.037
F	-8.23×10^{-4}	-27.00×10^{-4}
G	14.01×10^{-4}	27.15×10^{-4}
H	-1.93×10^{-4}	-10.75×10^{-4}

[1] Excluding $T_{max} < 750$ °C reached during $t_{max} < 60$ min

5.3 Applicability of the AITP t_e for RC Columns

In this section, the methodology of the AITP t_e is assessed in view of 4-sided fire exposure. A parametric study was conducted to assess its suitability for a wide range of possible design fire exposures and cross-section dimensions as follows.

5.3.1 Test Parameters

Design fires were constructed using the defining parameters of t_{max}, t_{final}, and T_{max}. The accepted values for each parameter were selected at intervals such that the developed design fires are reasonably spaced. Values for t_{max} were chosen at 5-min intervals until 30 min, then at 17-min intervals until 115 min; values for t_{final} were chosen at 20-min intervals throughout; and T_{max} values were chosen starting from 350°C at 100°C intervals until 650°C, then at 50°C intervals until 1200°C. Any combination with $t_{max} \geq t_{final}$ was immediately excluded, resulting in a total of 1290 design fires. Knowing the defining parameters, the full design fire curve was developed using the Eurocode approach for the heating branch and a linear profile for the cooling branch (EN 1991-1-2, 2002). The derived t_e duration is based on the ISO standard fire (ISO 834, 2014).

Similar to the study in Chapter 3, cross-sections were evaluated with width and height combinations of 250 x 500, 400 x 500, 600 x 500, and 800 x 500 mm. Additionally, four square cross-sections were evaluated having dimensions of 250, 400, 600, and 800 mm. Normal strength concrete (NSC) with siliceous aggregate was consistently used throughout the study. The thermal properties of NSC with siliceous aggregate were taken as defined in Lie (1992). Considering the 1290 design fires and eight cross-sections, 10,320 test cases were analyzed based on the AITP mean and conservative criteria.

5.3.2 Conservative AITP t_e Evaluation

The conservative t_e for 4-sided exposure was found to be highly similar in duration to that of the previously identified 3-sided t_e. Figure 5.2 displays the percent difference in the t_e duration between 3-sided and 4-sided exposure versus the column t_e duration in minutes. The values on the figure were numerically derived using the methodology of Section 5.2. A positive percentage change indicates the column t_e is longer, while a negative change indicates the opposite. From the figure, the column t_e can be seen to exhibit a relatively similar duration to the beam t_e. Of the evaluated cases, none required a decrease in the t_e duration. Although, several test cases do require a minor increase to the column t_e.

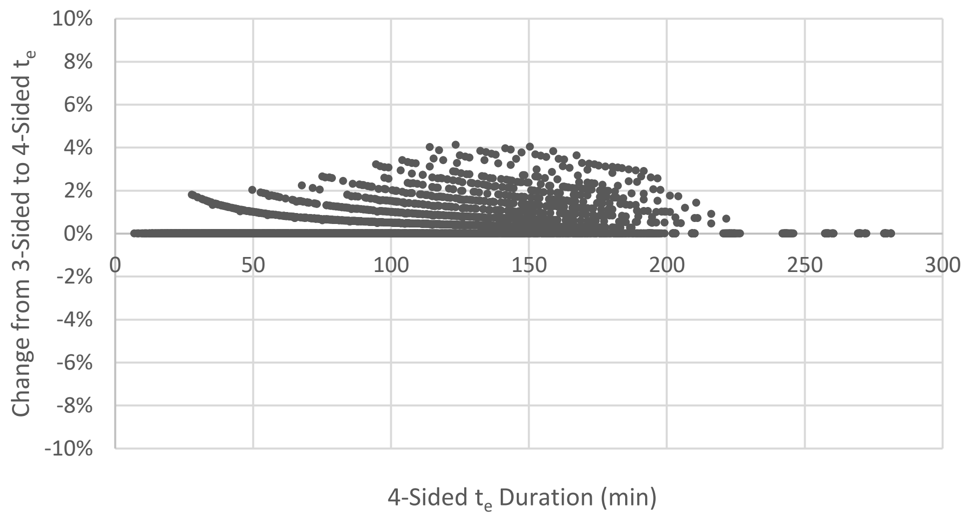

Fig. 5.2 Change in Conservative t_e from 3-Sided to 4-Sided Exposure

The necessary increase in the column t_e is attributed to the presence of the two variable zones on the AITP profile. In general, the two variable zones have no impact on the conservative t_e duration; as the column profile is identical in temperate to the beam profile, and simply symmetrical about the neutral axis. However, when a section is short in height, or a design fire is long in duration, the variable zones can overlap at the section's interior. In such a case, the AITP will experience higher internal temperatures, requiring an increase in the t_e duration. Of the evaluated cases, 27 % experienced the overlapping effect. Despite this overlapping presence, it's impact on the AITP t_e duration is relatively minor. On average, cases experiencing overlap required only a 0.29 % increase to the column t_e. Likewise, the maximum required change presented on Figure 5.2 is only 4.13 %, representing an addition of 5.5 min.

Given the similarity of the numerically derived conservative t_e for columns and beams, the AITP t_e equation derived for 3-sided heating is proposed for application with RC columns undergoing 4-sided exposure. Figure 5.3 highlights the suitability of the AITP t_e and ψ_{size} given in Equation 5.1 and 5.2 by examining the 5160 test cases undertaken on the four square cross-sections. The numerical and equation results indicate a good fit, satisfying the use of the existing AITP t_e equation. Application of the ψ_{size} results in a t_e with far superior fit, demonstrating the validity of the existing ψ_{size} and the importance of considering section dimensions when determining a time equivalent for RC elements.

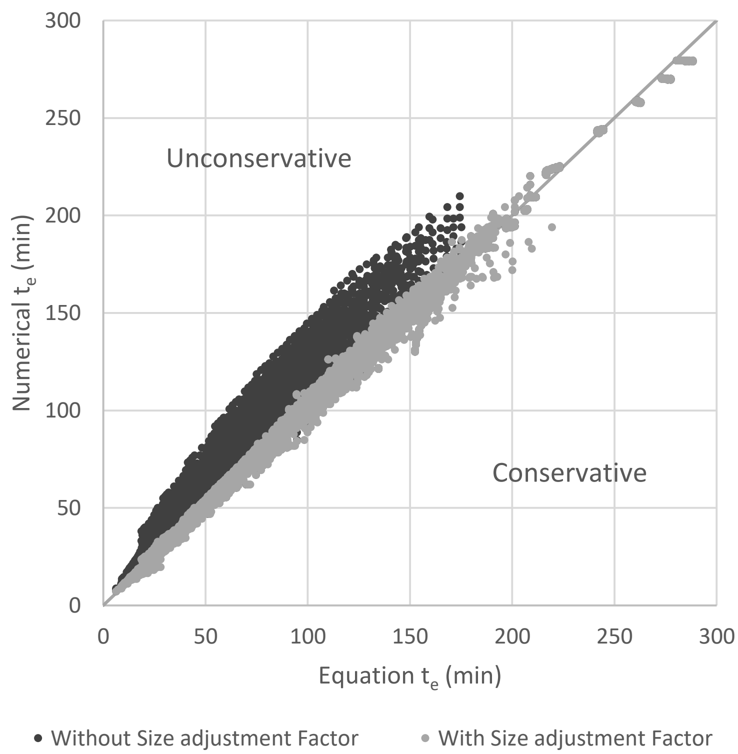

Fig. 5.3 Conservative Numerical vs. Equation t_e with and without ψ_{size}

5.3.3 Mean AITP t_e Evaluation

Figure 5.4 displays the percent change in the column versus the mean t_e duration. Unlike the conservative results, the mean t_e displays far greater variation between 3-sided and 4-sided exposure. From the test cases, 10 % recorded no significant change, 6 % recorded a decrease in the t_e duration, and 84 % recorded an increase in the t_e duration. At the most significant extent, the column t_e required a 33.8 % increase from the beam t_e. The presence of the second variable zone is the cause of the change in the t_e duration. For the mean t_e, the influence of the variable zone varies greatly depending on the design fire and cross-section dimensions. Given the results presented in Figure 5.4, the existing mean t_e equation (Equation 5.1) is deemed unsuitable for the application with RC columns undergoing 4-sided fire exposure.

Before deriving a new equation to calculate the column t_e, considerations should be made for the average error. The average error was defined in Section 5.2 as the absolute average of the percent difference between AITP-D and AITP-S at every layer of the section. The average error for the 3-sided exposure is displayed in Figure 5.5a. For 3-sided exposure, error was found to be greater than 10 % for 12 % of the evaluated cases. To ensure accuracy of the mean time equivalent, Table 5.2 outlines the conditions that were placed on the valid range of the beam t_e to eliminate the high error data points when applying Equation 5.1. A similar error analysis is presented for 4-sided exposure in Figure 5.5b. In contrast to the 3-sided results, the average error is found to vary significantly, with 36 % of the test cases recording an error greater than 10 %. More importantly however, for 3-sided exposure the high error points corresponded to smaller fires, as indicated by lower t_e durations. The 4-sided exposure results do not display this same error congregation, with high error data points existing through the entire range of design fires. Due to this error spread, development of new conditions to eliminate the high error data points is unfeasible. The introduction of two transient zones simply proves unrealistic for the standard fire to accurately approximate. As such, no mean t_e is proposed for the analysis of RC columns.

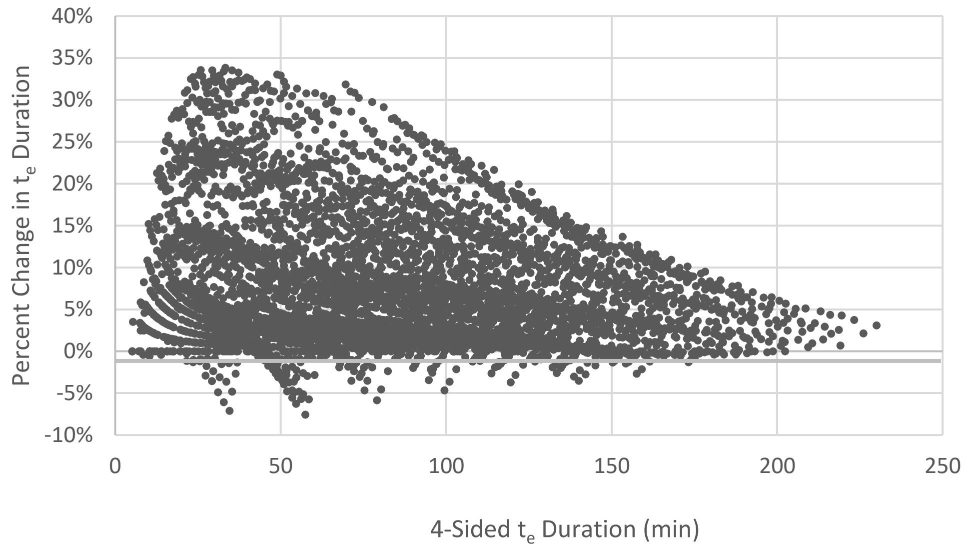

Fig. 5.4 Change in Mean t_e from 3-Sided to 4-Sided Exposure

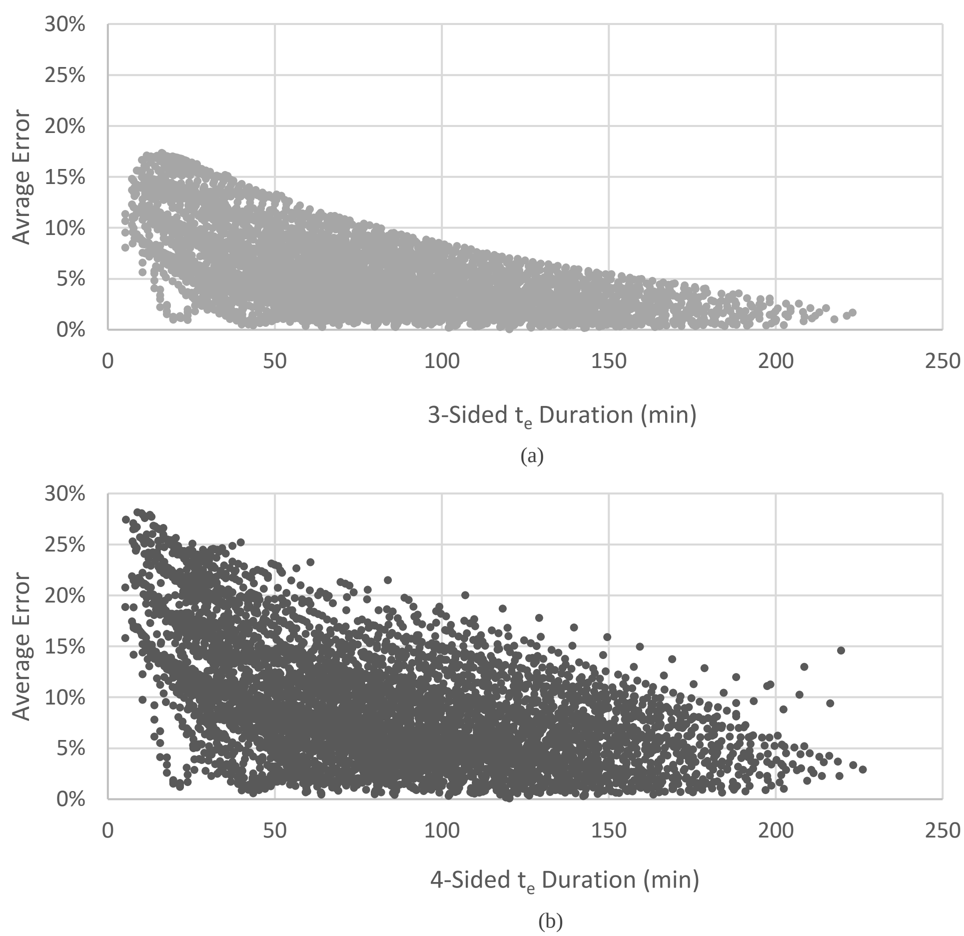

Fig. 5.5 Average Error due to (a) 3-Sided and (b) 4-Sided Exposure

5.4 Assessing the Moment-Axial Response of Fire-Exposed RC Columns using an Equivalent Standard Fire

A study is presented to assess the application of the conservative AITP t_e equation in the performance-based design of RC columns undergoing natural fire exposure. Performance-based requirements are often defined by serviceability and ultimate limit states. For RC columns, these two limit states can be best satisfied by the calculation of a section's moment-curvature (M-φ) relationship at difference axial load levels and the axial-strain (P-ε) relationship.

5.4.1 Sectional Analysis Method

The M-φ and P-ε relationship of RC columns during fire exposure can be simply established using a structural analysis program developed by El-Fitiany and Youssef (2009). The analysis is based on a finite difference method (FDM) and has three main steps: (1) determine the internal thermal gradients of the section, (2) evaluate the concrete thermal and transient strains at elevated temperature, and (3) complete a sectional analysis. Considering the axial-moment relationship of columns, a section can be evaluated at a given axial load by first determining the section's P-ε relationship, then using the axial strains to determine the subsequent M-φ response. The program makes the following assumptions: (1) plane sections remain plane during fire exposure, as previously validated up to 1200°C by El-Fitiany and Youssef (2011); (2) perfect bond exists between steel and concrete; (3) normal strength concrete (NSC) is used, and thus, explosive spalling can be ignored; (4) influence of concrete tensile cracks on heat flow is minor and can be ignored; and (5) geometrical nonlinearity is not considered.

5.4.2 Study Methodology

Using the structural analysis program of Section 5.4.2, RC columns were evaluated during both natural and standard fire exposure. The natural design fire is defined by the Eurocode approach using selected compartment parameters (EN 1991-1-2, 2002), and the standard fire is applied at a given conservative AITP t_e duration.

Comparison of a section's M-φ and P-ε relationships during natural and standard fire exposure is used to assess the accuracy of the AITP t_e. Considering the impracticality of presenting full M-φ and P-ε relationships for a large number of cross-sections and fire exposures, four key responses are identified from the relationships for general evaluation. These responses are the equivalent thermal induced strain recorded at section mid-height (ε_T), the axial capacity at elevated temperature (P_T), the moment capacity at elevated temperature (M_T), and the initial curvature at elevated temperature (φ_{iT}). For each section, these four responses are identified from the M-φ and P-ε relationships. It is necessary when analyzing columns to consider various axial load levels, of which, there are three load levels of particular importance: pure axial ($1.0P$), pure bending ($0.0P$), and the balanced condition ($0.4P$). It was identified by Yemen et al. (2008) that the balance condition at ambient temperature falls within a range of 30 % and 50 % of the maximum axial load. El-Fitiany and Youssef (2018) observed a similar range for columns evaluated at elevated temperatures. In this study, the balance condition is taken as approximately 40 % of P. Evaluation of a section at these three load levels allows for determination of the pure axial capacity (P_{rT}) at $1.0P$, the balance condition axial capacity (P_{bT}) at $0.4P$, the corresponding balanced condition moment capacity (M_{bT}) at $0.4P$, and the pure moment capacity (M_{rT}) at $0.0P$. Knowing these responses, a section's moment-axial (M-P) relationship can be approximated defining the section's load capacity. Considering the four responses and the three axial load levels, twelve responses are recorded in total for each cross-section and fire exposure.

5.4.3 Study Parameters

Five column sections were selected for evaluation, Table 5.3 displays their properties. The studied parameters are: concrete strength at ambient temperature (f'_c), section width (b_c), section height (h_c), steel reinforcement ratio (ρ_s), and aggregate type (*agg.*) of either siliceous (*sil.*) or calcareous (*cal.*). Thermal properties for normal strength concrete (NSC) with siliceous and calcareous aggregate are applied from Lie (1992). The steel ratio was represented as six bars, with three on the top and three on the bottom. The bars were spaced symmetrically about the centerline at 55 mm on center from the column edge surfaces. A general cross-section detail is presented in Figure 5.6.

Table 5.3 Parametric Study Column Properties

<table>
<tr><th>ID</th><th>F_y
MPa</th><th>f'_c
MPa</th><th>b_c
mm</th><th>h_c
mm</th><th>ρ_s
%</th><th>agg.
---</th></tr>
<tr><td>**C1**</td><td rowspan="5">400</td><td rowspan="2">30</td><td>300</td><td>300</td><td>2.0</td><td rowspan="3">sil.</td></tr>
<tr><td>**C2**</td><td>400</td><td>400</td><td>1.5</td></tr>
<tr><td>**C3**</td><td rowspan="2">40</td><td>600</td><td>600</td><td>1.5</td></tr>
<tr><td>**C4**</td><td>600</td><td>600</td><td>1.5</td><td rowspan="2">cal.</td></tr>
<tr><td>**C5**</td><td>30</td><td>500</td><td>800</td><td>1.0</td></tr>
</table>

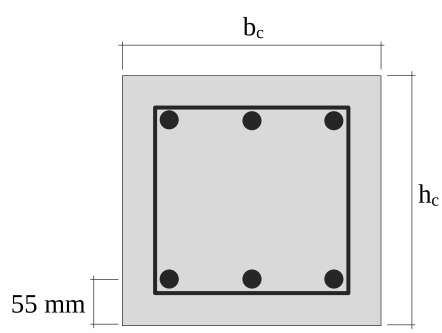

Fig. 5.6 Cross Section of Parametric Study RC Beam

For the fire exposure conditions, five design fires are identified in Figure 5.7. The five fires were developed using the Eurocode approach (EN 1991-1-2, 2002) to represent a range of possible natural fires as presented by Dembsey et al. (1995), Kirby et al. (1994), Lennon (2014), and Implementation of Eurocodes (2005). The fires can be broadly classified as medium, big, small, rapid hot, and long cool. To determine the conservative AITP t_e, the key points of t_{max}, t_{final}, and T_{max} can be graphically identified from the fire curves in Figure 5.7 and substituted into Equations 5.1 and 5.2. Table 5.4 records the AITP t_e duration with the applied φ_{size} for the given design fires and cross-section dimensions. In total, the study considers 125 test cases using the five column sections, five design fire exposures, five time equivalent standard fire exposures, and three axial load levels.

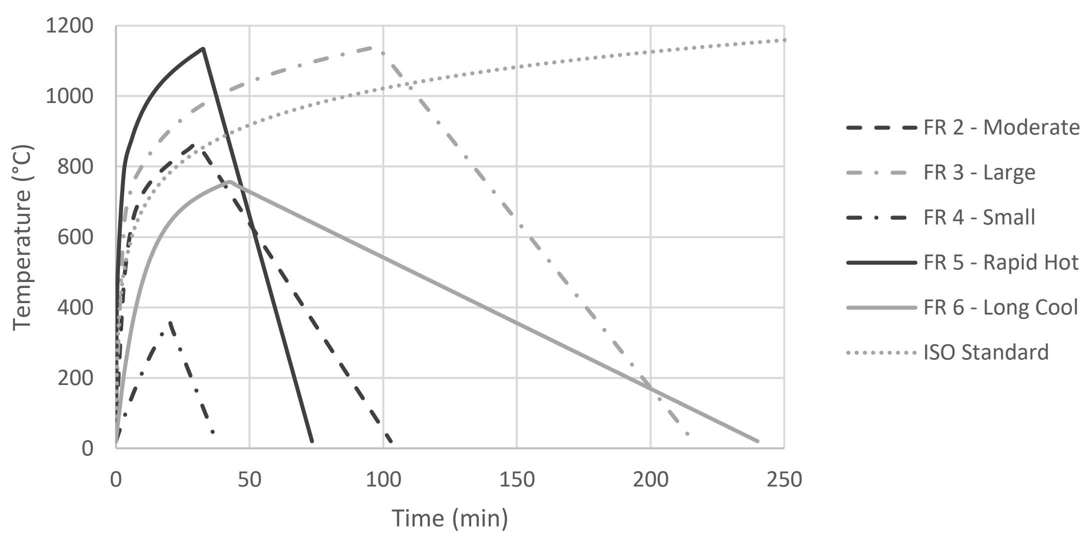

Fig. 5.7 Representative Design Fire Profiles

Table 5.4 Conservative AITP t_e for Study Design Fires and Cross-Sections

	Conservative te *(min)*				
	300 x 300	**400 x 400**	**600 x 600**	**500 x 800**	
FR 2	67.0	68.9	72.7	70.8	Moderate
FR 3	195.5	195.5	195.5	195.5	Large
FR 4	10.4	11.1	12.4	11.7	Small
FR 5	128.4	128.4	128.4	128.4	Rapid Hot
FR 6	90.2	96.2	108.2	102.2	Long Cool

5.4.4 Moment-Axial Assessment

Figure 5.8 displays the full results for C1 exposed to the medium design fire FR 2 and the conservative t_e standard fire. The ambient response is also provided as a baseline. The figure shows good correlation between the two fire events.

For the P-ε response, the two fires induce a near identical trend and value throughout. At the initial point when no axial load is applied, the thermal strain (ε_T) is found as -0.005 for both exposure fires. Strain increases with axial load similarly for both fires until the maximum axial load is identically reached at 2440 kN. For the M-φ response, the relationship at 0.0P shows a strong correlation with the AITP t_e recording only minorly conservative values throughout. At 0.4P, the AITP t_e deviates from the design fire response, but does so conservatively with lesser moment capacity and larger curvature. The final M-P relationship defines the load capacity of the section. The four responses used to approximate the curve are identified and labelled. The AITP t_e closely approximates the response of the design fire, with minorly conservative moment and axial responses.

Figures 5.9 to 5.12 display the comparison of the design fire and time equivalent standard fire in view of the four responses of ε_T, φ_{iT}, P_T, and M_T. For each of the 125 test cases, the AITP t_e conservatively approximates the design fire result. This entails lesser moment and axial capacities, and larger initial curvatures and fire induced strains. The ε_T displays the greatest variability, as concrete strain is highly susceptible to small changes in temperature. These figures confirm the application of the conservative AITP t_e in approximating the mechanical response of RC columns undergoing four-sided fire exposure.

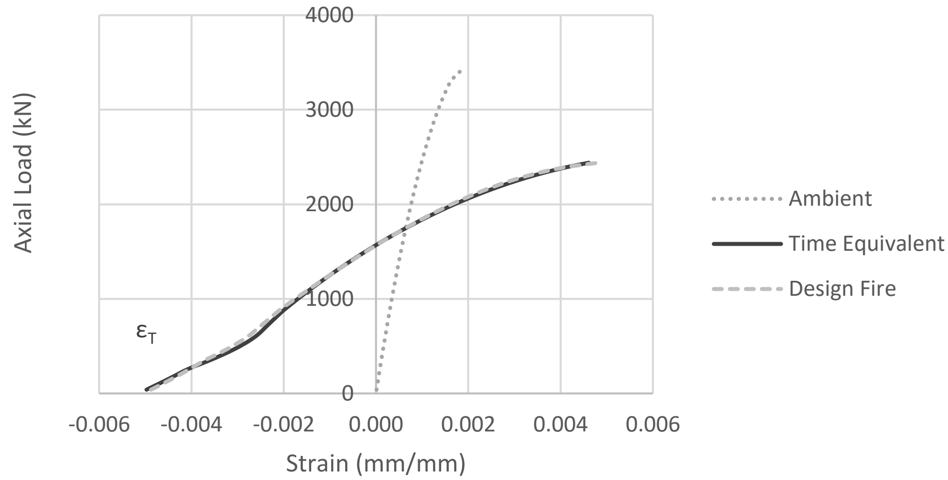

(a)

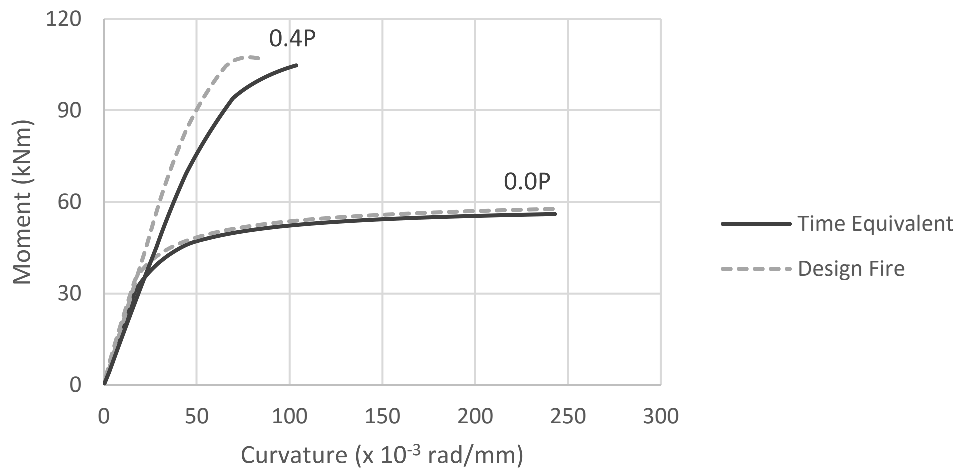

(b)

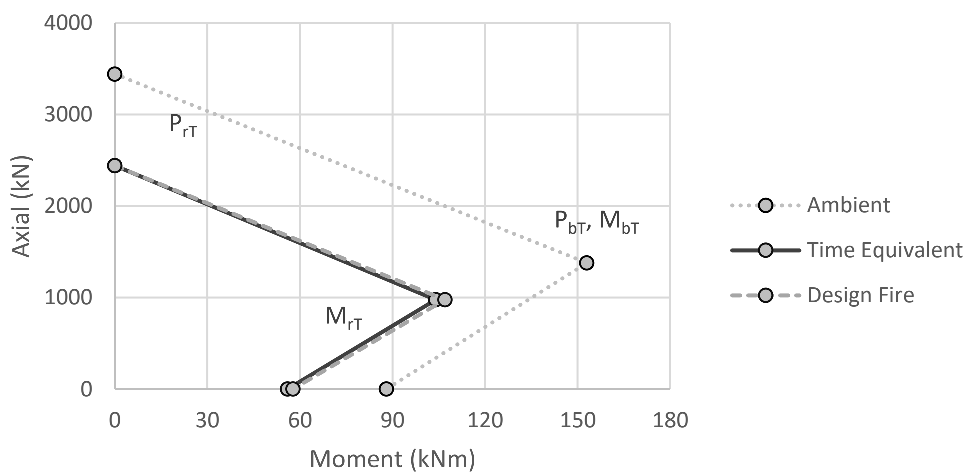

(c)

Fig. 5.8 (a) C1 Axial-Strain Relationship, (b) C1 Moment-Curvature Relationship, (c) C1 Moment-Axial Relationship

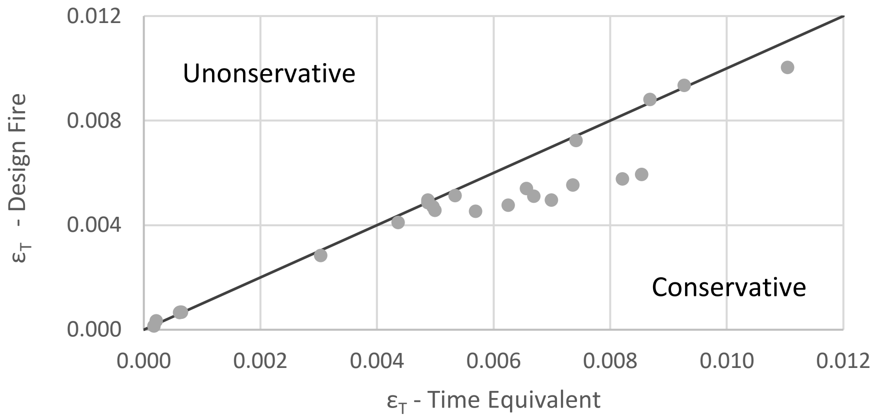

Fig. 5.9 Design vs. Time Equivalent Influence on ε_T

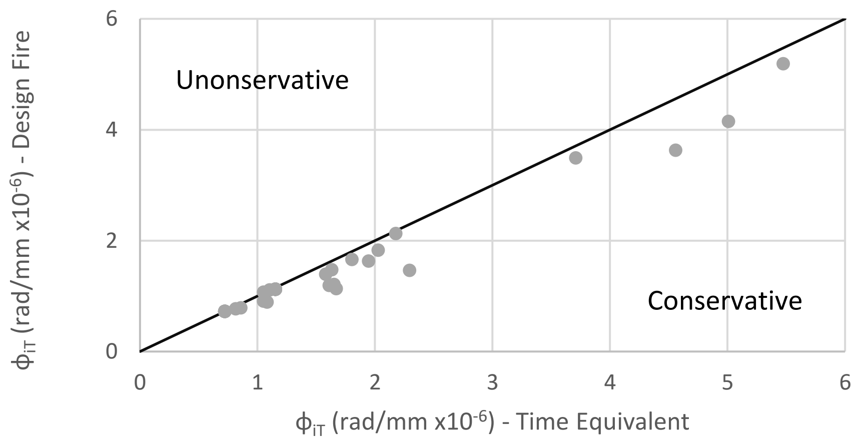

Fig. 5.10 Design vs. Time Equivalent Influence on φ_{iT}

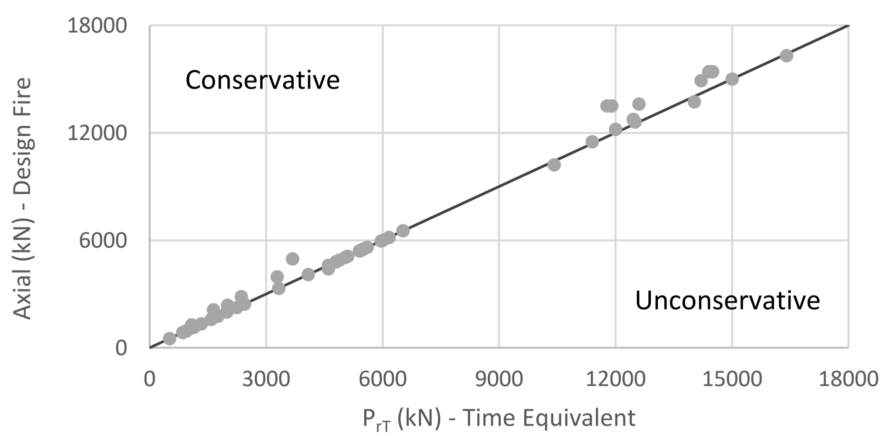

Fig. 5.11 Design vs. Time Equivalent Influence on P_{rT}

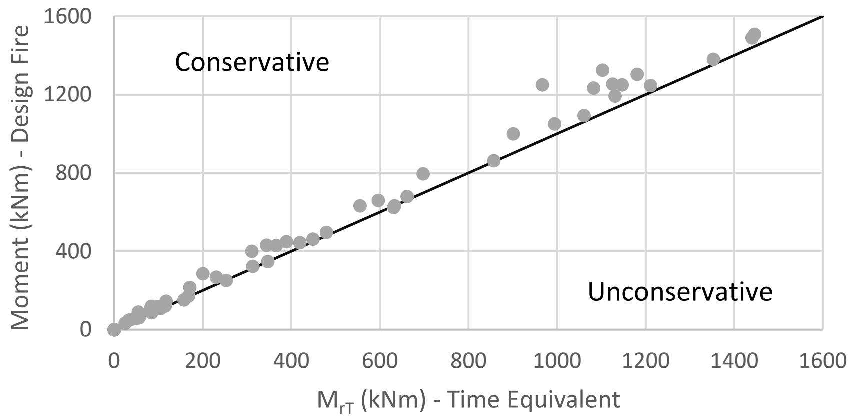

Fig. 5.12 Design vs. Time Equivalent Influence on M_{rT}

5.5 Comparison with Existing Methods

There are a number of time equivalent methods already existing in the literature; the earliest of which was proposed by Ingberg (1928). These methods vary greatly in their methodology, basing time equivalency on maximum element temperature, energy transfer, and load capacity. Chapter 3 of this thesis presents a brief literature review on the existing time equivalent methods. Despite the range of existing methods, few are applicable for reinforced concrete sections, and to the best of the author's knowledge, none consider the effect of 4-sided fire exposure. In this section, a comparison is provided with two major existing time equivalent methods to demonstrate the accuracy of the AITP t_e and the importance of considering the unique effects of 4-sided fire exposure for RC columns.

The existing methods presented by the Eurocode (EN 1991-1-2, 2002) and by Kodur et al. (2010) were selected for comparison. The Eurocode method was derived based on the work of Pettersson (1975) for protected steel columns. A modification factor is provided in the code for application to RC sections. Despite the code's stated applicability to RC sections, Thomas et al. (1997) and Xie et al. (2017) have proven the method provides unreliable time equivalent values for RC members when assessing load capacity during natural fire exposure. In Chapter 3, the suitability of the method in representing the AITP of RC beams was found to be unacceptable. Regardless, the wide spread use of the

Eurocode makes it a highly suitable method for comparison. Kodur et al.'s method (2010) was derived for RC beams based on the energy transfer of a fire event. This method was found in Chapter 3 to be reasonably accurate in representing the AITP of sections undergoing 3-sided fire exposure. Comparison with Kodur's method will best demonstrate the importance of considering 4-sided fire exposure when determining a time equivalent value.

Figure 5.13 displays the comparison between the conservative AITP t_e, EN 1991-1-2 (2002), and Kodur et al. (2010). The comparison was made for column C2 (400 x 400 mm) based on exposure to the five design fires given in Figure 5.7. Each of the four key responses is assessed at the axial load levels of 1.0P, 0.4P, and 0.0P. The key responses are recorded as a percent error from the value calculated using the design fire. A positive error indicates the time equivalent overestimates the actual design fire response, and a negative error indicates the opposite. It should be noted that some of the responses do not apply for every load level, therefore the figure is left blank for those cases. Furthermore, the ε_T response is identical for each load level because it is only affected by temperature, not load.

The results presented in Figure 5.13 highlight the conservative nature of the AITP t_e in relation with the existing methods. For every section response, design fire and axial load level; the AITP t_e resulted in a conservative estimate of the design fire severity. In contrast, the Eurocode method rarely produced conservative results, often significantly over-approximating the section capacity and under-approximating the developed stains. Given the derivation of the Eurocode method for steel section's, this lack of applicability for RC columns is expected. Kodur's method is far more accurate than the Eurocode, but still demonstrates a fair number of unconservative results. There does not appear to be any pattern in Kodur's method for when it conservatively or un-conservatively approximates a design fire. As such, the method cannot be used to reliable approximate the severity of a concrete section undergoing 4-sided fire exposure.

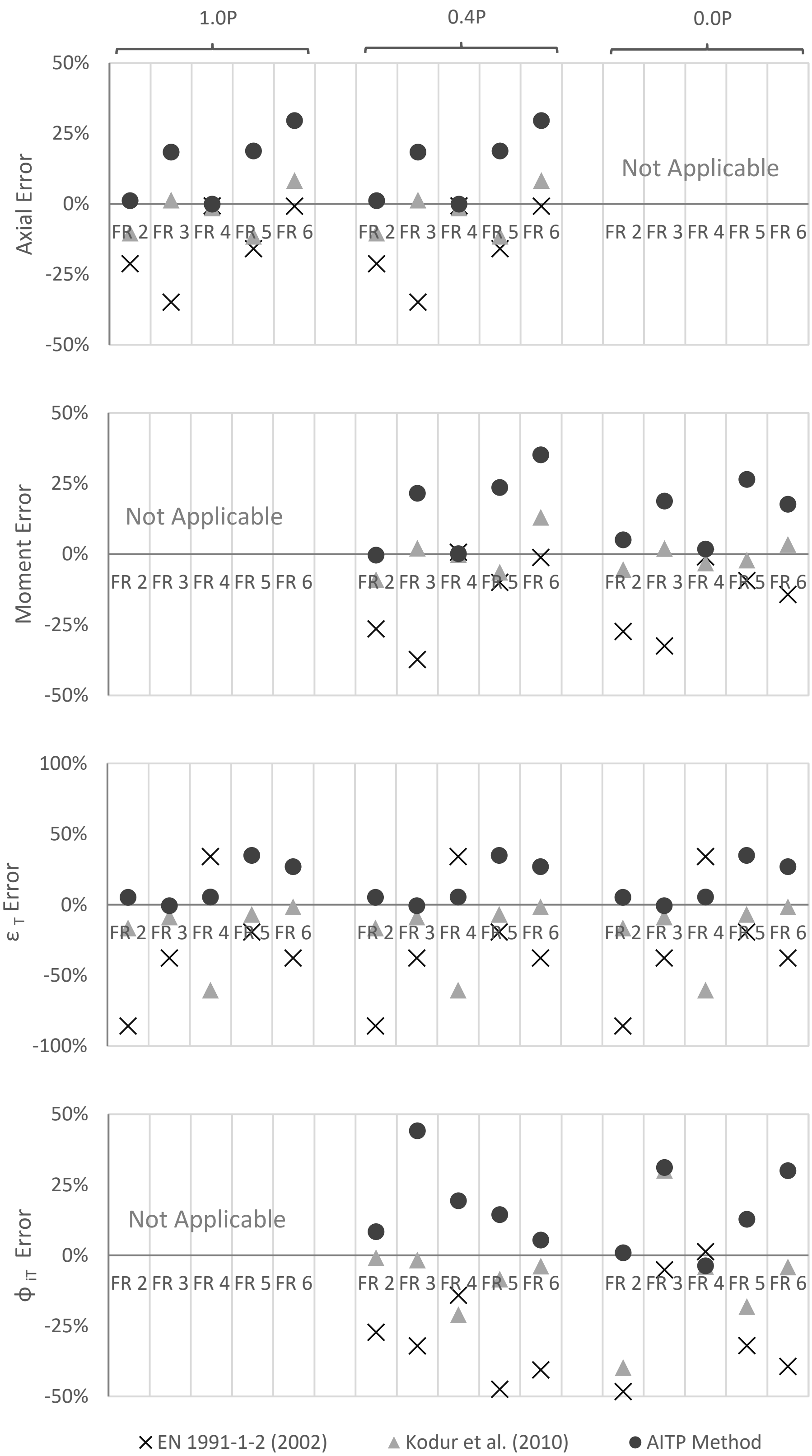

Fig. 5.13 M-P Response of C2 for Existing Time Equivalent Methods

5.6 Conclusion

During a fire event, typical interior RC columns undergo 4-sided fire exposure. The existing time equivalent methods are entirely focused on protected steel members or concrete beams undergoing 3-sided fire exposure. Due to the unique thermal properties of concrete, the methods derived for protected steel members, such as given in EN 1991-1-2 (2002), are highly unreliable. Also, the methods developed for RC beams undergoing 3-sided exposure, are equally inaccurate in representing fire severity as they ignore the additional thermal gradients that develop during 4-sided heating. To address the gap in the literature, a new AITP time equivalent method is proposed. The method is based on the actual internal gradients that develop within a concrete column section during 4-sided fire exposure. Using a section's AITP, which defines the sections average temperature as a function of height, the AITP t_e is identified as the shortest duration standard fire that generates equal or greater average temperatures at every layer along the section's height. Following a parametric study, a general equation is presented to calculate the AITP t_e within the valid fire ranges of 350°C $\leq T_{max} \leq$ 1200°C, 15 min $\leq t_{max} \leq$ 115 min, 20 min $\leq t_{final} \leq$ 240 min. To account for variable RC column dimension, a size adjustment factor was proposed to be used in conjunction with the t_e within the valid size ranges of 200 $\leq b_c \leq$ 800 mm and 200 $\leq h_c \leq$ 800 mm. The suitability of the AITP method was evaluated using a sectional analysis method. When assessing the moment-curvature, axial load-axial strain, and moment-axial load relationships; the AITP t_e always produced conservative results in comparison to the true design fire response. Based on the results of the study, it is concluded that the proposed time equivalent method allows designers to reliably approximate the severity of a natural fire on an RC column for performance-based design.

5.7 References

Dembsey, N.A., P.J. Pagni, and R.B. Williamson. "Compartment Fire Experiments: Comparison with Models." *Fire Safety Journal*, vol. 25, no. 1, 1995, pp. 187-227.

Elbahy, Y., M.A. Youssef, and M.L. Nehdi. "Stress Block Parameters for Concrete Flexural Members Reinforced with Superelastic Shape Memory Alloys." *Material and Structures*, vol. 42, no. 10, 2008, pp.1335-1351.

El-Fitiany, S.F. and M.A. Youssef. "Assessing the Flexural and Axial Behaviour of Reinforced Concrete Members at Elevated Temperatures Using Sectional Analysis." *Fire Safety Journal*, vol. 44, no. 5, 2009, pp. 691-703.

El-Fitiany, S.F. and M.A. Youssef. "Practical Method to Predict the Axial Capacity of RC Columns Exposed to Standard Fire." *Journal of Structural Fire Engineering*, vol. 9, no. 4, 2018, pp. 266-286.

El-Fitiany, S.F. and M.A. Youssef. "Stress-Block Parameters for Reinforced Concrete Beams during Fire Events." *ACI Special Publication: Innovations in Fire Design of Concrete Structures*, SP-279, 2011, pp. 1-40.

EN 1991-1-2. *Eurocode 1: Actions on Structures - Part 1-2: Actions on Structures Exposed to Fire*. European Committee for Standardization. Brussels, Belgium. 2002.

Implementation of Eurocodes. *Handbook 5 - Design of Buildings for the Fire Situation*. Leonardo Da Vinci Joint Research Project, 2005.

ISO 834. *Fire Resistance Tests – Elements of Building Construction*. International Organization for Standards. Geneva, Switzerland. 2014.

Kirby, B.R., D.E. Wainman, L.N. Tomlinson, T.R. Kay, and B.N. Peacock. "Natural Fires in Large Scale Compartments." *International Journal on Engineering Performance-Based Fire Codes*, vol. 1, no.2, 1999, pp. 43-58.

Kodur, V.K.R., P. Pakala, and M.B. Dwaikat. “Energy Based Time Equivalent Approach for Evaluating Fire resistance of Reinforced Concrete Beams.” *Fire Safety Journal*, vol. 45, no. 4, 2010, pp. 211-220.

Lennon, T. *Results and Observations from Full-Scale Fire Test at BRE Cardington*. no. 215-741, Building Research Establishment, Cardington, UK, 2004.

Lie, T.T. *Structural Fire Protection*. ASCE, 1992.

Chapter 6

6.0 Thesis Conclusion

Performance-based fire design provides engineers with the means to design structures to withstand fire events without the need for prescriptive measures. This thesis presented simple, practical, and rational methods to facilitate the evaluation of reinforced concrete (RC) elements during natural fire exposure. Considering the internal temperature gradients that develop within RC sections, a time equivalent (t_e) has been proposed to approximate the severity of a given natural fire event in terms of an equivalent standard fire duration. The methodology of this process was assessed for a range of natural fires, RC beam-sections, and RC column-sections. The proposed method has been assessed in view of existing experimental work and finite element analysis. In the following sections, the work completed in each chapter of this thesis is summarized, highlighting the important conclusions. The author's recommendations for future work are also included at the end of this chapter.

6.1 Literature Review

A literature review was conducted to investigate the influence of natural fires on the stress-strain relationship of concrete. Natural fire events were identified to have four main variabilities that influence the response of concrete: heating rate, maximum temperature, fire duration, and cooling rate. From the existing literature, experimental work was selected to evaluate the influence of each of the four variabilities. Given the large range of reported testing scenarios and mix designs, collected experimental work was limited to the following criteria: (a) unstressed tests, (b) unconfined tests, (c) unsealed tests, (d) ordinary portland cement (OPC) specimens (no additives such as fly ash, silica, fibers, etc.), and (e) normal strength concrete (NSC) specimens. The conclusions of the literature review found that maximum temperature has the most significant impact on the stress-strain relationship of concrete. At lower temperatures, circa 500°C, cooling rate has a comparable influence as maximum temperature, but, this impact diminishes greatly with increasing temperature.

Exposure duration only impacts strength until a uniform internal temperature gradient is reached. Long term exposure was not found to lead to further degradation. Heating rate was identified to have no noticeable impact on the stress-strain response. Given the impact of natural fires on the stress-strain relationship of concrete, properly identifying and accounting for these four fire variabilities will assist engineers in the future evaluation of concrete at elevated temperatures.

6.2 Equivalent Standard Fire Duration to Evaluate Internal Temperatures in Natural Fire Exposed RC Beams

A new time equivalent method was proposed in this chapter based on the internal temperatures that develop within an RC beam exposed to a natural fire event. The basis of the proposed method lays in the evaluation of a section's average internal temperature profile (AITP). AITP's record a section's average temperature as a function of section depth. Using AITP's, two-dimensional temperature gradients can be simply approximated by a single profile, greatly simplifying sectional analysis. The AITP time equivalent method is derived following two criteria: mean and conservative. Mean criterion was based on accurately matching the internal temperature profiles of a natural fire to that of a standard; while the conservative criterion was based on selecting the shortest duration standard fire that produces equal or larger temperatures at every point in the section. A parametric study was conducted to numerically determine the AITP t_e for a variety of natural fires. The study resulted in the development of two equations that allow for the simple calculation of the AITP t_e for mean and conservative criteria. The influence of beam dimensions was also considered. Beam height demonstrated no influence on the t_e duration, but beam width had a major effect on the required duration. A size adjustment factor (ψ_{size}) was subsequently derived to be used in conjunction with the AITP t_e. The thermal predictions of the proposed AITP t_e was then compared to those of existing time equivalent methods. To the best of the author's knowledge, the AITP t_e is the only time equivalent that considers the influence of cross-section dimensions. The comparison demonstrated the existing methods' lack of suitability for RC beams and the importance of considering beam dimensions. Using the proposed AITP t_e and size adjustment factor, designers will be capable of quickly evaluating the severity of a natural fire for a RC beam.

6.3 Assessing the Flexural Response of Fire-Exposed RC Beams using an Equivalent Standard Fire

To assess the suitability of the proposed AITP t_e in representing the severity of a natural fire event, selected flexural responses were evaluated using natural fire properties and the AITP equivalent standard fire. A simple sectional analysis method, developed by El-Fitiany and Youssef (2009), was used to calculate the moment-curvature relationship of RC beams during fire exposure. A parametric study was undertaken for a variety of natural fires and RC sections. For each test case, three key points from the moment-curvature profile were recorded for comparison: maximum moment, initial curvature, and initial stiffness. These points were identified as the critical points to define the relationship and allow for performance-based design. The study found the predictions based on the mean t_e to be in good agreement with the responses calculated using the design fire exposure. The initial curvature and stiffness demonstrated greater variability, but their error on the conservative side was less than 10 %. The conservative time equivalent led to conservative predictions for all cases. The chapter concluded with a case study demonstrating the application of the AITP t_e in the simplified analysis of an RC beam. The simplified analysis proceeded by determining the natural fire severity, calculating the section internal temperatures, and evaluating the sectional moment capacity. The approach was validated using a finite element model and experimental findings from Ellingwood and Lin (1991). The conclusions of the chapter indicate the validity of the AITP t_e and its suitability in the performance-based design process.

6.4 Equivalent Standard Fire Duration to Evaluate Internal Temperatures in Natural Fire Exposed RC Columns

In this chapter, the proposed time equivalent method for RC beams was assessed for RC columns. During fire exposure, a major change arises for typical interior columns, as they are heated from all four faces, not just from the three lower faces as is experienced by a typical beam. The additional exposure face was found to greatly influence the internal thermal gradients that develop within a section. For RC columns, the mean criterion methodology was found to be no longer suitable for application, as the internal gradients that developed were too variable to be represented accurately by an equivalent standard time. The conservative criterion methodology however, was found to work perfectly for RC columns. A study was undertaken to assess the conservative t_e equation for column sections of 300 x 300, 400 x 400, 600 x 600, and 800 x 800 mm. The study determined that the existing conservative time equivalent equation from Chapter 3 is still valid for RC columns. Similar to Chapter 4, the mechanical response of columns during time equivalent exposure was assessed based on the sectional moment-curvature, axial load-axial strain, and moment-axial load relationship. The three relationships were assessed at three load levels: pure axial; pure bending; and the balance condition, which was assumed to occur at 40% of the maximum axial load. For every section response, load case, cross-section, and natural fire considered, the conservative AITP t_e produced a conservative approximation of the natural fire result. A comparison with existing methods was further provided demonstrating the improved suitability of the AITP t_e for RC columns undergoing four-sided fire exposure.

6.5 Thesis Limitations

The proposed AITP t_e and size adjustment factor were derived based on a parametric study. As such, the method has a well-defined valid range based on the extents of the study:

The method is valid for natural fires within:

- 350°C ≤ maximum temperature ≤ 1200°C,
- 15 min ≤ time at maximum temperature ≤ 115 min
- 20 min ≤ overall fire duration ≤ 240 min

The method is valid for RC sections within:

- 200 mm ≤ beam width ≤ 800 mm
- 200 mm ≤ beam height ≤ 800 mm
- 300 mm ≤ column width ≤ 800 mm
- 300 mm ≤ column height ≤ 800 mm

Furthermore, the AITP methodology is only applicable for elements resisting un-axial bending. Columns resisting bi-axial bending were not considered in this study. The parametric study was only undertaken considering NSC, which allowed for the omission of explosive spalling.

6.6 Recommendations for Future Work

This thesis has revealed that additional experimental and analytical work is needed in the following subjects:

1) Further experimental testing is needed on the stress-strain response of concrete during natural fire exposure.
2) Experimental testing of RC elements exposed to natural fire exposure. To the best of the author's knowledge, no experimental work is readily available recording the flexural or shear failure of RC elements during natural fire exposure.
3) Assessment of the AITP method for plane RC elements such as walls and slabs.
4) Extending the AITP method for T or I shaped beam sections.
5) Consideration of the AITP method for application with high-strength concrete (HSC), which will require consideration of explosive spalling.

Appendix A

Finite Difference Modelling

In this thesis, a simple heat transfer model from Lie (1992) was implemented to determine the section internal temperatures of a concrete element during fire exposure. This appendix describes the implemented finite difference method (FDM), the validation approach, and method limitations. A full description of the equations needed for the FDM is provided by Lie (1992).

To calculate section temperatures, the cross-section is first divided into a fine two-dimensional mesh (Figure A.1). The mesh is oriented at 45 degrees, with square elements used in the interior and triangular elements used at the surface. Heat retention and transfer is conducted at the center of the square mesh elements. For the triangular elements, transfer is conducted at the center of the hypotenuse. This location of the triangular elements represents the boundary nodes of the section.

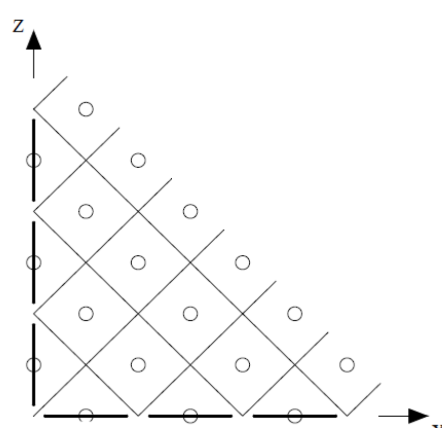

Fig. A.1 Heat Transfer Mesh Detail

Mesh size ($\Delta\xi$) was determined by a sensitivity analysis. Evaluating the internal temperatures of the section during standard fire exposure, the mesh size was iteratively decreased until a temperature change of less than 1% was observed. Based on the sensitivity analysis, the number of required horizontal mesh divisions can be related to the section width using equation A.1; where b_c is the section width in meters. Individual mesh size can be subsequently determined assuming a square mesh shape.

$$number\ of\ horizontal\ mesh\ divisions = b_c * 200 \qquad \text{(A.1)}$$

Application of the FDM requires knowledge of several concrete thermal properties. They include: the thermal conductivity (k), specific heat (c_s), and density (ρ). Temperature dependent relationships for these material parameters were implemented into the model based on equations presented in Lie (1992). Additional constants such as the Stefan Boltzmann constant (σ), the conductivity constant (h_{max}), and the emissivity (ε_f) were also specified based on the recommendation of Lie (1992).

Fire conditions are imposed on the section using a temperature-time relationship. At a given time, the temperature of the fire is identified, and applied evenly to the desired boundaries of the element. Depending on element geometry, the fire exposed boundaries (3-side heating, 4-side heating, etc.) are specified during implementation. The maximum time step for fire iteration is specified in the method based on mesh size, section geometry, and material properties.

Lie (1992) provides an Energy Equation to account for heat transfer due to conduction and radiation. Heat flow (q) due to conduction and radiation is undertaken consistent with the general energy relationships presented in Equations A.2 and A.3. Starting at the section boundaries, heat transfer is evaluated from the compartment fire to the exterior triangular mesh elements. Subsequent interior elements are solved for by iteratively applying the head transfer until the full section is evaluated. The time step is then increased, and the process continued until the final fire duration is reached.

$$q_{radiation} = \varepsilon\sigma(T_e^4 - T_r^4) \tag{A.2}$$

$$q_{conduction} = k(T_e - T_r) \tag{A.3}$$

Validation of the FDM was accomplished using the standard temperature profiles presented in the Implementation of Eurocodes (2005) handbook. These standard profiles are provided for a variety of specific aggregate types, section dimensions, and fire exposures. Evaluation of the FDM using the same parameters of these studies validates the accuracy of the implemented method in determining section internal temperatures.

The limitations of the proposed method are as follows:

1. Moisture movement within the section is omitted. This is a conservative assumption, as it leads to higher internal temperatures. Furthermore, for an established concrete structure, it is reasonable to assume moisture levels would be negligible.
2. The energy equation for radiation transfer is assumed for that of an ideal black body. This was shown my Lie (1992) to produce only very minor errors.
3. Fire is applied as a uniform temperature along the section's boundaries. This is consistent with the commonly implemented uniform compartment temperature.
4. The valid temperature range of the method is governed by the limitations of the specified material properties.
5. Heat transfer due to convection is ignored at the element's surface. This is proven be Lie (1992) to result in only very minor errors.
6. A stability equation is provided by Lie (1992) as a general limitation for the method. The equation accounts for mesh size, thermal properties, and iteration time step.
7. Normal strength concrete (NSC) is assumed, thus allowing for the omittance of explosive spalling.

Appendix B

Finite Element Modelling (ABAQUS)

A finite element (FE) model was utilized in Section 4.0 as part of the presented case study. This appendix describes the FE modelling and validation techniques implemented as part of that work.

The FE model was implemented in ABAQUS, a widely utilized FE software package. In order to capture the variation in heat transfer within the RC-section, solid elements were specified in the model. RC sections consist of both concrete and reinforcing steel. These elements were modelled as separate solid parts, and subsequently merged together as a combined assembly. Mechanical constraints were applied to the end faces of the element consistent with pin and roller connections. The roller connection permits the release of thermal expansion stresses, allowing for the model and case-study to omit the influence of restrain actions.

Material properties for the steel and concrete were implemented in ABAQUS consistent with values presented in Lie (1992). Materials were defined as temperature-dependent, allowing for greater accuracy during the fire event. Fire exposure was applied along the bottom and two side faces of the beam section. Considering the assumption of a uniform compartment temperature, the fire event was applied uniformly over the selected boundaries. Fire exposure was defined as a temperature-time relation. Along the element boundaries, heat transfer between the compartment and the beam was specified for radiation and conduction conditions.

Final mesh layout and sizing was selected based on a sensitivity study. Mesh size plays an important role in both the heat transfer and stress analysis, therefore both responses were evaluated in the sensitivity study. Element temperature was evaluated at the location of the steel reinforcement and the maximum deflection was recorded during ambient conditions for a uniform surface load. These responses were measured for a variety of mesh layouts, until a difference of less than 1 % was recorded between iterations. The final selected mesh is presented in Figure B.1. Due to stress concentrations at the steel location, a finer mesh is utilized in this region.

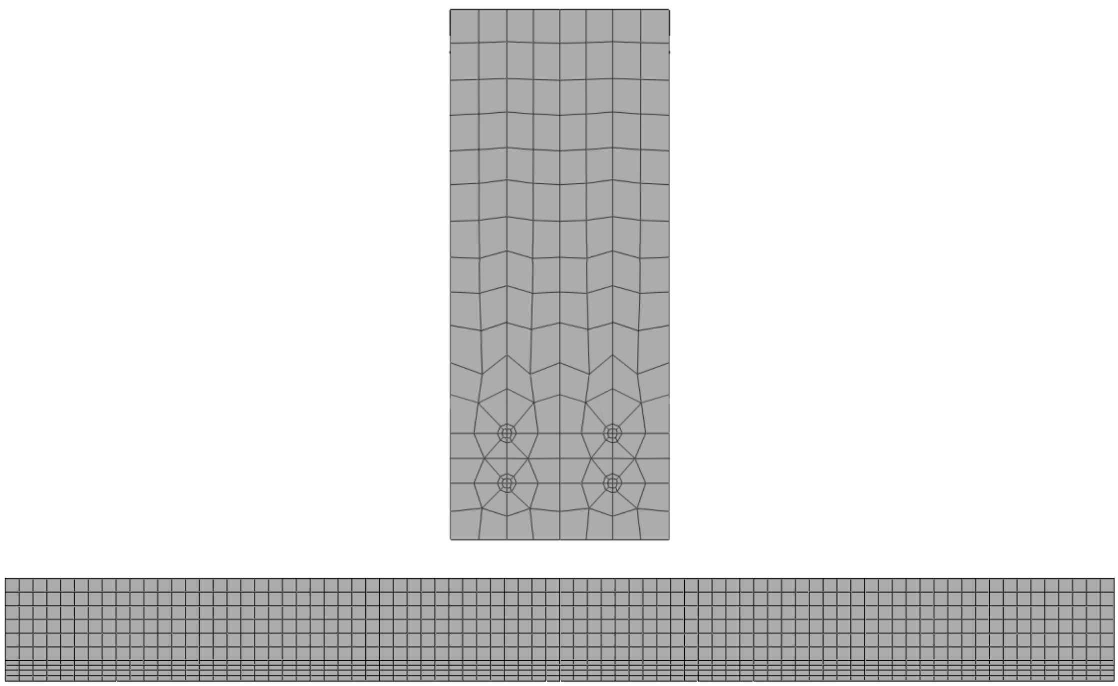

Fig. B.1 Element Meshing in Cross-Section and Elevation View

Running the model involves a two-step process: heat-transfer and stress analysis. In the heat-transfer step, the beam is exposed purely to the fire scenario and the internal temperatures are recorded with time. Secondly, the internal temperatures are loaded into the model as a pre-define condition, and a stress analysis is completed. In order to determine the moment capacity of the fire exposed section, a constant uniformly distributed load is applied to the top face of the element during the stress analysis. This load is manually increased between runs until failure is observed based on strain non-convergence. ABAQUS does allow for a coupled loading event in which both heat transfer and stress analysis can be completed simultaneously. However, both approaches provide identical results, and it is the author's opinion that this two-step process provides better compartmentalization for error checking.

Model validation was undertaken at both steps of the analysis. In the heat-transfer step, validation was performed by comparing section temperatures with the finite difference model (FDM) from Appendix A and the experimental work performed by Ellingwood and Lin (1991). In the stress analysis step, validation was undertaken with and without the fire exposed pre-defined condition. Doing so allowed for the moment capacity of the section to be easily validated at ambient temperatures, and then subsequently validated during the fire-exposed condition. At the fire exposed-condition, validation was achieved by comparison with the proprietary structural analysis program described in Section 4.1 of this thesis.

Curriculum Vitae

Name:	Robert Thomas Kuehnen
Post-secondary Education and Degrees:	Western University London, Ontario, Canada 2013-2017 B.E.Sc.
Honours and Awards:	Western University Continuing Admissions Scholarship 2013
	Peter A. Rosati Award for Outstanding Teaching in the Civil and Environmental Engineering Department 2018
	Western University Three Minute Thesis (3MT) 2nd Place Finalist 2019
Related Work Experience:	Teaching Assistant The University of Western Ontario 2017-2019

Journal Publications:

Kuehnen, R.T. and M.A. Youssef. “Equivalent Standard Fire Duration to Evaluate Internal Temperatures in Natural Fire Exposed RC Beams.” *Fire Safety Journal*. Manuscript submitted for publication, Nov 2018.

Kuehnen, R.T., M.A. Youssef, and S. El-Fitiany. “Performance-Based Design of RC Beams Exposed to Natural Fire: A Case Study.” *CSCE 7th International Specialty Conference on Engineering Mechanics and Materials*, Laval, Canada, 2019. Conference paper submitted for publication, Oct 2018.